International Doctorate Program in Molecular Oncology and Endocrinology

Doctorate School in Molecular Medicine

XXII cycle - 2006–2009
Coordinator: Prof. Giancarlo Vecchio

"Control of breast cancer cell growth by adipocyte-released factors"

Vittoria D'Esposito

University of Naples Federico II

Dipartimento di Biologia e Patologia Cellulare e Molecolare

"L. Califano"

Administrative Location

Dipartimento di Biologia e Patologia Cellulare e Molecolare “L. Califano”
Università degli Studi di Napoli Federico II

Partner Institutions

Italian Institutions
Università degli Studi di Napoli “Federico II”, Naples, Italy
Istituto di Endocrinologia ed Oncologia Sperimentale “G. Salvatore”, CNR, Naples, Italy
Seconda Università di Napoli, Naples, Italy
Università degli Studi di Napoli “Parthenope”, Naples, Italy
Università del Sannio, Benevento, Italy
Università di Genova, Genoa, Italy
Università di Padova, Padua, Italy
Università degli Studi “Magna Graecia”, Catanzaro, Italy
Università degli Studi di Firenze, Florence, Italy
Università degli Studi di Bologna, Bologna, Italy
Università degli Studi del Molise, Campobasso, Italy
Università degli Studi di Torino, Turin, Italy
Università di Udine, Udine, Italy

Foreign Institutions
Université Libre de Bruxelles, Brussels, Belgium
Universidade Federal de Sao Paulo, Brazil
University of Turku, Turku, Finland
Université Paris Sud XI, Paris, France
University of Madras, Chennai, India
University Pavol Jozef Šafàrik, Kosice, Slovakia
Universidad Autonoma de Madrid, Centro de Investigaciones Oncologicas (CNIO), Spain
Johns Hopkins School of Medicine, Baltimore, MD, USA
Johns Hopkins Krieger School of Arts and Sciences, Baltimore, MD, USA
National Institutes of Health, Bethesda, MD, USA
Ohio State University, Columbus, OH, USA
Albert Einstein College of Medicine of Yeshiwa University, N.Y., USA

Supporting Institutions
Ministero dell’Università e della Ricerca
Associazione Leonardo di Capua, Naples, Italy
Dipartimento di Biologia e Patologia Cellulare e Molecolare “L. Califano”, Università degli Studi di Napoli “Federico II”, Naples, Italy
Istituto Superiore di Oncologia (ISO), Genoa, Italy
Università Italo-Francese, Torino, Naples, Italy
Università degli Studi di Udine, Udine, Italy
Agenzia Spaziale Italiana
Istituto di Endocrinologia ed Oncologia Sperimentale “G. Salvatore”, CNR, Naples, Italy

Italian Faculty

Giancarlo Vecchio, MD, Co-ordinator
Salvatore Maria Aloj, MD
Francesco Saverio Ambesi Impiombato, MD
Francesco Beguinot, MD
Maria Teresa Berlingieri, MD
Angelo Raffaele Bianco, MD
Bernadette Biondi, MD
Francesca Carlomagno, MD
Gabriella Castoria, MD
Angela Celetti, MD
Mario Chiariello, MD
Lorenzo Chiariotti, MD
Vincenzo Ciminale, MD
Annamaria Cirafici, PhD
Annamaria Colao, MD
Alma Contegiacomo, MD
Sabino De Placido, MD
Gabriella De Vita, MD
Monica Fedele, PhD
Pietro Formisano, MD
Alfredo Fusco, MD
Michele Grieco, MD
Massimo Imbriaco, MD
Paolo Laccetti, PhD
Antonio Leonardi, MD
Paolo Emidio Macchia, MD
Barbara Majello, PhD
Rosa Marina Melillo, MD
Claudia Miele, PhD
Francesco Oriente, MD
Roberto Pacelli, MD
Giuseppe Palumbo, PhD
Silvio Parodi, MD
Nicola Perrotti, MD
Giuseppe Portella, MD
Giorgio Punzo, MD
Antonio Rosato, MD
Guido Rossi, MD
Giuliana SalvatoreMD,
Massimo Santoro, MD
Giampaolo Tortora, MD
Donatella Tramontano, PhD
Giancarlo Troncone, MD
Giuseppe Viglietto, MD
Roberta Visconti, MD
Mario Vitale, MD

Foreign Faculty

Université Libre de Bruxelles, Belgium
Gilbert Vassart, MD
Jacques E. Dumont, MD

Universidade Federal de Sao Paulo, Brazil
Janete Maria Cerutti, PhD
Rui Monteiro de Barros Maciel, MD PhD

University of Turku, Turku, Finland
Mikko Laukkanen, PhD

Université Paris Sud XI, Paris, France
Martin Schlumberger, MD
Jean Michel Bidart, MD

University of Madras, Chennai, India
Arasambattu K. Munirajan, PhD

University Pavol Jozef Šafàrik, Kosice, Slovakia
Eva Cellárová, PhD
Peter Fedoročko, PhD

Universidad Autonoma de Madrid - Instituto de Investigaciones Biomedicas, Spain
Juan Bernal, MD, PhD
Pilar Santisteban, PhD

Centro de Investigaciones Oncologicas, Spain
Mariano Barbacid, MD

Johns Hopkins School of Medicine, USA
Vincenzo Casolaro, MD
Pierre A. Coulombe, PhD
James G. Herman MD
Robert P. Schleimer, PhD

Johns Hopkins Krieger School of Arts and Sciences, USA
Eaton E. Lattman, MD

National Institutes of Health, Bethesda, MD, USA
Michael M. Gottesman, MD
J. Silvio Gutkind, PhD
Genoveffa Franchini, MD
Stephen J. Marx, MD
Ira Pastan, MD
Phillip Gorden, MD

Ohio State University, Columbus, OH, USA
Carlo M. Croce, MD
Ginny L. Bumgardner, MD PhD

Albert Einstein College of Medicine of Yeshiwa University, N.Y., USA
Luciano D'Adamio, MD
Nancy Carrasco,

“Control of breast cancer cell growth by adipocyte-released factors”

TABLE OF CONTENTS

LIST OF PUBLICATIONS

This dissertation is based upon the following publications:

1. Esposito I, Proto MC, Gazzerro P, Laezza C, Miele C, Alberobello AT, **D'Esposito V**, Beguinot F, Formisano P, Bifulco M. *The cannabinoid CB1 receptor antagonist rimonabant stimulates 2-deoxyglucose uptake in skeletal muscle cells by regulating the expression of phosphatidylinositol-3-kinase.* Mol Pharmacol. 2008 Dec;74(6):1678-86.

2. Alberobello AT*, **D'Esposito V***, Marasco D, Ruvo M, Bianco R, Tortora G, Esposito I, Fiory F, Miele C, Beguinot F, Formisano P. *Selective disruption of Insulin-like Growth Factor-1 signalling via Phosphoinositide-dependent Kinase-1 prevents protective effects of IGF-1 on human cancer cell death.* J Biol Chem. Pending revision.
   * Equally contributed to the study.

ABSTRACT

"CONTROL OF BREAST CANCER CELL GROWTH BY ADIPOCYTE-RELEASED FACTORS"

Obesity is one of the most challenging and growing health problems, worldwide. Epidemiologic studies now provide compelling evidence that obesity is a risk factor for both cancer incidence and mortality. In particular, obesity increases rates of breast cancer in postmenopausal women and is associated with poorer survival and increased recurrence of disease, regardless the menopausal status. It is now becoming clear that adipocytes, which represent very abundant cell types surrounding cancer cells, particularly in the mammary gland, could influence several aspects of tumorigenesis, from promoting local invasion to angiogenesis and metastasis. However, the molecular mechanisms involved in the adipocyte control of the malignant phenotype remain poorly understood. I have studied the mechanisms by which adipocytes may integrate metabolic and nutritional inputs and produce signals affecting breast cancer cell phenotypes. I have obtained evidence that conditioned media from 3T3-L1 cells induce growth of MCF7 cells, in a time-dependent manner. In particular, conditioned media from fully differentiated adipocytes are 2-fold more effective than conditioned media from pre-adipocytes in inducing MCF7 growth. Cell cycle analysis by flow cytometry revealed that these changes are due to reduced apoptosis instead of increased proliferation. Pre-incubation with low glucose medium or insulin reduces the effect of adipocyte conditioned media on MCF7 growth. Cytokines/growth factors screening of conditioned media from pre-adipoctyte and adipocyte, cultured in presence or in absence of low glucose medium or insulin, revealed that KC, RANTES and IGF1 could be good candidates in mediating pro-tumorigenic effect of adipocyte conditioned media. Moreover, IGF1R inhibitor AG1024 is able to revert adipocyte conditioned media effect. In conclusion, adipocyte-derived factors promote breast cancer cell growth inhibiting the apoptosis. This effect is more evident in adipocytes than in pre-adipocytes and is altered by insulin or nutritional factors such as glucose. The effects are likely mediated by IGF-1.

1. BACKGROUND

1.1 Obesity

Overweight and obesity are clinically defined indicators of a disease process characterized by the accumulation of body fat due to an excess of energy intake (nutritional intake) relative to energy expenditure (physical activity). When energy intake exceeds energy expenditure over a prolonged period of time, the result is a positive energy balance (PEB), which leads to the development of obesity (Fair and Montgomery 2009).

Several measures are used to define obesity. The most utilized parameter is body mass index (BMI, also called Quetelet's Index) (weight in kilograms divided by height in meters squared), a measure of overall overweight status. The World Health Organization (WHO) defined an overweight status as a BMI of 25.0 or higher. The overweight category is then divided into four categories: preobese, 25.00 to 29.9 kg/m^2; obese class I, 30.00 to 34.99 kg/m^2; obese class II, 35.00 to 39.99 kg/m^2; and obese class III, $\geq$ 40.00 kg/m^2 (World Health Organization 2000) .

Obesity is one of the most challenging and growing health problems (Van Roermund and Witjes 2007). The prevalence of obesity has reached epidemic levels in many parts of the world. Worldwide, more than 1 billion adults are overweight (BMI >25) and at least 300 million of them are obese (BMI >30) (Fig. 1) (Power et al. 2007). Obesity rates are slightly higher in men, and increase from youth to middle age (Moayyedi 2008). In the United States, 59 million adults (31%) are obese and 4.7% are considered morbidly obese (BMI $\geq$ 40) (Power et al. 2007). The situation in Europe is somewhat better. The prevalence of adult obesity in the states of EU is lower than in the USA: in males between 8-25%, in females between 8-27%. The highest obesity prevalence is in Central Europe, especially in the Czech Republic and in England (Ginter and Simko 2008). The problem is not restricted to industrialized societies: obesity rates are increasing in urban areas of developing countries, particularly those in transition. Of special concern are the increasing numbers of overweight children and adolescents in many countries (Aranceta et al. 2009).

It is clear from family, twin, and adoption studies that genetic factors contribute to the obesity phenotype. Such studies, conducted in countries where food is plentiful, suggest that 40–70% of individual variability in body mass in these settings may be explained by hereditable factors (Calle and Thun 2004).
Genes that influence energy balance in humans may operate through multiple central and peripheral homeostatic pathways that influence caloric intake, expenditure, and/or storage. Energy balance is mediated through endocrine and neural signals coming from a variety of peripheral tissues to the central nervous

system. Afferent signals received in the hypothalamus modulate the release of peptides and generate efferent signals that regulate energy expenditure (through the sympathetic and parasympathetic nervous systems and thyroid hormones) and energy intake. Genes and proteins that play a role in common obesity may regulate appetite and satiety (e.g. cholecystokin, neuropeptide Y, melanocortins, leptin), insulin sensitivity and glucose metabolism in muscle and other peripheral tissues (e.g. insulin and insulin receptor), and energy storage and expenditure in adipose tissue (e.g. lipoprotein lipase) (Calle and Thun 2004).

Over 200 association studies have been conducted relating genetic variation in candidate genes to obesity phenotypes. These studies generally have observed small, uncertain, or inconsistent effects. Significant positive associations have been observed in five or more studies for about 15 genes, including common polymorphisms in the beta-adrenergic receptors (β-AR2, β-AR3), the peroxisome proliferator- activated receptor gamma (PPARγ), LEP, LEPR, uncoupling protein genes (UCP-1, UCP-2, and UCP-3), and tumor necrosis factor alpha (TNFα) (Chagnon et al. 2003).

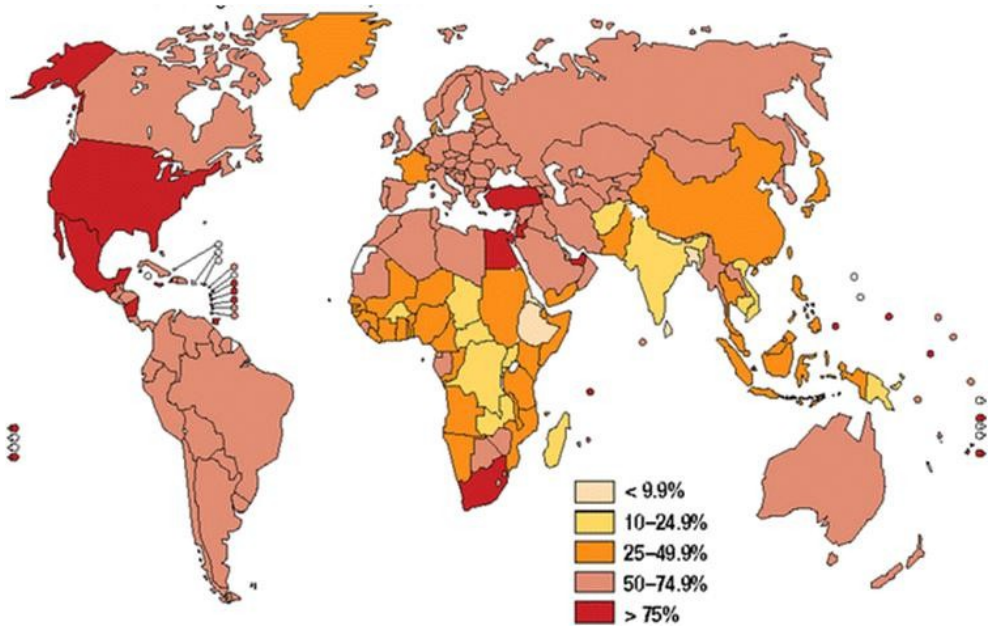

Fig. 1: Prevalence of overweight worldwide (BMI>25)

While single gene mutations rarely account for obesity in humans, it is likely that obesity is influenced by the interaction of multiple genes, each with modest effects, and further interactions with environmental factors such as energy availability, physical activity, and smoking (Calle and Thun 2004).

It should be noted that genetic and biologic determinants of obesity only become manifest in social environments that provide abundant calorie-dense foods and facilitate physical inactivity. Genetic factors predispose

individuals to gain weight. Only environmental factors cause sudden large shifts in the prevalence of obesity in populations. An obesogenic environment is probably the primary cause of the recent trends in obesity (Aranceta et al. 2009).

There is consistent evidence that obesity is associated with an increase in all cause mortality, and in the United States obesity is estimated to cause over 100,000 excess deaths annually. The mean loss of life years attributed to obesity is at least 2 years, and in young men this figure could be as high as 10–20 years. The effects of obesity are more marked in men, and there are racial differences, although obesity is associated with reduced life expectancy in all ethnic groups. The impact of obesity on mortality is less in subgroups where the competing causes of death are increased, such as the elderly and smokers (Moayyedi 2008).

There are a variety of diseases associated with obesity that contribute to excess mortality. Obesity has long been recognized to be an important cause of type II diabetes mellitus, hypertension, and dyslipidemia (National Task Force on the Prevention and Treatment of Obesity 2000). Cohort studies suggest more than a 10- to 20-fold increase in risk of developing diabetes in those with a BMI $\geq$35 kg/m^2 (Field et al. 2001). The adverse metabolic effects of excess body fat are known to accelerate atherogenesis and increase the risk of coronary heart disease, stroke, and early death. Obesity is also predictive of diseases that cause serious morbidity, such as osteoarthritis and sleep apnea, and is linked to an increase in hospital admissions (Calle and Thun 2004; Moayyedi 2008). There are also considerable psychosocial consequences of obesity (Ginter and Simko 2008).

Moreover, epidemiologic studies provide sufficient evidence that obesity is a risk factor for both cancer incidence and mortality (Pan and DesMeules 2009).

1.2 Epidemiologic studies of obesity and cancer

The available literature on weight and cancer has contributed to the knowledge that a PEB or obese status is related to elevated cancer risk (Malin et al. 2005). The association of overweight and obesity with noncancer outcomes is generally stronger than the association with all cancer or specific cancer sites (Calle and Thun 2004). Moreover, a meta-analysis suggested that, in Europe, 72,000 cancer cases each year could be attributed to an excess body mass (Bergström et al. 2001).

The International Agency for Research on Cancer (IARC) Working Group on the Evaluation of Cancer Preventive Strategies recently published a comprehensive evaluation of the available literature on weight and cancer that considered epidemiologic, clinical, and experimental data. Their report concluded that the avoidance of weight gain reduces the risk of developing

cancers of the colon, breast (in postmenopausal women), endometrium, kidney (renal cell), and esophagus (adenocarcinoma) (IARC 2002). These conclusions are based on epidemiologic studies of overweight and/or obese individuals compared to leaner individuals, not on studies of individuals who have lost weight. Unfortunately, few individuals lose and maintain significant amounts of weight, making it extremely difficult to examine cancer outcomes in large populations of weight losers. Consequently, the IARC report concluded that there is inadequate evidence in humans for a cancer-preventive effect of intentional weight loss for any cancer site. An association between overweight and obesity and cancer at many sites is consistent with animal studies showing that caloric restriction dramatically decreases spontaneous and carcinogen-induced tumor incidence, multiplicity, and size (Calle and Kaaks 2004).

Type of cancer	Relative risk[a] with BMI of 25–30 kg/m²	Relative risk[a] with BMI of ≥30 kg/m²	PAF (%) for US population[b]	PAF (%) for EU population[c]
Colorectal (men)	1.5	2.0	35.4	27.5
Colorectal (women)	1.2	1.5	20.8	14.2
Female breast (post-menopausal)	1.3	1.5	22.6	16.7
Endometrial	2.0	3.5	56.8	45.2
Kidney (renal cell)	1.5	2.5	42.5	31.1
Esophageal (adeno-carcinoma)	2.0	3.0	52.4	42.7
Pancreatic	1.3	1.7	26.9	19.3
Liver	ND	1.5–4.0	ND[d]	ND[d]
Gallbladder	1.5	2.0	35.5	27.1
Gastric cardia (adeno-carcinoma)	1.5	2.0	35.5	27.1

Tab 1: Obesity-related cancers
Relative risks (RRs) associated with overweight and obesity, and the percentage of cases attributable to overweight and obesity in the USA . *BMI* , body mass index; *ND* , not determined; *EU* , European Union; *PAF* , population attributable fraction.. b Data on prevalence of overweight and obesity are from the National Health and Nutrition Examination Survey (1999 – 2000) for men and women from the United States aged from 50 to 69 years. c Data on prevalence of overweight and obesity are from a range of sources of adult men and women residing in 15 European countries in the 1980s and 1990s. d PAFs were not estimated because the magnitude of the RRs across studies are not sufficiently consistent.

The literature on the relationship between body size and the colon and rectal cancers has demonstrated a positive association between risk of colorectal cancer and body fat distribution as indicated by BMI. Studies that

have examined association with obesity (BMI > 30.0 kg/m^2) found nearly twice the risk for colorectal cancer compared with those reporting association for overweight status or a BMI of over. The risk of colon cancer in men with a BMI > 30 increased up to 80%. Obesity has been consistently associated with higher risk of colorectal cancer in men (RRs, ~1.5 – 2.0) and women (RRs, ~1.2 – 1.5) in both case-control and cohort studies (Tab. 1).

Endometrial cancer (cancer of the uterine lining) was the first cancer to be recognized as being related to obesity. A linear increase in the risk of endometrial cancer with increasing weight or BMI has been observed in most studies ranging from twofold to fivefold in overweight and/or obese women (Tab. 1) (Fair and Montgomery 2009).

Studies of population worldwide have revealed that the risk of kidney cancer (specifically, renal-cell cancer) is 1.5-3 times higher in overweight and obese individuals than in normal weight men and women (Tab. 1). Most studies reported a dose- response relationship with increasing weight or BMI (Calle and Kaaks 2004).

Obesity is associated with a two- to threefold increase in risk for adenocarcinoma of the esophagus with stronger associations seen in nonsmokers (Tab. 1) (Hoyo and Gammon 2006).

There have been few previous studies of gall bladder cancer and obesity, and most have been relatively small (Tab. 1). Available studies have consistently found elevated risks for women (of about twofold), but generally have had too few cases to evaluate the association in men (Calle and Kaaks 2004).

Several recent studies have suggested that high body mass may be associated with approximately a doubling of risk for pancreatic cancer in men and women. However, smaller, earlier studies did not support an association and further research is needed (Berrington de Gonzalez et al. 2003).

Few studies have investigated the association of body mass with cancers of the liver, stomach, uterine cervix, and hematopoietic system. Three studies that have examined obesity and liver cancer found excess relative risk in both men and women in the range of 2.0–4.0. Importantly, obesity has been consistently shown to increase rates of breast cancer in postmenopausal women by 30 – 50% (Tab. 1) (Calle and Kaaks 2004).

1.3 Obesity and breast cancer

Breast cancer is the most commonly diagnosed cancer in the female population and is second in cancer related deaths in the United States. While the mortality has decreased slightly in recent years, the number of cases diagnosed annually has remained relatively steady. According to the American Cancer Society, over 178000 new cases are diagnosed each year, with an

estimated 40 400 deaths from breast cancer in 2008. Five year survival rates of breast cancer patients is almost 90%, although higher in patients over 40, as women diagnosed at a young age typically have amore aggressive cancer that is less responsive to treatment. Though both incidence rates and mortality rates have decreased in recent years, the healthcare costs and the emotional costs of breast cancer remain high (Jemal et al. 2008).

A number of risk factors are associated with development of breast cancer. The greatest risk factors are age and gender, with females developing breast cancer 100 times more frequently than males. As a woman ages, her risk of developing breast cancer increases, from 1 in 233 between the ages of 30–39 to 1 in 27 between the ages of 60–69. While age and gender are the greatest risk factors, there are also hormonal risk factors associated with breast cancer development, including age at first menarche, age at menopause, and lifetime exposure to estrogen. Furthermore, a family history of breast cancer and a history of previous benign breast disease are risk factors associated with breast cancer. Interestingly, some risk factors are modifiable, such as diet and obesity (Carter and Church 2009).

Many epidemiologic studies since the 1970s have assessed the association between anthropometric measures and breast cancer occurrence and/or prognosis (Stephenson and Rose 2003). Early studies established that the association between body size and risk of breast cancer differed according to menopausal status, and that heavier women were at increased risk of postmenopausal, but not premenopausal breast cancer. In fact, among premenopausal women, there is consistent evidence of a modest reduction in risk among women with high (≥28) BMI (IARC 2002).

Obesity has been shown consistently to increase rates of breast cancer in postmenopausal women by 30–50% (tab. 1). Some studies have found central adiposity to be an independent predictor of postmenopausal breast cancer risk beyond the risk attributed to overweight alone. In addition, adult weight gain has generally been associated with a larger increase in risk of postmenopausal breast cancer than has BMI, in studies that examined both (Calle and Thun 2004).

Studies of breast cancer mortality and survival among breast cancer cases illustrate that adiposity is associated both with poorer survival and increased likelihood of recurrence among those with the disease, regardless of menopausal status and after adjustment for stage and treatment. Very obese women (BMI ≥40.0) have breast cancer death rates that are three times higher than very lean (BMI ≤20.5) women. The greater risk of death among heavier women likely reflects both a true biological effect of adiposity on survival and delayed diagnosis in heavier women (Petrelli et al. 2002).

The mechanism behind the relationship of increased incidences of breast cancer in obese individuals is poorly understood; however, the literature concerning this association has increased in recent years (Carter and Church 2009).

The breast is a very heterogeneous tissue, composed of a number of different cell types. Epithelial cells make up the parenchyma of the tissue, forming the ducts and glands involved in milk production, storage, and secretion. Surrounding these epithelial cells is a network of fibroblasts, which generate the proteins of the breast connective tissue. Another key component of breast tissue is adipose, composed of mesenchymal precursor cells and the mature adipocytes (Crum et al. 2003).

The tumor microenvironment provides a number of signals and resources to the tumor cells, promoting proliferation, survival, and motility. In that regard, adipocytes, or their precursor cells, may provide key factors in breast tissue needed for tumor development, progression, or even enable tumor cell invasion. Collectively, these results imply that excess amounts of adipose in either the breast or other distant fat depots could provide a climate amenable to development of carcinoma of the breast (Carter and Church 2009).

1.4 Adipose tissue

Adipose tissue, commonly called 'fat', is a type of loose connective tissue comprised of lipid-filled cells (adipocytes) surrounded by a matrix of collagen fibers, blood vessels, fibroblasts and immune cells. In certain areas, for example, subcutaneous and mesentery regions, adipose tissue is organized into large lobular structures (Ahima and Flier 2000). Adipose tissue itself is composed of not only adipocytes but also by other cell types found in the stroma-vascular fraction, which include macrophages, fibroblasts, pericytes, blood cells, endothelial cells, and adipose precursor cells, among others (Fig. 2) (Frühbeck 2008).

White adipose tissue, the predominant type of adipose tissue in humans, is characterized by adipocytes with a single lipid inclusion and eccentrically located nucleus (Ahima and Flier 2000).

White adipose tissue has long been recognized as the main site of storage of excess energy derived from food intake. White adipocytes store dietary energy in a highly concentrated form as triglyceride, mostly in a single large lipid droplet. These structures are associated with a unique complement of proteins, which enable the sequestration or mobilization of lipids. In times of caloric need, these triglycerides can be rapidly hydrolysed by lipases (a process known as lipolysis) and the resulting fatty acids are transported to other tissues to be oxidized in mitochondria as an energy source. By contrast, brown fat is specialized primarily for non-shivering thermogenesis, a cold climate adaptation in many homeotherms. Brown adipocytes are characterized by multiple, smaller droplets of triglyceride, which are accessible for rapid hydrolysis and rapid oxidation of the fatty acids. Brown fat depots are present

in human infants and recent evidence suggests that dispersed brown adipocytes might persist in adults (Guilherme et al. 2008).

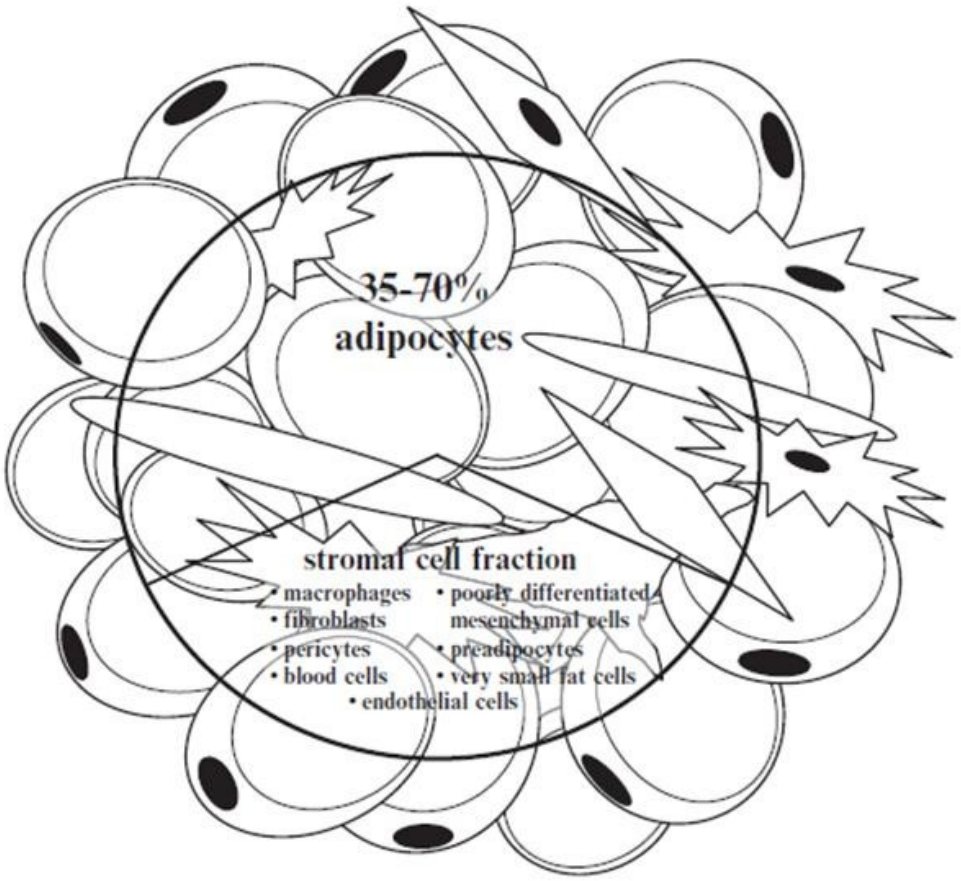

Fig. 2: Schematic representation of the multicellularity of adipose tissue with approximate quantitative contribution of adipocytes compared to the stromavascular fraction

White adipose tissue is actively involved in cell function regulation through a complex network of endocrine, paracrine, and autocrine signals that influence the response of many tissues, including the hypothalamus, pancreas, liver, skeletal muscle, kidneys, endothelium, and immune system, among others. Furthermore, adipocytes are uniquely equipped to participate in the regulation of other functions such as reproduction, immune response, blood pressure control, coagulation, fibrinolysis, and angiogenesis, among others (Fig. 3) (Schäffler 2006).

The identification of adipose tissue as a multifunctional organ has been brought about by the emerging body of evidence gathered during the last decades, which opposes the static view of adipose tissue as a merely passive organ devoted to the storage of excess energy in the form of fat. This pleiotropic nature is based on the ability of fat cells to secrete a large number

of hormones, growth factors, enzymes, cytokines, complement factors, and matrix proteins, collectively termed as adipokines or adipocytokines (Fig. 4), at the same time as expressing receptors for most of these factors, which warrants an extensive crosstalk at a local and systemic level in response to specific external stimuli or metabolic changes. The vast majority of adipocyte-derived factors have been shown to be dysregulated in the alterations accompanying adipose tissue mass changes (Frühbeck 2008).

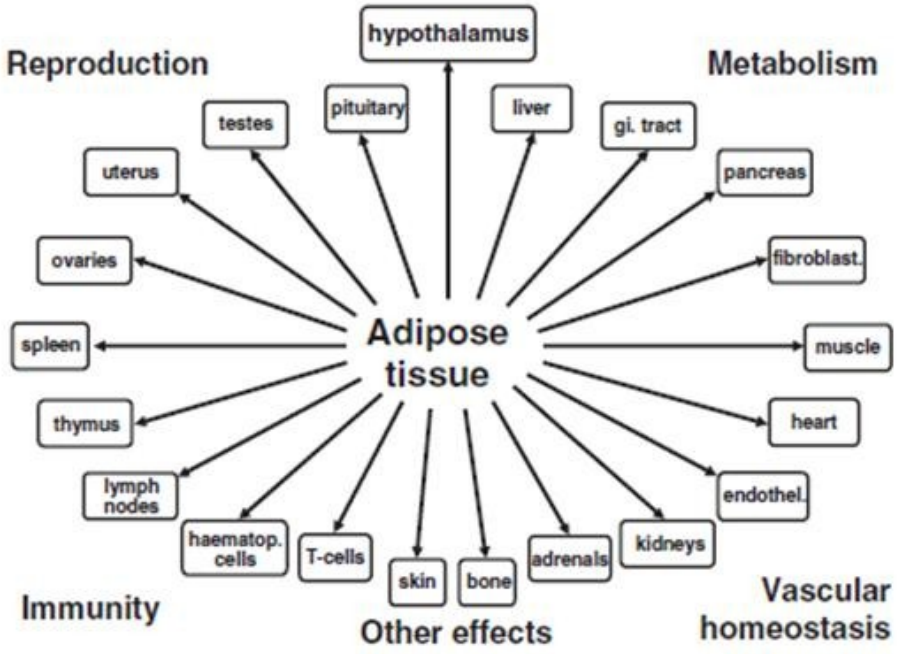

Fig. 3: Dynamic view of white adipose tissue based on the pleiotropic effects exerted on quite diverse organs and their respective physiological functions

It is now evident that adipose tissue is the source of production of a multiplicity of secretory factors, which vary considerably in terms of structure, function, and cellular origin. For instance, classical cytokines include TNF-α and interleukin-1, 6, 10, and 18 (IL-1, IL-6, IL-10, IL-18), whereas monocyte chemoattractant protein-1 (MCP-1), macrophage migration inhibitory factor (MIF), and IL-8 belong more to the subgroup of chemokines. The diversity of secreted molecules includes also factors involved in lipid and glucose metabolism such as lipoprotein lipase (LPL), apolipoprotein E (apoE), cholesteryl ester transfer protein, PPAR, glucocorticoids, sex steroids, prostaglandins, adipsin, acylation stimulating protein, leptin, resistin, adiponectin/Acrp30/adipoQ, osteonectin, and cathepsins, among others. Finally, secreted growth factors include insulin-like growth factor 1 (IGF1), nerve growth factor (NGF), macrophage colony-stimulating factor, transforming growth factor-β (TGF-β), vascular endothelial growth factor (VEGF), heparin-binding epidermal growth factor, leukemia inhibitory factor, and bone morphogenetic proteins (Fruhbeck 2008).

The adipocyte is therefore an excellent candidate cell to play an important role in influencing tumor behavior through heterotypic signaling processes and may prove to be critical for tumor survival, growth, and metastasis in the breast. However, it is not known how adipocytes influence breast tumor cell behavior or whether any of the paracrine factors secreted by adipocytes cause changes in the phenotypic behavior of the malignant cells (Iyengar et al. 2003).

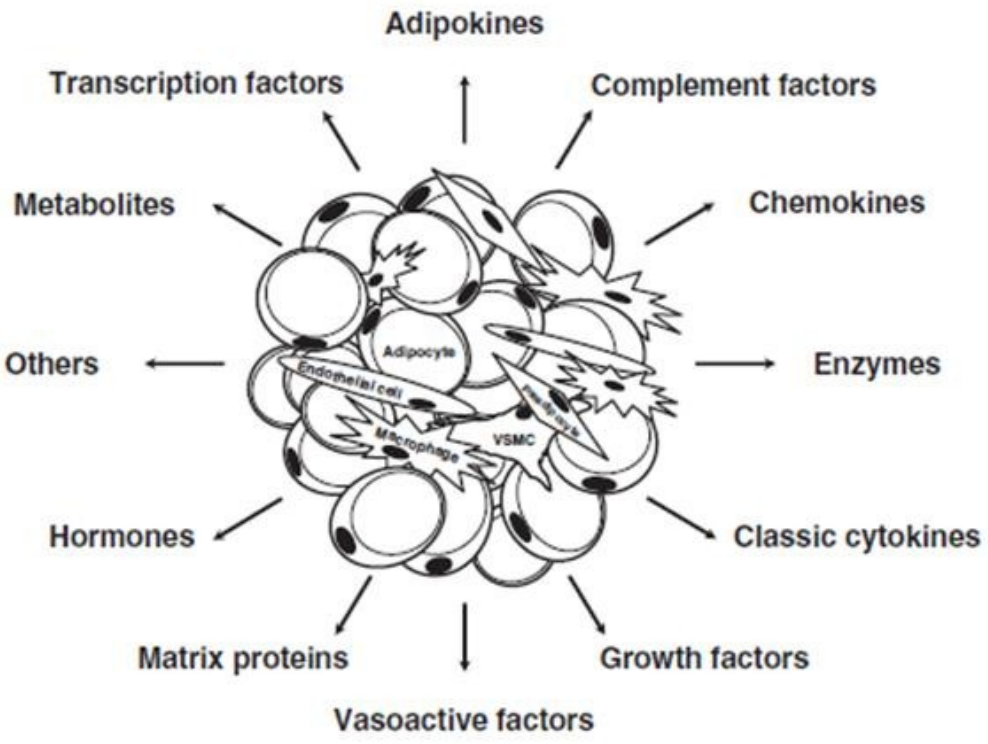

Fig. 4: Diagram of the multiple adipose-derived factors

1.5 Proposed mechanisms relating adiposity to cancer risk

The biological mechanisms that link overweight and obesity to many forms of cancer are poorly understood. Obesity-associated changes in hormone metabolism (insulin, insulin-like growth factor1, sex steroids), in adipocyte-released factors and in inflammatory response may contribute to tumorigenesis, tumor progression and metastatic potential (Calle and Kaaks 2004, Harvie and Howell 2006).

- ***Endogenous hormones: Insulin, IGF1 and sex steroids***

The association between excess body weight with cancer risk may be explained by alterations in the metabolism of endogenous hormones –

including insulin, insulin-like growth factors and sex steroids – which can lead to distortion of the normal balance between cell proliferation, differentiation, and apoptosis. However, the pathophysiological and biological mechanisms underpinning these associations are only starting to be understood (Osório-Costa et al. 2009).

Excess body weight, increased plasma triglyceride levels, low levels of physical activity and certain dietary patterns can all favor elevated circulating insulin levels. In the early 1990's, McKeown-Eyssen (1994) and Giovannucci (1995) noted that the risk factors for Westernized cancer were remarkably similar to those for insulin resistance, and suggested that hyperinsulinemia might contribute to cancer development through the growth-promoting effect of elevated levels of insulin. In addition to its importance in glucose homeostasis, it is well established that insulin is a crucial hormone in anabolic processes involved in early growth and development, and may be also a strong mediator of the adverse effect of obesity on cancer prognosis (Osório-Costa et al. 2009).

Chronically increased insulin levels have been associated with colon cancer pathogenesis and with cancers of the breast, pancreas and endometrium. These tumorigenic effects of insulin could be directly mediated by insulin receptors in the (pre) neoplastic target cells, or might be due to related changes in endogenous hormone metabolism, secondary to hyperinsulinemia. For example, insulin has effect on the synthesis and biological availability of insulin-like growth factor 1 and sex hormones including androgens, progesterone and oestrogens (Calle and Kaaks 2004).

The IGF1 is a peptide hormone with a molecular structure very similar to that of insulin. The principal stimulus for the synthesis of IGF1 in liver, which is the source of over 80% of circulating IGF1, is provided by Growth Hormone (GH). Nutritional energy balance can have profound effects on its synthesis and biological activity (Pollak et al. 2004; Kaaks and Lukanova 2001).

IGF1 plays an important role in regulating cell proliferation, differentiation, apoptosis, and transformation.

IGF1 exert its actions by interacting with a specific receptor on the cell membrane, namely, the IGF1 receptor (IGF-1R), and the interaction is regulated by a group of specific binding proteins (IGFBP) (Yu and Rohan 2000). At least 75% of IGF1 in the circulation is bound to IGFBP3, whereas most of the remainder is bound to at least five additional binding proteins (IGFBP1, IGFBP2, IGFBP4, IGFBP5 and IGFBP6). The IGFBPs have many functions, including the stabilization of a large pool of IGF1 in the circulation and the regulation of the availability of IGF1 for binding to its receptor (Clemmons 1998), in particular, IGFBP-1 is considered the chief acute regulator of IGF1 bioactivity (Harvie and Howell 2006).

Recently, a number of epidemiologic studies have shown consistently that high circulating levels of IGF1, are associated with increased risk for several common cancers, including those of the breast, prostate, lung, and colorectum (LeRoith and Helman 2004). These findings were confirmed in animal models,

where reduced circulating IGF1 levels result in significant reductions in cancer development, growth, and metastases, whereas increased circulating IGF1 levels are associated with enhanced tumor growth (Wu et al. 2003).

Aberrant expression of the IGF-1R has been implicated in malignant transformation of cells. IGF-1R is normally activated by binding of the secreted growth factor ligand to the extracellular domain. This, in turn, triggers a number of cellular signalling pathways, including the phosphatidylinositol 3-kinase (PI3K) pathway, the main mechanism by which IGF-1R protects cells from apoptosis (Alberobello et al.).

There are also several lines of evidence that dysregulation of the IGF1 system is involved in resistance to certain anticancer therapies, including cytotoxic chemotherapy, hormonal agents, biological therapies, and radiation (Ryan and Goss 2008).

Finally, it has been shown that the level of IGFBP3, a major IGF1-binding protein in serum that, in most situations, suppresses the mitogenic action of IGF1, is inversely associated with the risk of these cancer (Yu and Rohan 2000).

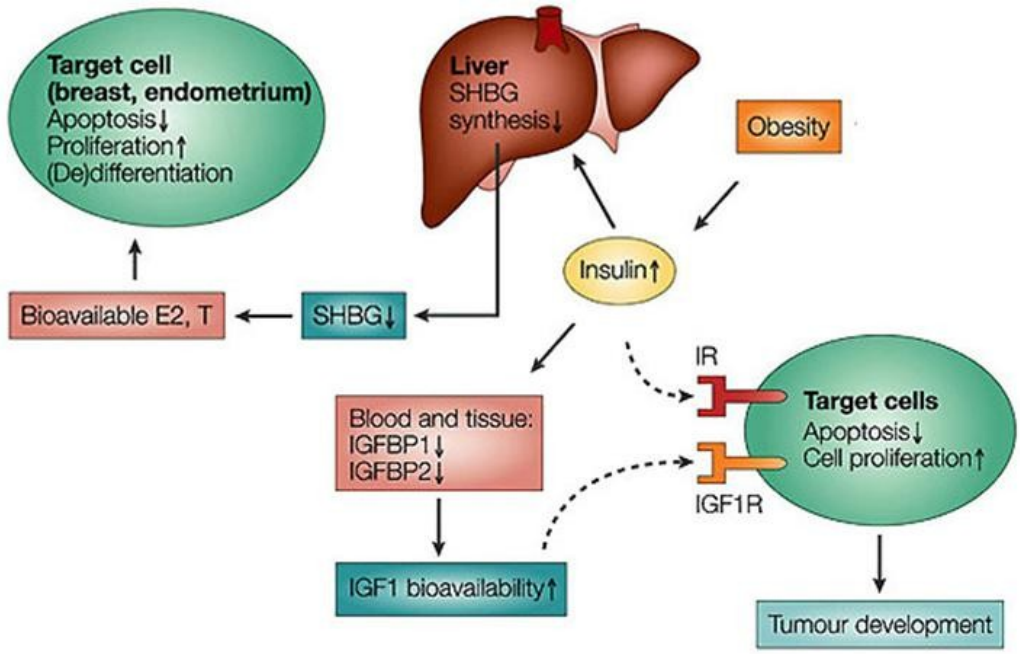

Fig. 5: Effect of obesity on growth factor and hormone production.
Obesity leads to hyperinsulinemia, which in turn causes a reduction in IGFBP and SHBP synthesis. This results in increased levels of bioavailable IGF1, E2 and T. Insulin and IGF1 signal through the insulin receptors (IRs) and IGF1 receptor (IGF1R), respectively, to promote cellular proliferation and inhibit apoptosis in many tissue types. E2 and T can diffuse to target cells, where they bind to oestrogen and androgen receptors. The effects of sex steroids binding their receptors can vary, depending on the tissue types, but in some tissues (for example, breast epithelium and endometrium) they promote cellular proliferation and inhibit apoptosis. Adapted from Calle and Kaaks (2004).

Chronically increased insulin concentrations lead to reduced liver synthesis and blood levels of IGFBP1, and probably also reduce IGFBP1 synthesis locally in other tissues. Increased fasting levels of insulin in the plasma are generally also associated with reduced levels of IGFBP2 in the blood. This results in increased levels of free bioavailable IGF1 and concomitant changes in the cellular environment, that favor tumor development (Fig. 5). It is also suggested that IGF1 can synergize with other growth factors to produce enhanced mitogenic effects, and may operate via an endocrine, paracrine or autocrine manner to regulate cell growth, cell survival, cell transformation, and cell differentiation (Calle and Kaaks 2004; Osório-Costa et al. 2009).

With regard to sex steroids, adiposity influences the synthesis and bioavailability of the hormones — the oestrogens, the androgens and progesterone — through at least three mechanisms. First, adipose tissue expresses a variety of sex-steroid-metabolizing enzymes, like aromatase, that promote the formation of estrogens from androgenic precursors, which are secreted by the gonads or adrenal glands. Adipose tissue is the major site of estrogen synthesis in men and postmenopausal women, with levels of aromatase and circulating levels of estrone and estradiol strongly related to BMI. A second hypothesis is that obesity results in an increase in circulating levels of insulin and IGF1 bioactivity. Insulin and IGF1 both inhibit the synthesis of sex hormone-binding globulin (SHBG) – the major carrier protein for testosterone and estradiol in the plasma – and may lead to an increase in the amount of unbound sex-steroid available for bioactivity (Fig. 5). In women, decreases in SHBG generally also lead to increased levels of bioavailable testosterone. In men, by contrast, decreases in SHBG generally lead to reductions in total testicular testosterone production, and no increase in bioavailable testosterone. The combined effect of increased formation of oestrone and testosterone, along with reduced levels of SHBG, leads to an increase in the bioavailable fractions of E2 and T that can diffuse to target cells, where they bind to oestrogen and androgen receptors. The effects of sex steroids binding their receptors can vary, depending on the tissue types, but in some tissues (for example, breast epithelium and endometrium) they promote cellular proliferation and inhibit apoptosis. Finally, high insulin levels can increase ovarian, and possibly also adrenal, androgen synthesis, and can cause the development of the polycystic ovary syndrome in some genetically susceptible pre-menopausal women (Calle and Kaaks 2004).

- ***Adipocyte released factors: adipokines and inflammatory cytokines***

Current epidemiologic and experimental studies of the obesity-cancer association focus on the role of increased adipose tissue, particularly the increase in circulating adipocyte-derived factors (adipokines).

Multiple factors from adipose tissue, such as leptin, adiponectin, cytokines, and other secreted products, including growth factors, hormone-like

molecules, acute phase reactants, complement-related proteins, and extracellular matrix proteins, influence processes involved in carcinogenesis. In addition, reduction of adiposity by calorie restriction or physical activity suppresses tumor development and lowers circulating levels of many adipokines, further implicating them in tumor development. (Nunez et al. 2006; Iyengar et al. 2003).

Adipocytokines were shown to participate to some extent in the process of carcinogenesis, however most if not all of these positive data come from *in vitro* studies on cancer cell lines.

Leptin, the most widely studied member of a family, is a multifunctional neuroendocrine protein with wide ranging biological activities including appetite regulation, bone formation and reproductive function and angiogenesis. It stimulates growth, migration and invasion of cancer cells *in vitro* and also potentiates angiogenesis, thus displaying a capacity for promoting malignant biological behavior of cancer *in vitro* (Housa et al. 2006; Rose et al. 2004).

Adiponectin is one of the most studied adipokines with a high expression level in adipose cells and with high concentrations in serum. It is exclusively secreted by the adipose cells and exerts many different effects in obesity-related disorders. Much remains to be learnt about its physiological functions, but evidence is accumulating for a role in the inhibition of inflammatory processes, modulation of endothelial function, and protection against the consequences of the insulin resistance syndrome. Also, in contrast to other adipocytokines, adiponectin has been reported to suppress angiogenesis by a process which involves activation of members of the caspase group of apoptotic enzymes (Andersson et al. 2008; Rose et al. 2004). Although there have been no studies of the effect of adiponectin on proliferation of normal breast or breast cancer cells, a recent *in vitro* study showed adiponectin to be a potent inhibitor of endothelial cell proliferation and primary tumour growth of a sarcoma mouse model via inhibition of angiogenesis. Two medium-sized case–control studies demonstrated significant inverse associations between circulating adiponectin and breast cancer (Harvie and Howell 2006).

VEGF, HGF and IGF1 are not usually found on a list of the adipocytokines, but they are produced by adipose cells, where they have important functions.

VEGF has a critical role in the angiogenic process, being a specific mitogen for vascular endothelial cells; it also promotes angiogenesis by inducing matrix metalloproteinase (MMP) expression, and stimulating vascular endothelial cell migration .

Like VEGF, HGF stimulates vascular endothelial cell proliferation and migration *in vitro*, induces MMP expression, and stimulates angiogenesis in *in vivo* models (Rose et al. 2004). Several investigations have shown that the serum concentrations of HGF are often elevated in breast cancer patients, and particularly so in those with advanced disease (Vona-Davis and Rose 2007).

Until now, the role of IGF1 signaling in white adipose tissue has remained unclear. *In vitro* IGF1 is an essential regulator of differentiation, and it was recently shown that IGF-1 stimulates both cell growth and lipogenesis during differentiation of human mesenchymal stem cells into adipocytes *in vitro*. However, the physiological role of IGF1 signaling in adipose tissue *in vivo* has not been systematically studied (Klöting et al. 2008).

Inflammation has also been implicated in obesity and tumorigenesis, it is thought to underlie some of the cancer effects of excess adiposity (Nunez et al. 2006; Harvie and Howell 2006). Inflammation has been linked to risk of breast and other obesity related cancers such as colorectal cancer (Harvie and Howell 2006). Indeed, the consistent results from epidemiologic studies linking adiposity and the risk of several adult cancers turns plausible the hypothesis that the molecular mechanisms of carcinogenesis may be mediated by inflammatory pathways (Osório-Costa et al. 2009), however the mechanism by which it happens is not yet known.

Adipose tissue produces and secretes a lot of inflammatory cytokines, for example TNFα and IL-6. Cytokine expression and plasma levels increase in proportion to adiposity and as a result of changes in energy balance. An increasing number of immune mediators produced from adipocytes found in adipose tissues are being identified (Fair and Montgomery 2009).

TNFα is a pro-inflammatory cytokine which can inhibit tumour cell proliferation and promote cellular apoptosis, but also stimulates oestrogen biosynthesis by way of aromatase induction, and angiogenesis. Under physiological conditions, TNFα is produced in adipose tissue in relatively large quantities. However, the TNFα derived from adipose tissue originates only in part from the adipocytes; a considerable portion may be secreted by infiltrating macrophages, and particularly so in obesity (Rose et al. 2004). In obese adipose tissue, infact, there is macrophage recruitment, which, in turn, results in a pro-inflammatory state. Macrophages that are infiltrated in other tissues are known to secrete large amount of TNF, leading to a chronic inflammatory state with impaired triglyceride deposition and increased lipolysis, the excess of circulating triglyceride and free fatty acids results in disruption of normal metabolic functions such as mitochondrial oxidative phosphorylation and insulin-stimulated glucose transport (Osório-Costa et al. 2009). TNFα has been reported to stimulate angiogenesis in *in vivo* models.

Also the other main pro-inflammatory cytokine, IL-6, has activities related to insulin resistance, angiogenesis, and tumour cell biology. Like leptin and TNFα, IL-6 can stimulate oestrogen biosynthesis by the induction of aromatase activity. Human adipocytes secrete sizeable amounts of IL-6. *In vitro*, IL-6 stimulated invasion of a metastatic human breast cancer cell line, and in breast cancer patients elevated serum IL-6 levels were associated with aggressively metastatic disease (Rose et al. 2004).

2. AIM OF THE STUDY

Since the 1980's, the world has been living a striking increase in the prevalence of overweight and obesity. This phenomenon has had its beginning in developed countries, but, nowadays, it is also common to many other populous regions over the world, as Asia and Latin America, and it is becoming a Public Health concern (Osório-Costa et al. 2009). Since obesity has long been recognized as an important cause of diabetes and cardiovascular diseases, the relationship between obesity and different types of cancer has received less attention than its cardiovascular effects. Results from epidemiological studies that largely began in the 1970s indicate that adiposity contributes to the increased incidence and/or death from cancers of the colon, breast (in postmenopausal women), endometrium, kidney (renal cell), oesophagus (adenocarcinoma), gastric cardia, pancreas, gallbladder and liver, and possibly other cancers. It has been estimated hat 15–20% of all cancer deaths in the United States can be attributed to overweight and obesity. As the worldwide obesity epidemic has shown no signs of abating, insight into the mechanisms by which obesity contributes to tumour formation and progression is urgently needed, as are new approaches to intervene in this process (Calle and Kaaks 2004)

Current epidemiologic and experimental studies of the obesity-cancer association focus on the role of increased adipose tissue, particularly the increase in circulating adipocyte-derived factors (Nunez et al. 2006).

Adipocyte represents one of the most abundant cell types surrounding cancer cells and could influence several aspects of tumorigenesis, from promoting local invasion to angiogenesis and metastasis to distant sites that are fat enriched (such as the bone marrow). In fact, adipose tissue expresses and secretes a variety of adipokines and proinflammatory cytokines, but also extracellular matrix proteins, complement and coagulant-related proteins, acute phase reactants, tissue factors and different growth factors such as vascular endothelial growth factor (VEGF), hepatocyte growth factor (HGF) and insulin-like growth factor 1 (IGF1) (Iyengar et al. 2003, Klöting et al. 2008; Ahima and Flier 2000). All of these factors may be envisioned as contributing factors for cancer onset and/or progression (Feldmann 2008). In addition, reduction of adiposity by calorie restriction or physical activity suppresses tumor development and lowers circulating levels of many adipokines, further implicating them in tumor development (Nunez et al. 2006).

The aim of this study is to identify the molecular mechanisms by which adipocytes control breast cancer cells growth. Indeed, adipose tissue is a highly relevant component of the mammary gland and may influence the function of mammary epithelial cells (Hovey et al. 1999). In particular, the work aims to demonstrate that metabolic perturbations affect the production/secretion of adipocyte factors (adipokines, inflammatory cytokines and growth factors) potentially involved in cancer cell growth control.

3. MATERIALS AND METHODS

3.1 Cell culture

The MCF-7 human breast cancer cells and 3T3-L1 murine fibroblast cells were available in host laboratory. They were grown in Dulbecco's modified Eagle's medium (DMEM) supplemented with 10% fetal bovine serum (FBS), 100 IU/ml penicillin, 100 IU/ml streptomycin, and 2% L-glutamine in a 5% humidified CO_2 incubator. 3T3-L1 cells were differentiated as previously described (Engelman et al. 1998). In brief, after 2 days from confluence (Day 0), the DMEM 10% FBS was changed and new DMEM 10% FBS was added to the cells with the addition of 160 nm insulin, 250 nm dexamethasone, and 0.5mm 3-isobutyl-1-methylxanthine. After 2 days (Day 2), this medium was replaced with fresh DMEM 10% FBS containing only 160 nm insulin. After another 2 days, the cells were then propagated in only 10% FBS medium. Adipogenesis was scored by analysis of the expression of adipocyte-specific genes (aP2 and peroxisome proliferator-activated receptor γ (PPARγ)) (Chavey et al. 2003) and by lipid accumulation using microscopic analysis or oil red O staining (Ramirez-Zacarias et al. 1992). Human adipose tissue was digested with collagenase as previously reported (Rotter et al. 2003) and incubated in Minimum Essential Medium (MEM) supplemented with 1% human albumin.

3.2 Conditioned media system

The conditioned media was isolated in the following way: confluent 3T3-L1 adipocyte or 3T3-L1 fibroblast plates were identified, the 10% FBS removed, the plates washed two times with sterile phosphate-buffered saline (PBS), and 3–5 ml of serum-free DMEM 0,25%BSA (DMEM-BSA) added to the plates and incubated for approximately 8h. After the incubation, the DMEM-BSA was collected and centrifuged at 14000xg to remove cellular debris. The centrifuged conditioned media was then placed on MCF-7 cells for variable periods of time as indicated in the respective experiments. Often, to prevent the treated MCF-7 cells from becoming sick due to harmful metabolites that may have leached into the DME-BSA, low levels of serum (0.1% FBS) were added to the conditioned media (protective agent). This small amount of serum was added across all samples.

3.3 Cell proliferation assay

MCF-7 cells were seeded in 6-well culture plates at a concentration of $1 \cdot 10^5$ cells/well in a complete medium. The following day, the cells were refed with serum-free DMEM 0,25%BSA for 16h in an atmosphere of 5% CO_2. Then, the cells were incubate with conditioned media for different times, trypsinized and centrifuged, and cell pellets were resuspended in PBS. Cell count was performed by Bürker chamber. Three replicate wells were used for each data point, and the experiment was performed three times.

3.4 Flow cytometry

Cells were fixed with ethanol and routinely kept at -20°C overnight. For analysis, cells were centrifuged, resuspended in PBS containing 0.1mg/ml RNaseA and 40 μg/ml propidium iodide and incubated in dark for 30 min at room temperature. Samples were kept on ice and the analysis was performed using FACS Cyan cytometer (Dako Cytomation, USA). A minimum of 30000 events were collected for each sample. Sub-G1 phase cells were identified using Summit V 4.3 software (Dako).

3.5 Western Blot analysis

MCF7 were lysed in lysis buffer (50mM HEPES pH 7.6, 150mM NaCl, 10mM EDTA, 10mM $Na_4P_2O_7$, 2mM Na_3VO_4, 100mM NaF, 10% glycerol, 1mM PMSF, 100 IU/ml aprotinin, 20μM leupetin, 1% Triton X-100), for 2 h at 4 °C and lysates were centrifuged at 14,000 x g for 15 minutes to remove cellular debris. Cell lysates were separated by sodium dodecyl sulfate-polyacrylamide gel electrophoresis (SDS-PAGE) and analyzed by western blot as previously described (Laemmli 1970). Nitrocellulose membranes were probed with antibodies to phospho-Ser^{473}Akt/PKB, phospho-Thr^{202}/Tyr^{204} ERK and actin (CELL-SIGNALING Techology). Immunoreactive bands were detected by enhanced chemiluminescence according to the manufacturer's instructions (GE Healthcare, NJ).

3.6 Bioplex Cytokine and Growth Factor Assay

Supernatants were collected after 12 h of plating the different cells. Concentrations of IL-1a, IL-1b, IL-2, IL-3, IL-4, IL-5, IL-6, IL-9, IL-10, IL-

12 (p40), IL-12(p70), IL-13, IL-17, Eotaxin, G-CSF, GM-CSF, IFN-γ, KC, MCP-1, MIP-1α, MIP-1β, RANTES, TNF-α, PDGF, VEGF and IGF1 were determined using the Bioplex multiplex Mouse Cytokine and Growth factor assay kits (Bio-Rad, Hercules, CA) according to the manufacturer's protocol. Briefly, 50 µl of the culture supernatant or cytokine standard was plated in a 96 well filter plate coated with a multiplex of beads coupled to antibodies against the above mentioned cytokines and incubated for 30 min on a platform shaker at 300 rpm at RT. After a series of washes to remove the unbound proteins, a mixture of biotinylated detection antibodies, each specific for a different epitope was added to the reaction resulting in the formation of antibodies assimilated around the target proteins. Streptavidin-phycoerythrin (streptavidin-PE) was then added to bind to the biotinylated detection antibodies on the bead surface. The data from the reaction were then collected and analyzed by using the Bio-Plex suspension array system (or Luminex 100 system) from Bio-Rad Laboratories (Hercules, CA).

3.7 Real-time PCR

Total RNA was isolated from 3T3 L1 pre-adipocytes and adipocytes by using the Rneasy Kit (Qiagen Sciences) according to the manufacturer's instruction. For real-time RT-PCR analysis, 1 µg cell RNA was reverse transcribed using SuperScript II Reverse Transcriptase (Invitrogen). PCR were analyzed using SYBR Green mix (Invitrogen). Reactions were performed using Platinum SYBR Green Quantitative PCR Super-UDG using an iCycler IQ multicolour Real-Time PCR Detection System (Biorad Hercules, CA). All reactions were performed in triplicate and GAPDH was used as an internal standards. Primer sequences used were as follows: IGF1 forward primer 5'-TGG ATG CTC TTC AGT TCG TG -3', reverse primer 5'- TTT TGT AGG CTT CAG TGG GG -3'.

3. RESULTS AND DISCUSSION

4.1 Evaluation of the effect of the adipocyte conditioned media on breast cancer cell growth.

The adipocyte represents one of the most abundant cell types surrounding cancer cells and could influence several aspects of tumorigenesis, from promoting local invasion to angiogenesis and metastasis to distant sites that are fat enriched (Iyengar et al. 2003). However, it is not known how adipocytes influence breast tumor cell behaviour or whether any of the paracrine factors secreted by adipocytes cause changes in the malignant phenotype.

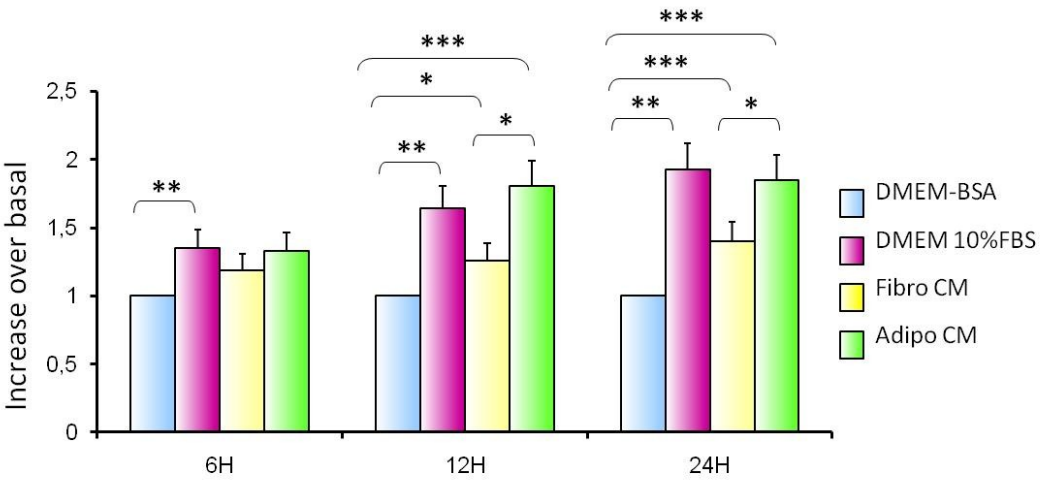

Fig. 6: Effect of adipocyte conditioned media on MCF7 cell growth. Undifferentiated 3T3-L1 cells or mature 3T3-L1 adipocytes have been incubated with serum-free DMEM for 8h. Media have been collected (respectively Fibro CM, yellow bar, and Adipo CM, green bar) and added to serum-starved MCF-7 breast cancer cells for 6, 12 and 24 h, as indicated. As a control, MCF7 cells have also been incubated with DMEM without serum supplementation (DMEM-BSA, blue bar) or with 10% fetal bovine serum (DMEM 10%FBS, purple bar). Then, cells have been counted and the results reported as fold-increase over basal (cell count in DMEM-BSA). Asterisks denote statistically significant values (* $p<0.05$; ** $p<0.01$; *** $p<0.005$).

I studied whether adipocyte-derived factors may affect the growth of breast cancer cells. For these studies 3T3-L1 cells, an established model of differentiating adipocytes, and MCF-7, a well studied breast cancer cell line were chosen. In conditioned media ('CM') assay, 3T3-L1 fibroblasts and adipocytes were allowed to secrete factors into serum-free medium ('DMEM-BSA'). After 8h, medium was collected and applied to MCF-7 cells for 6, 12 and 24h (respectively 'Fibro CM' and 'Adipo CM'). As control, MCF-7 cells were incubated for the same time in the presence of DMEM-BSA (negative control), or in presence of DMEM 10% FBS (standard growth conditions for MCF-7 cells), as positive control. MCF-7 cells were subsequently trypsinized and counted. As shown in fig. 6 conditioned media obtained from 3T3-L1 cells

induced growth of MCF-7 cells, in a time-dependent manner. Breast cancer cell growth reached levels similar to those observed for cells incubated with DMEM 10%FBS. Interestingly, however, conditioned media from fully differentiated adipocytes (green bar) are significantly more effective than conditioned media from pre-adipocytes (yellow bar) in inducing MCF-7 growth.

In order to address whether these changes are due to reduced cell death or to increased proliferation, I performed cytofluorimetric determinations of cell cycle phases.

To this aim MCF-7 cells were exposed to serum-free media for 16h and then incubated with 'Fibro CM' or 'Adipo CM' for 12h. The induction of apoptosis/necrosis was analyzed by a spectrum of flow cytometric assays. The phases of the cell cycle and the occurrence of a sub-G_1 peak were determined with propidium iodide staining.

The MCF-7 cells exposed to DMEM 10%FBS displayed a normal distribution among the phases of cell cycle while, serum-free media treatment (DMEM-BSA) induced significant accumulation of cells in the G_0/G_1 phase that is indicative of cell death. Interestingly, the incubation with conditioned media protected cells from serum starvation-induced cell death and 'Adipo-CM' was more effective than 'Fibro-CM' (Fig. 7).

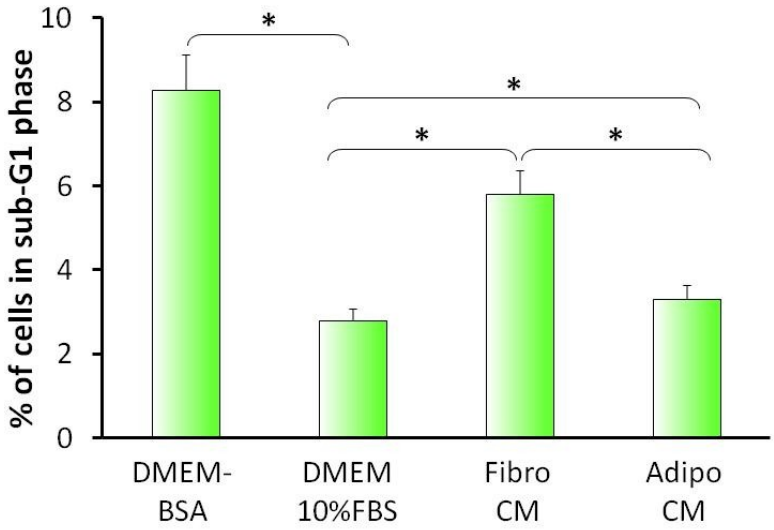

Fig. 7: Effect of conditioned media on MCF-7 apoptosis/necrosis. MCF-7 cells were starved for 16h and incubated with conditioned media from fibroblast (Fibro CM) or adipocyte (Adipo CM) for 12h. MCF-7 cells were treated with propidium iodide staining and ratio of sub-G1 phase was analyzed by flow cytometric assays (* $p<0.05$).

It has been clearly demonstrated that several growth factors, including IGF1, promote cell proliferation and protect cells from apoptosis activating MAPK and PI3K pathways (Robbins and Cotran 2004).

I therefore hypothesized that Adipo CM could contain growth factors able to activate these transduction pathways. AKT and ERK are the main proteins downstream PI3K and MAPK signaling respectively. AKT is activated by phosphorylation at Ser^{473},while ERK is activated when is phosphorylated on Thr^{202}/Tyr^{204}.

I evaluated AKT and ERK phosphorylation in MCF-7 cells upon Adipo CM treatment using phospho-specific antibodies.

MCF-7 cells have been treated with Adipo CM for 10 min and 12h or with 100 ng/ml IGF1 as positive control. As shown in fig. 8, Adipo CM rapidly induced the phosphorylation of ERK on Thr^{202}/Tyr^{204} and of AKT on Ser^{473} after 10 min of treatment. However, after 12h ERK phosphorylation was reduced while AKT phosphorylation was preserved.

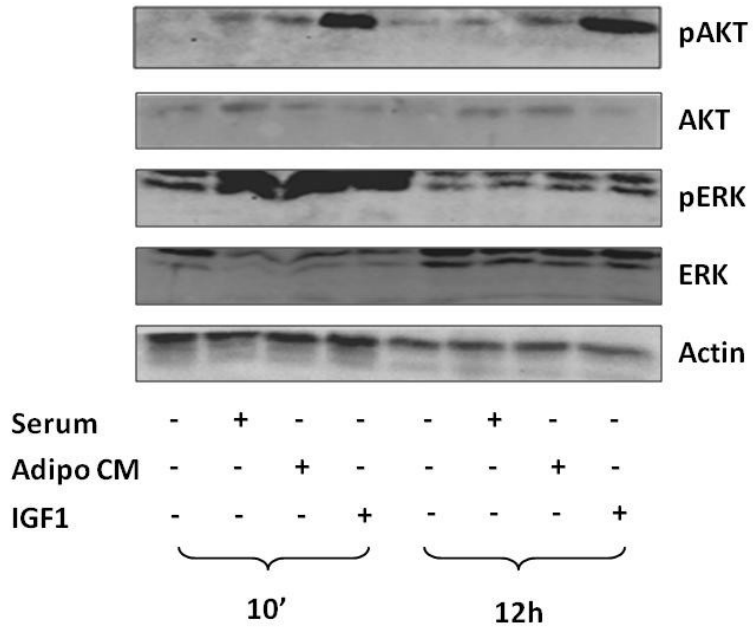

Fig. 8: Effect of Adipo CM on PI3K and MAPK signaling. MCF-7 cells were starved for 16 h and stimulated with Adipocyte conditioned media (Adipo CM) or with 100ng/ml IGF-1 for the indicated times. Then the cells were solubilysed as described in Materials and Methods. Cell lysates were blotted with specific anti-phospho-Serine473–Akt/PKB antibody (pAkt) and anti-phospho-Threonine202/Tyrosine204-ERK antibody (pERK).and then reblotted with anti-Akt/PKB and ERK antibodies. To ensure the equal protein transfer, membranes were blotted with actin antibodies

Next, I have investigated whether human adipocytes were as effective as murine cell lines. To this end I have isolated adipocytes by surgical specimens. I have incubated whole adipose tissue and isolated adipocytes in a specific culture media and, after 4h, I have collected the conditioned media and placed them onto MCF-7 for 8 and 24h. MCF-7 cells were subsequently trypsinized and counted. As shown in fig. 9, conditioned media from both whole adipose tissue and isolated adipocytes induced growth of MCF-7 cells.

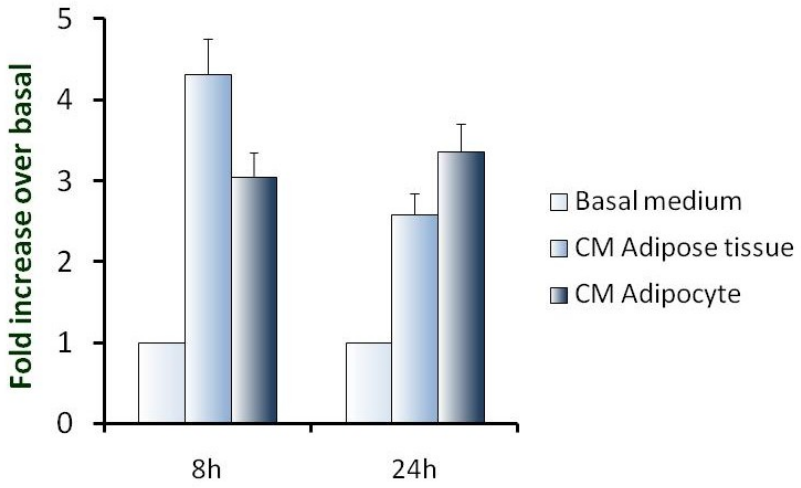

Fig. 9: Effect of humane adipocyte conditioned media on MCF-7 cell growth. 300mg of adipose tissue or of isolated adipocytes have been incubated with basal medium for 4h. Media have been collected and added to serum-starved MCF-7 breast cancer cells for 8 and 24 h, as indicated. As a control, MCF-7 cells have also been incubated with basal medium. Then, cells have been counted and the results reported as fold-increase over basal (cell count in basal medium).

4.2 Evaluation of the effect of insulin and glucose on adipocyte ability to promote breast cancer cell growth.

Metabolic disorders are strongly associated with obesity and an increased risk for several types of cancer. Therefore, I examined whether perturbations of the metabolic environment may affect the growth-promoting properties of adipocytes. To this end 3T3-L1 cells were incubated in the presence of low concentrations of glucose, prior to measure the ability of their conditioned media to induce growth of cancer cells. In detail, 3T3-L1 adipocytes were cultured either in regular medium (containing 25,5 mM glucose) or in low-glucose medium (5,5 mM glucose) for 24h, than the medium was changed and the cells were allowed to secrete factors into serum-free medium ('DMEM-BSA'). After 8h, medium was collected and applied to MCF-7 cells for 6, 12 and 24h. As control, MCF-7 cells were incubated for the same time in the presence of DMEM-BSA (negative control), or in presence of DMEM 10% FBS, as positive control. MCF-7 cells were subsequently trypsinized and counted. As shown in fig. 10, the treatment of adipocytes with low glucose (fig. 10a, orange bar) impairs their ability to induce growth of MCF-7 cells.

Similarly, when 3T3-L1 adipocytes were treated with insulin (fig. 10b), in order to increase glucose utilization, their conditioned medium failed to increase MCF-7 cell growth.

All together, these data suggest that glucose metabolism in adipocytes may affect their ability to promote cancer cell growth.

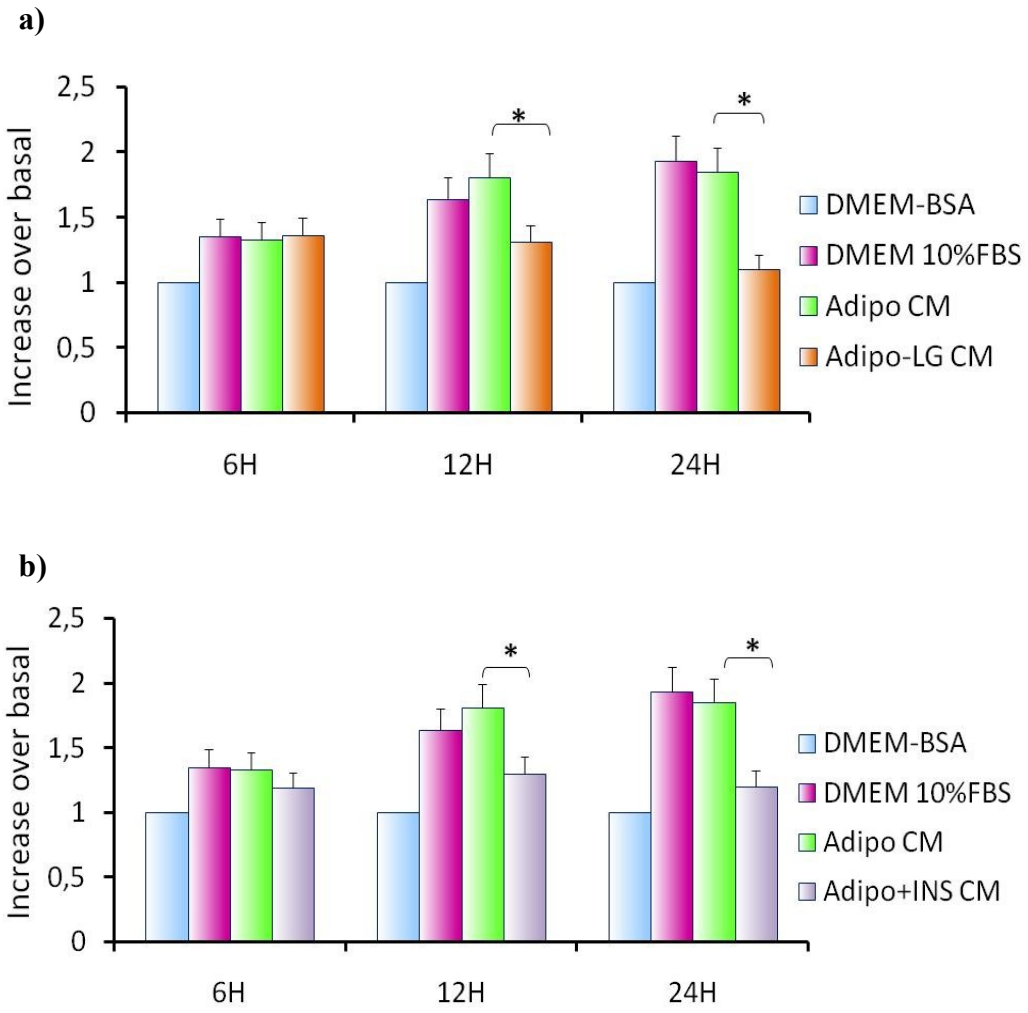

Fig. 10: Effect of glucose or insulin on adipocyte growth-promoting action. 3T3-L1 adipocytes have been pre-incubated with regular DMEM containing 25 mM glucose or with DMEM containing 5 mM glucose (Low Glucose medium) for 24 h (a) or with 100 nM insulin for 16h (b). Then, they have been further incubated with regular serum-free DMEM for 8 h. Media have been collected and added to serum-starved MCF-7 breast cancer cells for 6, 12 and 24h, as indicated. As a control, MCF-7 cells have also been incubated with DMEM without serum supplementation (DMEM-BSA) or with 10% fetal bovine serum (DMEM 10%FBS). Then, cells have been counted and the results reported as fold-increase over basal (cell count in DMEM-BSA). Asterisks denote statistically significant values (* $p<0.05$).

4.3 Identification of the adipocyte factors controlling breast cancer cell phenotypes.

White adipose tissue expresses and secretes a variety of adipokines, proinflammatory cytokines and growth factors (Iyengar et al. 2003; Ahima and Flier 2000).

In order to identify the factors released from the adipocytes which may be contributing to the malignant phenotype of breast cancer cells I used ELISA/multiplex analysis. In particular, I analyzed the conditioned media for the content of growth factors and cytokines produced by pre-adipoctytes or adipocytes, in presence or absence of low glucose medium or insulin. Conditioned media were collected and tested for 23 cytokines and 3 growth factors by using the Bioplex multiplex cytokine assay kit and the Bioplex multiplex growth factor assay kit. In tab. 2 are shown all the cytokines and growth factors analyzed and their changes in both conditioned media. As shown, in Adipo CM there is an increase of IL-12 (p40), INF-γ, MIP-1α, RANTES and IGF1 and a reduction of KC, MCP-1 and MIP-1β compared to Fibro CM. The levels of IL-1β and IL-3 are similar in both media. Other cytokines were not detectable.

a)

Mouse 23-Plex Panel	Adipo CM (pg/ml)	Fibro CM (pg/ml)	Adipo-LG CM (pg/ml)	Adipo+INS CM (pg/ml)
IL-1a	ND	ND	ND	ND
IL-1b	13	12,7	8,59	12,96
IL-2	ND	ND	ND	ND
IL-3	0,10	0,07	0,16	0,07
IL-4	ND	ND	ND	ND
IL-5	ND	ND	ND	ND
IL-6	ND	ND	ND	ND
IL-9	ND	ND	ND	ND
IL-10	ND	ND	ND	ND
IL-12 (p40)	6,28	ND	5,05	7,58
IL-12 (p70)	ND	ND	ND	ND
IL-13	ND	ND	ND	ND
IL-17	ND	ND	ND	ND
Eotaxin	ND	ND	ND	ND
G-CSF	ND	ND	ND	ND
GM-CSF	ND	ND	ND	ND
IFN-γ	3	1,87	3,81	3,93
KC	505	2391,7	1275,05	3209,61
MCP-1	6806,27	8733,65	7101,21	5836,97
MIP-1a	70,02	56,58	82,94	90,67
MIP-1b	2,01	2,58	2,01	1,29
RANTES	2357,78	957,51	747,66	1097
TNF-a	ND	ND	ND	ND

b)

Mouse 3-Plex Panel	Adipo CM	Fibro CM	Adipo-LG CM	Adipo+INS CM
PDGF	ND	ND	ND	ND
VEGF	ND	ND	ND	ND
IGF1	32	12	25	20

Tab. 2: Screening of cytokines and growth factors present in Adipo CM. Supernatants from adipocytes (Adipo CM), fibroblast (Fibro CM), adipocyte pretreated with low glucose medium (Adipo-LG CM) or with insulin (Adipo+INS CM) were collected from 8h and tested for 23 cytokines and 4 growth factors by Bioplex multiplex assay.

It should be noted that IL-12 is secreted only by adipocyte, while RANTES, MIP-1a and IGF1 are secreted by both preadipocytes and adipocytes, but their concentration is higher in Adipo CM than in Fibro CM.

Incubation in Low glucose medium or with insulin led to changes in adipocyte-released factors. In Adipo-LG CM and Adipo +INS CM there was a decrease of RANTES and IGF1 and an increase of KC compared to Adipo CM. The levels of MCP-1 were similar in Adipo CM and Adipo-LG CM, but reduced in Adipo +INS CM.

In conclusion, in Adipo CM there was a reduction of KC and an increase of RANTES and IGF1 compared to Fibro CM. Low glucose or insulin treatment of adipocytes rescued these differences.

Except for the IGF1, the role of these cytokines in cancer is largely unknown, so it remains to elucidate how they may promote breast cancer cell survival or growth.

4.4 IGF1 expression and inhibition.

In order to investigate the molecular basis of the differential IGF1 secretion, I have measured the expression levels of IGF1 by real-time RT-PCR in pre-adipocytes and adipocytes cultured or not in presence of low glucose medium or insulin

As shown in fig. 11, in adipocytes the IGF1 mRNA levels were 3-fold higher than those detected in pre-adipocytes.

Incubation with either low glucose medium or insulin reduced IGF1 mRNA levels in adipocytes (Fig. 11).

Then I have tested the possibility that the growth effect of adipocyte conditioned media could be reverted by inhibiting IGF-1 pathway. Therefore, 3T3-L1 adipocytes conditioned media were collected and applied to MCF-7 cells for 12h in the presence of 10 μM AG1024, a specific IGF-1R tyrosine kinase inhibitor.

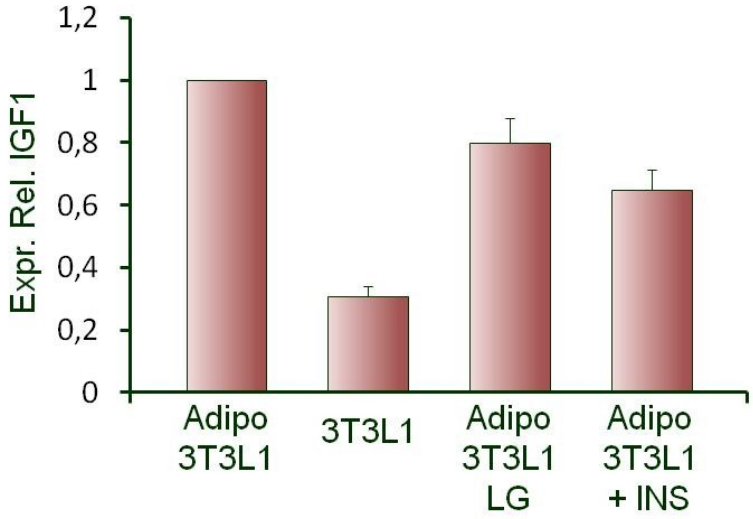

Fig. 11:IGF1 expression. The abundance of mRNA for IGF1 was determined by real-time PCR analysis of total RNA isolated from 3T3 L1, adipocyte 3T3L1 (Adipo 3T3L1), adipocyte 3T3L1preincubated 24h in low glucose medium (Adipo 3T3L1 LG) and adipocyte 3T3L1 pretreated with 100 nM insulin for 16h (Adipo 3T3L1+INS). Bars represent the mRNA levels in these cells and are relative to those in adipocyte 3T3 L1 cells.

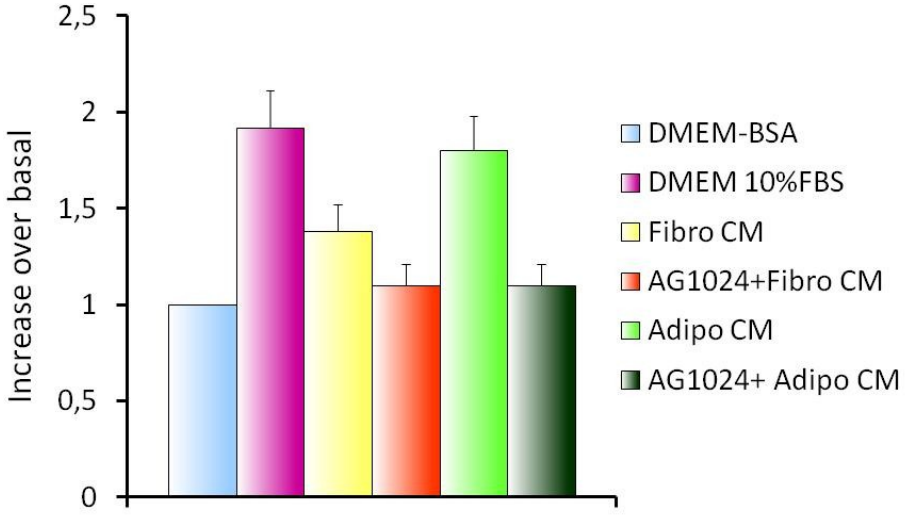

Fig. 12: Effect of AG1024 on adipocyte and pre-adipocyte growth-promoting action. MCF-7 cells have been treated with 10 μM AG1024 for 15min, then, they have been further incubated with Adipo CM or Fibro CM for 12h. As a control, MCF7 cells have also been incubated with DMEM without serum supplementation (DMEM-BSA) or with 10% fetal bovine serum (DMEM 10%FBS). Then, cells have been counted and the results reported as fold-increase over basal (cell count in DMEM-BSA).

As shown in fig. 12, the treatment of MCF-7 cells with IGF-1R inhibitor AG1024 (fig. 12, respectively red and dark green bars) impaired the ability of Adipo CM and Fibro CM to induce cell growth, suggesting the crucial role of adipocyte produced IGF1 in promoting cancer cell growth.

5. CONCLUSIONS

Adipocyte conditioned media stimulate MCF-7 cell proliferation; interestingly, conditioned media from fully differentiated adipocytes are significantly more effective than conditioned media from pre-adipocytes in inducing MCF-7 growth. This effect is obtained also with human adipocytes.

Adipocyte conditioned media reduce MCF-7 apoptosis and activate ERK1/2 and AKT resulting in protection from apoptosis.

The incubation of adipo 3T3L1 cells with low glucose medium or with insulin impair their ability to induce MCF7 growth suggesting that glucose metabolism in adipo 3T3L1 cells is crucial.

Finally, cytokines/growth factors screening revealed that KC, RANTES and IGF1 could be good candidates in mediating pro-tumorigenic effect of adipocyte conditioned media. In particular, adipocyte conditioned media proliferative effect is reverted by inhibiting IGF-1 pathway suggesting the crucial role of adipocyte produced IGF1 in promoting cancer cell growth.

6. ACKNOWLEDGEMENTS

Desidero ringraziare tutti coloro che mi hanno aiutato, scientificamente e moralmente, nello svolgimento di questo lavoro di tesi.

Ringrazio il prof. Beguinot per avermi concesso di far parte del suo gruppo di lavoro dandomi l'opportunità di realizzare questo progetto di tesi, per l'affetto e per essere stato sempre esempio di professionalità e serietà.

Ringrazio Pietro per essere stato amico e guida, per la fiducia mostratami, per la pazienza, l'entusiasmo e l'ottimismo.

Ringrazio Claudia, Francesco, Rossella, Francesca e Anna per essere stati punto di riferimento, per i consigli e la loro allegria.

Ringrazio tutti i membri del laboratorio Beguinot e del laboratorio Portella per la disponibilità, l'affetto e la simpatia.

Ringrazio Teresa per avermi insegnato a "vivere" e lavorare in laboratorio; Iolanda per la collaborazione, la calma e la dolcezza, Gregory per gli incoraggiamenti, i continui confronti e i suggerimenti; Alessia per la vivacità e i consigli; Giuseppe per essere stato sempre presente e disposto ad aiutarmi; Serena per il sostegno e la complicità; Flora per le risate e i momenti di svago; ma, soprattutto, ringrazio tutti loro per la profonda amicizia e disponibilità.

Ringrazio i miei "bimbi": Gabriele per le risate e per aver pensato con me a questo progetto; Federica per la presenza costante e instancabile, per l'entusiasmo e la perseveranza che hanno contribuito notevolmente allo svolgimento di questo lavoro.

Ringrazio Ginevra e Salvatore con i quali ho raggiunto questo traguardo, affrontando momenti belli e tempestosi, con stima e amicizia.

I would like to thank prof. Smith for his availability and for giving me the opportunity to attend his laboratory; I would like to thank Ann for her helpfulness and professionalism.

Ringrazio Alessandra, Peppe, Tonia, Giosuè e Alfonso per aver contribuito ad alleggerire le fatiche lavorative, per l'allegria e la forte amicizia.

Ringrazio mamma, papà, Luigi, zia Anna, zio Bruno, Marilena e il nonno per il continuo appoggio, la fiducia e l'infinito affetto.

Dulcis in fundo ringrazio Carmine, la sua pazienza, saggezza e il suo amore sono stati il mio più grande sostegno e incoraggiamento.

7. REFERENCES

Ahima RS, Flier JS. Adipose Tissue as an Endocrine Organ. Trends Endocrinol Metabolism. 2000;11:327-32.

Alberobello AT, D'Esposito V, Marasco D, Ruvo M, Bianco R, Tortora G, Esposito I, Fiory F, Miele C, Beguinot F, Formisano P. Selective disruption of Insulin-like Growth Factor-1 signalling via Phosphoinositide-dependent Kinase-1 prevents protective effects of IGF-1 on human cancer cell death. J Biol Chem. Pending revision

Andersson CX, Gustafson B, Hammarstedt A, Hedjazifar S, Smith U. Inflamed adipose tissue, insulin resistance and vascular injury. Diabetes Metab Res Rev 2008; 24: 595–603.

Aranceta J, Moreno B, Moya M, Anadón A. Prevention of overweight and obesity from a public health perspective. Nutr Rev. 2009;67.

Bergström A, Pisani P, Tenet V, Wolk A, Adami HO. Overweight as an avoidable cause of cancer in Europe. Int J Cancer 2001;91:421–30.

Berrington de Gonzalez A, Sweetland S, Spencer E. A meta-analysis of obesity and the risk of pancreatic cancer. Br. J. Cancer 2003;89, 519–523.

Calle EE, Kaaks R. Overweight, obesity and cancer: epidemiological evidence and proposed mechanisms. Nat Rev Cancer. 2004;4:579-91.

Calle EE, Thun MJ. Obesity and cancer. Oncogene 2004;23:6365-78.

Carter JC, Church FC. Obesity and Breast Cancer: The Roles of Peroxisome Proliferator-Activated Receptor-gamma and Plasminogen Activator Inhibitor-1. PPAR Res. 2009;2009:345320.

Chagnon YC, Rankinen T, Snyder EE, Weisnagel SJ, Pérusse L, Bouchard C. The human obesity gene map: the 2002 update. Obes Res. 2003;11:313-67.

Chavey C, Mari B, Monthouel MN, Bonnafous S, Anglard P, Van Obberghen E, Tartare-Deckert S. Matrix metalloproteinases are differentially expressed in adipose tissue during obesity and modulate adipocyte differentiation. J Biol Chem. 2003;278:11888-96.

Clemmons DR. Role of insulin-like growth factor binding proteins in controlling IGF actions. Mol. Cell Endocrinol. 1998;140:19–24.

Crum CP, Lester SC, Cotran RS. The female genital system and breast. In Kumar V, editor. Robbins Basic Pathology. Saunders, Philadelphia, Pa, USA, 2003.

Engelman JA, Lisanti MP, Scherer PE. J Biol Chem. 1998; 273: 32111–32120.

Fair AM, Montgomery K. Energy balance, physical activity, and cancer risk. Methods Mol Biol. 2009;472:57-88.

Feldmann M. Many cytokines are very useful therapeutic targets in disease. J Clin Invest. 2008;118:3533-6.

Field AE, Coakley EH, Must A, Spadano JL, Laird N, Dietz WH. Impact of overweight on the risk of developing common chronic diseases during a 10-year period. Arch Intern Med 2001;161:1581-1586.

Frühbeck G. Overview of adipose tissue and its role in obesity and metabolic disorders. Methods Mol Biol. 2008;456:1-22.

Ginter E, Simko V. Adult obesity at the beginning of the 21st century: epidemiology, pathophysiology and health risk. Bratisl Lek Listy. 2008;109:224-30.

Giovannucci E. Insulin and colon cancer. Cancer Causes Control. 1995;6(2):164-79.

Guilherme A, Virbasius JV, Puri V, Czech MP. Adipocyte dysfunctions linking obesity to insulin resistance and type 2 diabetes. Nat Rev Mol Cell Biol. 2008;9:367-77.

Harvie M, Howell A. Energy balance adiposity and breast cancer – energy restriction strategies for breast cancer prevention. Obes Rev. 2006;7:33-47.

Housa D, Housová J, Vernerová Z, Haluzík M. Adipocytokines and cancer. Physiol Res. 2006;5:233-44.

Hoyo C, Gammon MD. Obesity and overweight in relation to adenocarcinoma of the esophagus. In: McTiernan A, editor. Cancer Prevention and Management Through Exercise and Weight Control. Taylor & Francis, Boca Raton, FL: 2006. p. 269 – 282.

Hovey RC, McFadden TB, Akers RM. Regulation of mammary gland growth and morphogenesis by the mammary fat pad: a species comparison. J Mammary Gland Biol Neoplasia. 1999;4:53-68.

IARC. IARC Handbooks of Cancer Prevention. Weight Control and Physical Activity. International Agency for Research on Cancer. 2002, Lyon.

Iyengar P, Combs TP, Shah SJ, Gouon-Evans V, Pollard JW, Albanese C, Flanagan L, Tenniswood MP, Guha C, Lisanti MP, Pestell RG, Scherer PE. Adipocyte-secreted factors synergistically promote mammary tumorigenesis through induction of anti-apoptotic transcriptional programs and proto-oncogene stabilization. Oncogene 2003; 22: 6408-23.

Jemal A, Siegel R, Ward E, Hao Y, Xu J, Murray T, Thun MJ. Cancer statistics, 2008. CA Cancer J Clin 2008;58:71–96.

Kaaks R, Lukanova A. Energy balance and cancer: the role of insulin and insulin-like growth factor-I. Proc. Nutr. Soc. 2001;60:91–106.

Klöting N, Koch L, Wunderlich T, Kern M, Ruschke K, Krone W, Brüning JC, Blüher M. Autocrine IGF-1 action in adipocytes controls systemic IGF-1 concentrations and growth. Diabetes 2008; 57: 2074-82.

Laemmli UK. Cleavage of structural proteins during the assembly of the head of bacteriophage T4. Nature 1970;227:680-685.

LeRoith D, Helman L. The new kid on the block(ade) of the IGF-1 receptor. Cancer Cell 2004;5:201-202.

Malin A, Matthews CE, Shu XO, Cai H, Dai Q, Jin F, Gao YT, Zheng, W. Energy balance and breast cancer risk. Cancer Epidemiol Biomarkers Prev 2005;14:1496 – 1501.

McKeown-Eyssen G. Epidemiology of colorectal cancer revisited: are serum triglycerides and/or plasma glucose associated with risk? Cancer Epidemiol Biomarkers Prev. 1994;3(8):687-95.

Moayyedi P. The epidemiology of obesity and gastrointestinal and other diseases: an overview. Dig Dis Sci. 2008;53:2293-9.

National Task Force on the Prevention and Treatment of Obesity. Dieting and the development of eating disorders in overweight and obese adults. Arch Intern Med. 2000;160:2581-9.

Nunez NP, Oh WJ, Rozenberg J, Perella C, Anver M, Barrett JC, Perkins SN, Berrigan D, Moitra J, Varticovski L, Hursting SD, Vinson C. Accelerated tumor formation in a fatless mouse with type 2 diabetes and inflammation. Cancer Res. 2006;66:5469-76.

Osório-Costa F, Rocha GZ, Dias MM, Carvalheira JB. Epidemiological and molecular mechanisms aspects linking obesity and cancer. Arq Bras Endocrinol Metabol. 2009; 53: 213-26.

Pan SY, DesMeules M. Energy Intake, Physical Activity, Energy Balance, and Cancer: Epidemiologic Evidence. Methods Mol Biol. 2009;472:191-215.

Petrelli J, Calle E, Rodriguez C, Thun M. Body mass index, height, and postmenopausal breast cancer mortality in a prospective cohort of US women. Cancer causes control 2002;13:325-332.

Pollak MN, Schernhammer ES, Hankinson SE. Insulin- like Growth Factors and neoplasia. Nat Rev Cancer. 2004;4:505-518.

Power C, Miller SK, Alpert P. Promising new causal explanation for obesity and obesity-related diseases. Biol Res Nurs 2007;8:223-233.

Ramirez-Zacarias JL, Castro-Munozledo F, Kuri-Harcuch W. Quantitation of adipose conversion and triglycerides by staining intracytoplasmic lipids with Oil red O, Histochemistry 1992; 97:493–497.

Rose DP, Komninou D, Stephenson GD. Obesity, adipocytokines, and insulin resistance in breast cancer. Obes Rev. 2004;5:153-65.

Robbins SL, Cotran RS. Pathologic Basis of Disease, 2004, 7th ed, vol. 1, p100.

Rotter V, Nagaev I, Smith U. Interleukin-6 (IL-6) induces insulin resistance in 3T3–L1 adipocytes and is, like IL-8 and tumor necrosis factor-alpha, overexpressed in human fat cells from insulin-resistant subjects. J Biol Chem 2003;278:45777–45784.

Ryan PD, Goss PE. The emerging role of the insulin-like growth factor pathway as a therapeutic target in cancer. Oncologist 2008;13:16-24.

Schäffler A, Schölmerich J, Buechler C. The role of 'adipotropins' and the clinical importance of a potential hypothalamic-pituitary-adipose axis. Nat Clin Pract Endocrinol Metab 2006;2:374–383.

Stephenson G and Rose D. Breast cancer and obesity: an update. Nutr. Cancer 2003; 45:1–16.

van Roermund JG, Witjes JA. The impact of obesity on prostate cancer. World J Urol. 2007;25:491-7.

Vona-Davis L, Rose DP. Adipokines as endocrine, paracrine, and autocrine factors in breast cancer risk and progression. Endocr Relat Cancer. 2007;14:189-206.

World Health Organization. Obesity: preventing and managing the global epidemic. Report of a WHO consultation. 2000;894. Geneva, Switzerland, World Health Organization. WHO Technical Reports Series.

Wu Y, Cui K, Miyoshi K, Hennighausen L, Green JE, Setser J, LeRoith D, Yakar S. Reduced circulating insulin-like growth factor I levels delay the onset of chemically and genetically induced mammary tumors. Cancer Res 2003;63:4384.

Yu H, Rohan T. Role of the insulin-like growth factor family in cancer development and progression. J Natl Cancer Inst. 2000;92:1472-89.

0026-895X/08/7406-1678–1686$20.00
MOLECULAR PHARMACOLOGY
Vol. 74, No. 6
49205/3410717
Mol Pharmacol 74:1678–1686, 2008
Printed in U.S.A.

The Cannabinoid CB1 Receptor Antagonist Rimonabant Stimulates 2-Deoxyglucose Uptake in Skeletal Muscle Cells by Regulating the Expression of Phosphatidylinositol-3-kinase

Iolanda Esposito, Maria Chiara Proto, Patrizia Gazzerro, Chiara Laezza, Claudia Miele, Anna Teresa Alberobello, Vittoria D'Esposito, Francesco Beguinot, Pietro Formisano, and Maurizio Bifulco

Dipartimento di Biologia e Patologia Cellulare e Molecolare & Istituto di Endocrinologia ed Oncologia Sperimentale del Consiglio Nazionale delle Ricerche, Università degli Studi di Napoli "Federico II", Napoli, Italy (I.E., C.L., C.M., A.T.A., V. D.E., F.B., P.F.); and Endocannabinoid Research Group, Dipartimento di Scienze Farmaceutiche, Università degli Studi di Salerno, Fisciano (SA), Italy (M.C.P., P.G., M.B.)

Received May 26, 2008; accepted September 18, 2008

ABSTRACT

The endocannabinoid system regulates food intake, energy, and glucose metabolism at both central and peripheral levels. We have investigated the mechanism by which it may control glucose uptake in skeletal muscle cells. Detectable levels of the cannabinoid receptor type 1 (CB1) were revealed in L6 cells. Exposure of differentiated L6 myotubes to the CB1 antagonist rimonabant (SR141716) selectively increased 2-deoxyglucose uptake (2-DG) in a time- and dose-dependent manner. A similar effect was induced by genetic silencing of CB1 by small interfering RNA. Protein expression profiling revealed that both the regulatory p85 and the catalytic p110 subunits of the phosphatidylinositol-3-kinase (PI3K) were increased by SR141716. No significant change in the cellular content of other known molecules regulating PI3K was observed. However, phosphoinositide-dependent kinase-1, Akt/protein kinase B, and protein kinase Cζ activities were rapidly induced after SR141716 treatment of L6 cells in a PI3K-dependent manner. The stimulatory effect of SR141716 on PI3K expression and activity was largely prevented by *N*-[2-(4-bromocinnamylamino)ethyl]-5-isoquinoline (H-89), an inhibitor of the cAMP-dependent protein kinase. Moreover, SR141716-stimulated 2-DG uptake was blunted by the coincubation either with H-89 or with the PI3K inhibitor 2-(4-morpholinyl)-8-phenyl-1(4*H*)-benzopyran-4-one hydrochloride (LY294002), both in L6 cells and in mouse primary myocytes. Thus, modulation of CB1 regulates glucose uptake at the level of the PI3K signaling system in skeletal muscle cells. Interfering with CB1 signaling may therefore ameliorate glucoregulatory functions in peripheral tissues.

Type 2 diabetes (T2D) is a genetically determined disorder, affecting more than 150 million people worldwide. T2D is characterized by several metabolic defects, among which β-cell secretory dysfunction and peripheral insulin resistance are considered as hallmarks of the disease in humans (Kahn, 2003). Common forms of T2D arise because of the progressive failure of endocrine pancreas to adequately cope with the increased insulin demand in insulin-resistant states (Lazar, 2005). In particular, obesity is believed to play a central role as a causative factor of insulin resistance (Lazar, 2005). Moreover, genetic and functional abnormalities found in obese individuals show a certain degree of overlap with those detected in patients with T2D, suggesting that common molecular events may contribute to the onset and/or the progression of both disorders.

This study was supported in part by the European Community's FP6 EUGENE2 (LSHM-CT-2004-512013) and FP7 PREPOBEDIA (number 201-681), grants from the Associazione Italiana per la Ricerca sul Cancro (to F.B. and P.F.), the Ministero dell'Università e della Ricerca Scientifica (to F.B. and P.F. and FIRB Idea Progettuale RBIP0689BS), the Ministero della Salute, the European Federation for the Study of Diabetes, and by the Associazione Educazione e Ricerca Medica Salernitana (ERMES). The financial support of Telethon–Italy is also gratefully acknowledged. I.E. was awarded a travel grant from the Università di Napoli "Federico II"–International Exchange Program.

Article, publication date, and citation information can be found at http://molpharm.aspetjournals.org.

doi:10.1124/mol.108.049205.

ABBREVIATIONS: T2D, type 2 diabetes; 2-DG, 2-deoxyglucose; PKB, protein kinase B; CB1, cannabinoid receptor type 1; CHX, cycloheximide; CREB, cAMP response element-binding protein; DMEM, Dulbecco's modified Eagle's medium; ECS, endocannabinoid system; GLUT, glucose transporter; IRS, insulin receptor substrate; IRTX, iodoresinatoxin; PeSt, penicillin-streptomycin; PKCζ, protein kinase Cζ; PDK-1, phosphoinositide-dependent kinase-1; PI3K, phosphatidylinositol-3-kinase; PKA, protein kinase A; PTEN, phosphatase and tensin homolog; siRNA, small interfering RNA; SR141716, rimonabant; H-89, *N*-[2-(4-bromocinnamylamino)ethyl]-5-isoquinoline; LY294002, 2-(4-morpholinyl)-8-phenyl-1(4*H*)-benzopyran-4-one hydrochloride; PCR, polymerase chain reaction; RT-PCR, reverse transcriptase-polymerase chain reaction; PAGE, polyacrylamide gel electrophoresis.

These defects may affect feeding behavior, as well as energy expenditure and nutrient metabolism.

The endocannabinoid system, for instance, is an important regulator for all of those functions (Boyd, 2006; Pagotto et al., 2006). Elevated levels of the endogenous cannabinoids (anandamide and 2-arachidonoyl-glycerol) have been found in obese individuals (Engeli et al., 2005; Osei-Hyiaman et al., 2005, 2006) and correlate with intra-abdominal adiposity (Cote et al., 2007). Both exogenous cannabinoids and endocannabinoids increase food intake and promote weight gain by activating the specific CB1 receptor (Jamshidi and Taylor, 2001; Williams and Kirkham, 2002; Cota et al., 2003a). Mice carrying the ablation of the CB1 gene are lean and resistant to diet-induced obesity (Ravinet Trillou et al., 2004). It has been shown recently that rimonabant (SR141716), a CB1-receptor inverse agonist (Bouaboula et al., 1997), produces a marked and sustained decrease in body weight, which is associated with favorable modifications in serum biochemical and lipid profiles (Poirier et al., 2005; Pi-Sunyer et al., 2006).

Long-term blockade of the CB1 receptor is also accompanied by reduced blood pressure and fasting glucose and insulin levels (Ravinet Trillou et al., 2003; Poirier et al., 2005; Van Gaal et al., 2005). Nevertheless, whether these additional beneficial effects are merely the consequence of weight loss or are the result of peripheral actions of the CB1-targeted molecules is still unknown. It has been shown that CB1 receptors are expressed in several mammalian tissues relevant to insulin action (Engeli et al., 2005; Juan-Pico et al., 2006). For instance, pancreatic islets express functional cannabinoid receptors, which may regulate Ca^{2+} signals and insulin secretion (Juan-Pico et al., 2006). In the liver, the activation of CB1 increases de novo synthesis of fatty acids by activating the transcription factor sterol regulatory element binding protein 1c (Osei-Hyiaman et al., 2005). In addition, modulation of CB-1 activity in isolated mouse adipocytes increases the activity of the lipogenic enzyme lipoprotein lipase (Cota et al., 2003b) and adiponectin expression (Bensaid et al., 2003). Very little information is available, however, concerning cannabinoid receptor function in the skeletal muscle. Recently, CB1 expression has been detected in soleus muscle (Pagotto et al., 2006), and SR141716 has been shown to affect glucose uptake in the isolated soleus of genetically obese mice (Liu et al., 2005) and the expression of genes involved in oxidative metabolism (Cavuoto et al., 2007). However, the molecular mechanisms of CB1 action in skeletal muscle cells remain largely undefined.

We now show that in a skeletal muscle cultured cell model, the L6 cells, pharmacological regulation of the endocannabinoid system controls glucose uptake at the level of the phosphatidylinositol-3-kinase (PI3K). In particular, the CB1 inverse agonist SR141716 selectively increases PI3K expression and activity in a protein kinase A (PKA)-dependent manner. This, in turn, leads to changes of the PI3K downstream signaling and a consequent regulation of glucose uptake in the skeletal muscle cells.

Materials and Methods

General. Media, sera, and antibiotics for cell cultures were from Invitrogen Ltd. (Paisley, United Kingdom). Phospho-Ser241 PDK1, phospho-Ser473 PKB, phospho-serine, and phospho-Thr202/Tyr204 extracellular signal-regulated kinase antibodies were purchased from Cell Signaling Technology (Danvers, MA). Actin antibody was from Sigma (St. Louis, MO). Antibodies directed against CB1, GLUT1, GLUT4, extracellular signal-regulated kinases, phospho-Thr410 PKCζ, PKCζ, p110, PTEN, PKB, CREB, and phospho-Ser133 CREB were from Santa Cruz Biotechnology (Santa Cruz, CA). PDK1, IRS-1, IRS-2, and p85 antibodies were from Upstate Cell Signaling Technology (Lake Placid, NY). Electrophoresis and Western blot reagents were from Bio-Rad (Richmond, VA). 2-Deoxy-[^{14}C]-glucose and enhanced chemiluminescence reagents were from GE Healthcare (Chalfont St. Giles, Buckinghamshire, UK). Other reagents were from Sigma.

Cell Culture. The L6 skeletal muscle cells were plated (6×10^3 cells/cm^2) and grown in Dulbecco's modified Eagle's medium (DMEM) supplemented with 10% (v/v) fetal bovine serum and 2 mM glutamine. Cultures were maintained at 37°C in a humidified atmosphere containing 5% (v/v) CO_2. L6 differentiation was achieved as described previously (Caruso et al., 1997).

Mouse Primary Fibroskeletal Muscle Cell Culture. Skeletal muscle biopsies were obtained after C57 BL6 strain ($n = 9$) mice were sacrificed by pentobarbitone overdose, as described previously (Krämer et al., 2007). The biopsies were collected in cold phosphate-buffered saline supplemented with 1% PeSt (100 U/ml penicillin, 100 μg/ml streptomycin), dissected, finely minced, and transferred to a digestion solution (0.015 g Collagenase IV, 8% 10× trypsin, 0.015 g of bovine serum albumin, 1% PeSt, in DMEM supplemented with 10% fetal calf serum, 10,000 U/ml penicillin, 10 mg/ml streptomycin, and 2% L-glutamine) and incubated with gentle agitation at 37°C for 15 to 20 min. Thereafter, undigested tissue was allowed to settle, and the supernatant was collected and mixed with DMEM supplemented with 20% fetal calf serum and 1% PeSt. The remaining tissue was digested for a further 15 to 20 min at 37°C with fresh digestion solution. The resultant supernatant was then pooled with the previous cells and centrifuged for 10 min at 350*g*. The cell pellet was resuspended in DMEM supplemented with 20% fetal calf serum and 1% PeSt and was then seeded and grown in culture flask. After this, medium was again changed to DMEM supplemented with 10% fetal calf serum and 1% PeSt. Before any experiment, cells were incubated in serum-free media for 16 h and stimulated with insulin or with SR141716 as indicated.

Cell Treatment. For all of the experiments, L6 cells and myocytes were incubated in serum-free media supplemented with 0.25% bovine serum albumin. Unless specified, different concentrations of SR141716 (0.05, 0.1, 0.3, 1, and 10 μM) were simultaneously added to the media, as described in the figure legend. Likewise, 0.1 μM SR144528 and 0.3 μM iodoresinatoxin (IRTX) were added to the serum-free media for the indicated time. For PI3K inhibition studies, cells were pretreated with 10 μM LY294002 for 30 min followed by further incubation with LY294002 and 0.1 μM SR141716 for additional 24 h. For early times, the cells were serum-starved for 16 h and then pretreated with 10 μM LY294002 for 30 min, followed by further incubation with LY294002 and 0.1 μM SR141716 for an additional 30 min. For PKA inhibition studies, cells were pretreated with 15 μM H-89 for 30 min followed by combined treatment with H-89 and 0.1 μM SR141716 for an additional 30 min or 24 h as indicated. To study the SR141716 effect on protein synthesis, the cells were incubated with 40 μg/ml cycloheximide in presence of 0.1 μM SR141716 for 24 h.

Transient Transfection. For knocking down CB1 expression, a 21-nucleotide small interfering RNA duplex (Dharmacon Research, Lafayette, CO) was used, designed for specific silencing of CB1 (siRNA-CB1), covering the sequence sense 5′-CCCAAGUGAC-GAAAAACAUU-dTdT-3′. The cells were transfected using FuGENE (Roche, Indianapolis, IN) and 100 nM siRNA for each transfection, in accordance with the manufacturer's instruction. An equal concentration of Silencer Negative Control-1 siRNA (Ambion, Austin, TX) was used as negative control. Transfected L6 cells were serum-starved and incubated with 0.1 μM SR141716 and after 16 h assayed for

2-deoxy-D-glucose uptake. Specific silencing of CB1 gene was confirmed by RT-PCR and Western blot analysis for CB1 receptor.

Real-Time PCR. Total RNA was isolated from 3T3 L1 preadipocytes and L6 cells by using the RNeasy Kit (QIAGEN Sciences, Valencia, CA) according to the manufacturer's instruction. For real-time RT-PCR analysis, 1 μg of cell RNA was reverse-transcribed using SuperScript II Reverse Transcriptase (Invitrogen, Carlsbad, CA). PCR was analyzed using SYBR Green mix (Invitrogen). Reactions were performed using Platinum SYBR Green Quantitative PCR SuperUDG using an iCycler IQ multicolor Real-Time PCR Detection System (Bio-Rad, Hercules, CA). All reactions were performed in triplicate, and β-actin was used as an internal standard. Primer sequences used were as follows: CB1R sense, 5′-CTA CTG GTG CTG TGT GTC ATC-3′; antisense, 5′-GCT GTC TTT ACG GTG GAA TAC-3′; and β-actin: forward, 5′-GCGTGACATCAAAGAGAAG-3′; reverse, 5′-ACTGTGTTGGCATAGAGG-3′.

Immunoblot Analysis and Immunoprecipitation Procedure. Cells were solubilized for 20 min at 4°C with lysis buffer containing 50 mM HEPES, 150 mM NaCl, 10 mM EDTA, 10 mM $Na_4P_2O_7$, 2 mM sodium orthovanadate, 50 mM NaF, 1 mM phenylmethylsulfonyl fluoride, 10 μg/ml aprotinin, 10 μg/ml leupeptin, pH 7.4, and 1% (v/v) Triton X-100. The lysates were clarified by centrifugation at 12,000*g* for 20 min at 4°C. Proteins were separated by SDS-polyacrylamide gel electrophoresis and blotted on Immobilon-P membranes (Millipore, Billerica, MA). Membranes were blocked for 1 h in Tris-buffered saline (10 mM Tris-HCl, pH 7.4, and 140 mM NaCl) containing 4% (w/v) bovine serum albumin and then incubated with the indicated antibodies. Detection of blotted proteins was performed by enhanced chemiluminescence according to the manufacturer's instruction. Immunoprecipitation experiments were performed as described previously (Formisano et al., 1998). Densitometric analysis was performed using a Scion Image Analyzer. All of the data were expressed as mean ± S.D. Significance was assessed by Student's *t* test for comparison between two means. Data were analyzed with Statview software (Abacus Concepts, Piscataway, NJ) by one-factor analysis of variance. *P* values of less than 0.05 were considered statistically significant.

2-Deoxy-D-glucose Uptake. The measurement of 2-deoxy-D-[^{14}C]glucose uptake was taken as a measure of glucose uptake by muscle cells, as described previously (Klip et al., 1982). Cells were incubated in serum-free Dulbecco's modified Eagle's medium (DMEM) supplemented with 0.2% (w/v) bovine serum albumin for 18 h in the presence or absence of SR141716 at different concentrations. Cells were incubated in glucose-free 20 mM HEPES, pH 7.4, 140 mM NaCl, 2.5 mM $MgSO_4$, 5 mM KCl, 1 mM $CaCl_2$ (HEPES buffer) and exposed or not to 100 nM insulin for 30 min. Glucose uptake was measured by incubating cells with 0.15 mM 2-deoxy-D-[^{14}C]glucose (0.5 μCi/assay) for 15 min in HEPES buffer. The reaction was terminated by the addition of 10 μM cytochalasin B, and the cells were washed three times with ice-cold isotonic saline solution before lysis in 1 M NaOH. Incorporated radioactivity was measured in a liquid scintillation counter.

Measurement of Intracellular cAMP. Cells were plated in 12-well plates at a density of 5×10^5 cells/well. Cells were treated with 1 μM forskolin for 30 min and with 0.1 μM SR141716 for 24 h. After treatment, cells were washed twice with cold phosphate-buffered saline, and intracellular cAMP was extracted by the addition of 500 μl of 0.1 N HCl with 0.1% Triton, followed by three cycles of freezing and thawing. cAMP concentration was measured by radioimmunoassay (PerkinElmer Life and Analytical Sciences, Waltham, MA) (Nikodemova et al., 2003).

Results

Effect of CB1 Modulation on Glucose Uptake. To investigate whether the endocannabinoid system may operate in a skeletal muscle cell model, we measured the expression levels of the CB1 receptor by real-time RT-PCR and immunoblot experiments in the L6 myotubes (Fig. 1). As control, we used 3T3 L1 cells, in which CB1 expression has already been described previously (Yan et al., 2007). In L6 myotubes, the CB1 mRNA (Fig. 1A) and protein (Fig. 1, B and C) were expressed at levels similar to those detected in 3T3 L1 cells.

Next, 2-deoxy-glucose (2-DG) uptake was measured in the myotubes in the absence or presence of increasing concentrations of the CB1 receptor inverse agonist SR141716 (Fig. 2A). At variance, preincubation of L6 myotubes with 0.1 and 0.3 μM SR141716, respectively, led to 50 and 45% increases of 2-DG uptake ($p < 0.001$), only slightly lower than that observed upon acute insulin stimulation (100 nM for 30 min). No effect was observed with 0.05 μM SR141716 (Fig. 2A). Increasing SR141716 concentrations to 1 and 10 μM led to a progressive reduction of 2-DG uptake, however, consistent with a partial agonist effect. In addition, no significant effect was achieved after treatment of L6 cells with 0.1 μM SR144528 (a selective CB2 receptor antagonist) and 0.3 μM IRTX, a potent transient receptor potential vanilloid 1 receptor antagonist (Fig. 2A). Time course analysis revealed that the effect of 0.1 μM SR141716 was rapidly induced upon 30-min treatment and persisted up to 16 h (Fig. 2B) and longer (up to 72 h, data not shown).

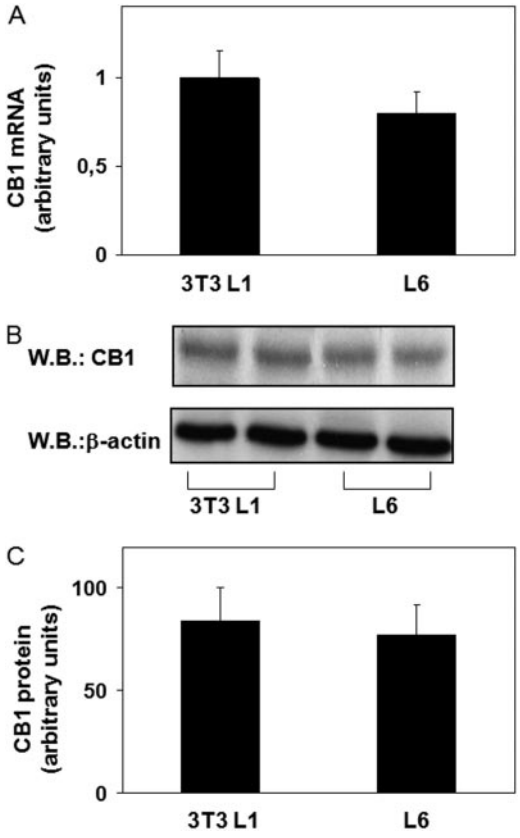

Fig. 1. CB1 expression in myoblasts and myotubes. A, the abundance of mRNA for CB1 was determined by real-time PCR analysis of total RNA isolated from 3T3 L1 cells and L6 myotubes. The results have been analyzed as described under *Materials and Methods*. Bars represent the mRNA levels in L6 myotubes and are relative to those in 3T3 L1 cells. Data are expressed as means ± S.D. of triplicate reactions for total RNAs from each cell type in five independent experiments. B, 3T3 L1 and L6 were solubilized, and cell lysates were separated on SDS-PAGE and immunoblotted with CB1 antibodies. The autoradiograph shown is representative of five independent experiments in duplicate. C, filters obtained in B have been analyzed by laser densitometry as described under *Materials and Methods*.

Protein Expression Profile upon CB1 Modulation. To address the mechanism by which CB1 may regulate glucose uptake in the L6 cells, protein lysates were obtained after-treatment with 0.1 μM SR141716 for 16 h. Protein expression profiling was achieved by immunoblot with specific antibodies (Table 1). The intracellular content of the regulatory (p85α) and the catalytic (p110α) subunits of class I PI3K was increased by 2.0- and 1.7-fold, respectively, upon SR141716 exposure (Table 1 and Fig. 3). No significant change, instead, was detected for the insulin receptor, IRS-1 and -2, phosphoinositide-dependent-kinase 1, and protein kinase Cζ, as well as for the lipid phosphatase PTEN and glucose transporters GLUT-1 and -4 (Table 1). The expression levels of protein kinase Bα/Akt1 were also increased by SR141716, although differences did not reach statistically significant values (Table 1). We then evaluated the timing of PI3K regulation by CB1. The treatment of L6 cells with SR141716 for 5 h led to a slight increase of p85 expression, which increased up to 24 h and remained stable for up to 72 h (Fig. 3C). No detectable change was observed upon 30-min exposure to SR141716. Very similar results were obtained with p110 (data not shown).

To assess whether CB1-mediated regulation of p85 expres-

TABLE 1

Effect of SR141716 on proteins involved in glucose uptake

The cells were incubated or not with 0.1 μM SR141716 for 16 h. Filters were immunoblotted with specific antibodies as indicated and analyzed by laser densitometry, as described under *Materials and Methods.* The values have been normalized to the actin levels and represent means ± S.D. of three independent experiments in duplicate.

Protein	SR141716
	% of control
Insulin receptor	108 ± 8.4
IRS1	107 ± 7.0
IRS2	100 ± 5.4
p85	196 ± 8.8***
p110	168 ± 9.3*
PDK1	99 ± 9.2
PKCζ	112 ± 5.6
Akt/PKB	123 ± 16.9
PTEN	107 ± 10.2
GLUT1	100 ± 11.2
GLUT4	108 ± 7.8

* $P < 0.05$; *** $P < 0.001$ (statistically significant difference of the samples obtained from treated versus untreated cells).

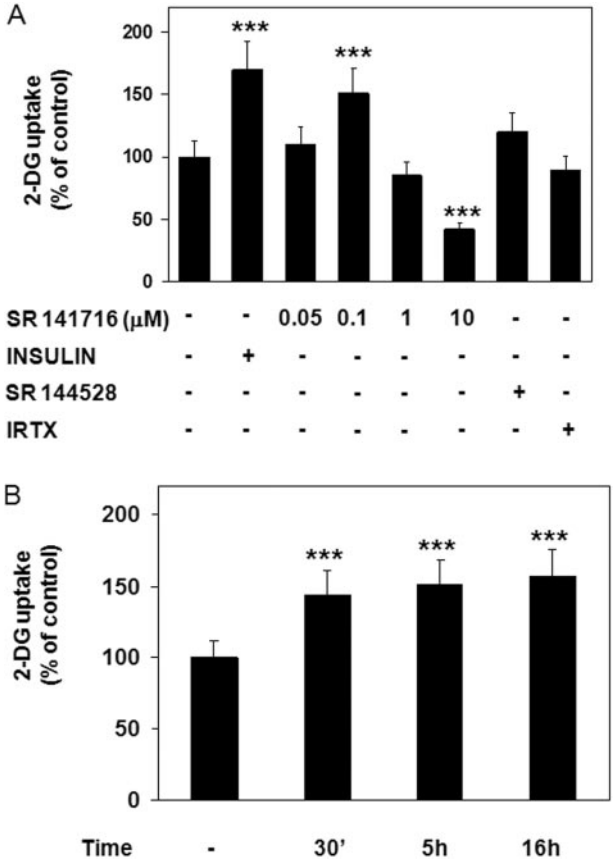

Fig. 2. 2-DG uptake upon SR141716 incubation. A, L6 myotubes were incubated in serum-free media for 16 h before exposure to 100 nM insulin for 30 min as indicated. On the other hand, increasing concentrations (0.05, 0.1, 0.3, 1, and 10 μM) of SR141716, or 0.1 μM SR144528 or 0.3 μM IRTX was simultaneously added to serum-free media for 16 h (in the absence of insulin). Then the cells were assayed for 2-DG uptake as described under *Materials and Methods*. Bars represent mean ± S.D. of three different experiments in triplicate. Asterisks indicate statistically significant differences versus untreated cells (***, $p < 0.001$). B, the cells were treated with 0.1 μM SR141716 for different times (as indicated). 2-DG uptake assay was performed as described under *Materials and Methods*. Bars represent mean ± S.D. of three different experiments in triplicate. Asterisks indicate statistically significant differences versus untreated cells (***, $p < 0.001$).

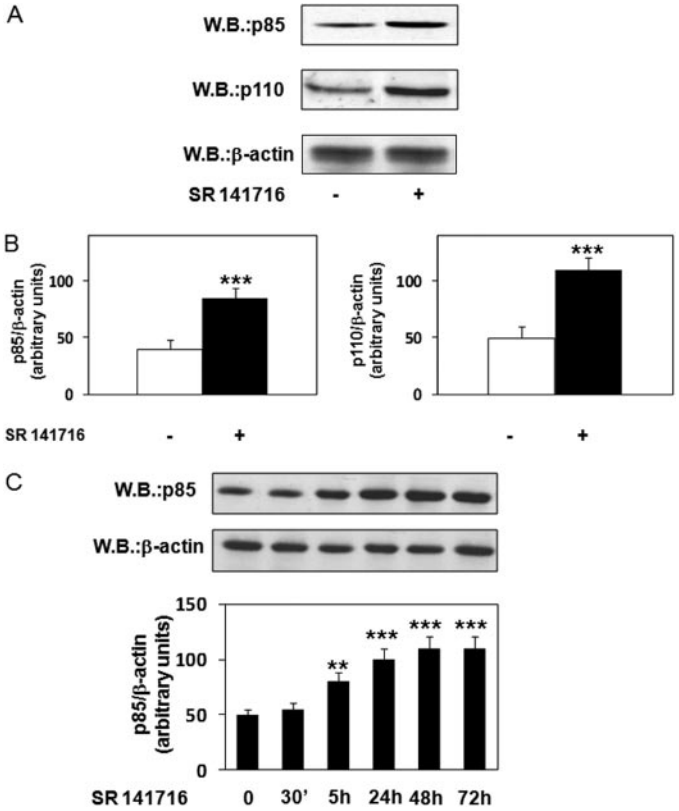

Fig. 3. p85 and p110 regulation by SR141716. A, L6 myotubes were serum-starved and incubated with 0.1 μM SR141716 for 16 h, as described in the legend to Fig. 2 and under *Materials and Methods*. Cell lysates were separated on SDS-PAGE and analyzed by p85, p110, and β-actin immunoblot. The autoradiographs shown are representative of five independent experiments. B, filters obtained in A were analyzed by laser densitometry as described under *Materials and Methods*. Asterisks indicate statistically significant differences (***, $p < 0.001$). C, cells were treated with 0.1 μM SR141716 for different times as indicated. Cell lysates were then analyzed by p85 and β-actin immunoblot as indicated. The autoradiographs shown are representative of five independent experiments. Then, filters obtained in C were analyzed by laser densitometry as described under *Materials and Methods*. Asterisks indicate statistically significant differences (***, $p < 0.001$; **, $p < 0.01$).

sion occurred at the level of protein synthesis, L6 cells were treated with 40 μg/ml cycloheximide (CHX). At the baseline, CHX treatment reduced p85 cellular abundance (Fig. 4, A and B). The treatment with SR141716, however, was still able to increase p85 immunodetection, indicating that regulation occurred at a post-translational level. Similar results were obtained with p110 (data not shown). Consistent with this hypothesis, CHX did not affect SR141716-induced 2-DG uptake (Fig. 4C).

It has been shown previously that CB1 receptor may regulate PKA activity (Bidaut-Russell et al., 1990). To investigate whether SR141716 may regulate PKA activity in the L6 cells, we evaluated the phosphorylation of its substrate, CREB. Immunoblot with specific antibodies revealed that SR141716 induced the phosphorylation of CREB on Ser133 (Fig. 5, A and B). We have therefore tested whether PKA inhibition was able to revert the SR141716 effect on p85. To this end, L6 cells were treated with H-89 (15 μM), a PKA inhibitor, in the absence or presence of SR141716. It is interesting that no increase of p85 cellular abundance was detected in cells treated with H-89 (Fig. 5, A and B). To further clarify the hypothesis that SR141716 may regulate PKA activity, we measured intracellular cAMP levels. Incubation of L6 myotubes with 0.1 μM SR141716 for 24 h led to a significant 5-fold increase of intracellular cAMP production ($p < 0.001$), approximately 50% lower than that observed upon short-term stimulation (30 min) with 1 μM forskolin, a well known adenylyl cyclase stimulator (Fig. 5C). Moreover, we have investigated whether SR141716 stimulates p85 phosphorylation via PKA. To this aim, L6 cells were pretreated with H-89 for 30 min and stimulated with SR141716 for additional 30 min. SR141716 treatment increased p85

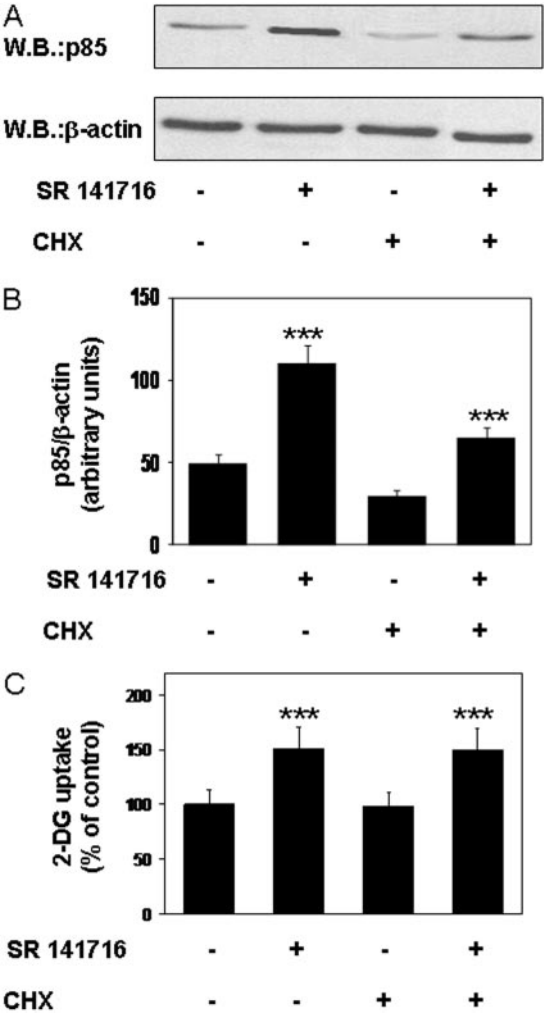

Fig. 4. Effect of CHX on p85 and 2-deoxyglucose uptake. A, cells were serum-starved and incubated with 40 μg/ml cycloheximide in the absence or in the presence of SR141716 for 24 h, as described in the legend to Fig. 1 and under *Materials and Methods*. Cell lysates were then analyzed by immunoblot with p85 and β-actin antibodies. The autoradiographs shown are representative of five independent experiments. B, filters obtained in A were analyzed by laser densitometry as described under *Materials and Methods*. Asterisks indicate statistically significant differences (***, $p < 0.001$). C, cells were treated as described above and assayed for 2-DG uptake as described under *Materials and Methods*. Bars represent mean ± S.D. of three different experiments in triplicate. Asterisks indicate statistically significant differences versus untreated cells (***, $p < 0.001$).

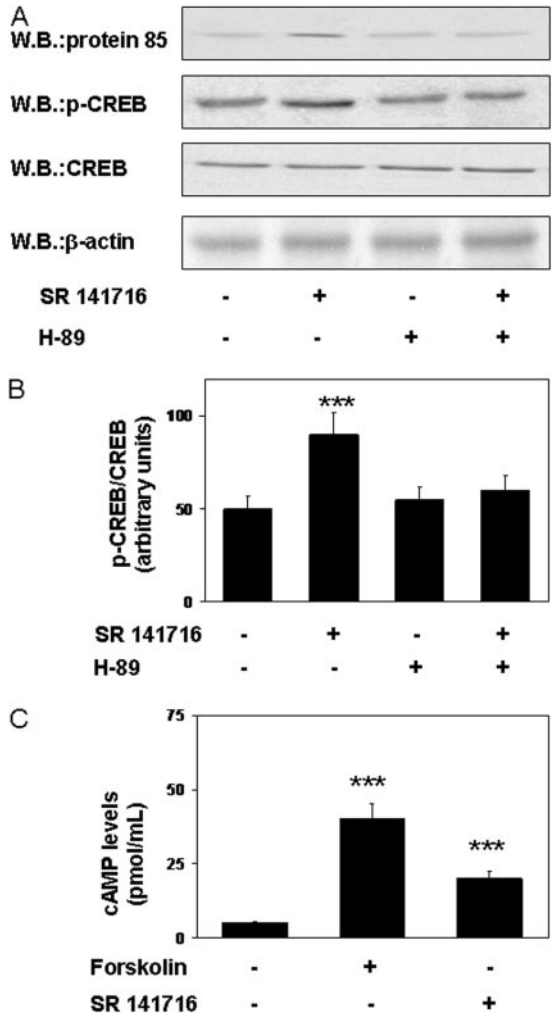

Fig. 5. SR141716 regulates p85 levels via PKA. A, cells were pretreated with 15 μM H-89 and incubated with 0.1 μM SR141716 for 24 h, as described in the legend to Fig. 2 and under *Materials and Methods*. Cell lysates were then analyzed by immunoblot with p85, CREB, phospho-CREB, and β-actin antibodies. The autoradiographs shown are representative of five independent experiments. B, filters obtained in A were analyzed by laser densitometry as described under *Materials and Methods*. Asterisks indicate statistically significant differences (***, $p < 0.001$). C, myotubes were exposed to 1 μM forskolin for 30 min and to 0.1 μM SR141716 for 24 h. Then the cells were assayed for cAMP production. Bars represent mean ± S.D. of three different experiments in triplicate. Asterisks indicate statistically significant differences versus untreated cells (***, $p < 0.001$).

serine phosphorylation, and this effect is prevented by H-89 pretreatment (Fig. 6).

Regulation of PI3K Signaling by CB1. Next, we investigated whether CB1 modulation affects signaling downstream PI3K. To this end, L6 cells have been treated with 0.1 μM SR141716. Immunodetection of the phosphorylated forms of PDK1, Akt/PKB, and PKCζ was taken as functional marker for PI3K activity (Fig. 7, A and B). Indeed, these kinases represent downstream targets of PI3K (Hirsch et al., 2007). Treatment with SR141716 increased the phosphorylation of all these proteins. The positive effect of SR141716 on PDK1, Akt/PKB, and PKCζ phosphorylation was already evident upon 30-min treatment and remained stable up to 24 h (Fig. 7, A and B). L6 myotubes were therefore pretreated with 10 μM LY294002, to block PI3K activity, or with 15 μM H-89, to block PKA activity, and stimulated with 0.1 μM SR141716 for 30 min or for 24 h. In both conditions, SR141716 failed to induce phosphorylation of PDK1, Akt/PKB, and PKCζ (Fig. 8, A and B). In addition, the effect of SR141716 on 2-DG uptake was blunted after LY294002 and H-89 pretreatment (Fig. 9A). Moreover, we investigated the SR141716 effect on 2-DG uptake in primary myocytes. Treatment with 0.1 μM SR141716 for 30 min or for 24 h stimulated 2-DG uptake ($p < 0.01$) by approximately 50%, a level similar to that observed upon short-term insulin stimulation (100 nM for 30 min) (Fig. 9B). In addition, the effect of SR141716 on 2-DG uptake was reverted after LY294002 and H-89 pretreatment (Fig. 9B).

Effect of CB1 Silencing on Glucose Uptake. Finally, we investigated whether CB1 silencing affects glucose uptake induced by SR141716. To this end, L6 cells were transfected with 100 nM siRNA-CB1, which specifically inhibited CB1 expression by approximately 80% (Fig. 10A). In untransfected L6 cells, SR141716 increased 2-DG uptake. It is interesting that the transfection of siRNA increased glucose uptake but abolished further increases induced by SR141716 (Fig. 10B). Moreover, the transfection of silencer negative control siRNA did not modify 2-DG uptake induced by SR141716 treatment (Fig. 10B).

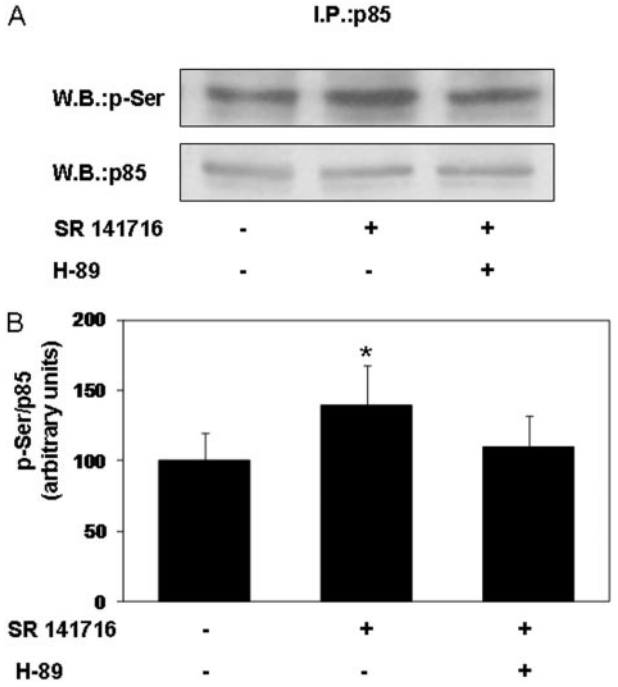

Fig. 6. SR141716 increases p85 phosphorylation via PKA. A, L6 myotubes were pretreated with 15 μM H-89 for 30 min and incubated with 0.1 μM SR141716 for additional 30 min, as described in the legend to Fig. 2 and under *Materials and Methods*. Cells were then solubilized, precipitated with anti-p85 antibodies, and immunoblotted with anti phosphoserine antibodies. The autoradiographs shown are representative of three independent experiments. B, filters obtained in A were analyzed by laser densitometry as described under *Materials and Methods*. Asterisks indicate statistically significant differences (*, $p < 0.05$).

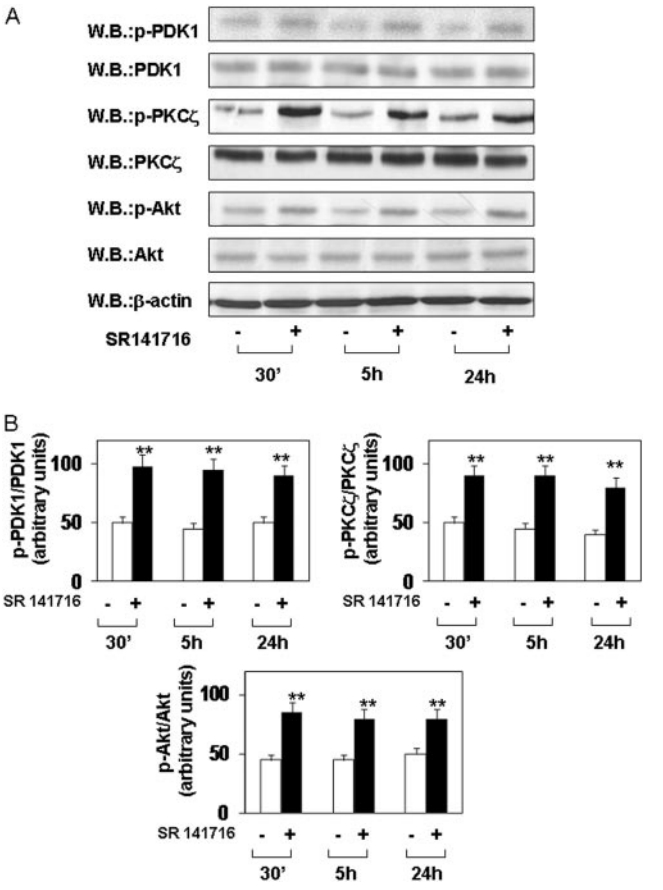

Fig. 7. Effect of CB1 modulation on PI3K signaling. A, L6 myotubes were incubated with 0.1 μM SR141716 for different times, as described in the legend to Fig. 2 and under *Materials and Methods*. Cells were then solubilized and phosphorylation and expression of PDK1, PKCζ, and Akt were analyzed by Western blot with specific antibodies (phospho-PDK1/PDK1, phospho-PKCζ/ PKCζ, phospho-Akt/Akt) as indicated. The autoradiographs shown are representative of three independent experiments. B, filters obtained in A were analyzed by laser densitometry as described under *Materials and Methods*. Asterisks indicate statistically significant differences (**, $p < 0.01$).

Discussion

The endocannabinoid system (ECS) is a crucial regulator of several physiological processes, including the control of energy balance (Osei-Hyiaman et al., 2006; Pagotto et al., 2006; Bifulco et al., 2007). Studies in genetically engineered murine models have, indeed, proven that removal of the CB1 receptor produces lean animals, with grossly modified feeding behavior and increased energy consumption (Ravinet Trillou et al., 2004). More recent evidence in humans has indicated that pharmacological blockade of CB1 is accompanied by significant reduction of body weight and of plasma levels of cholesterol and triglycerides (Despres et al., 2005;

Van Gaal et al., 2005). It also seems that ECS targeting reduces blood glucose levels (Hollander, 2007) and may directly regulate glucose metabolism in peripheral tissues. We have investigated the molecular mechanism by which CB1 exerts its modulatory action in the L6 cells, a well characterized model of differentiating skeletal muscle cells (Klip et al., 1982). Exposure of the myotubes to SR141716 significantly increased glucose uptake. No effect was elicited, instead, by SR144528 and IRTX, which are antagonists of CB2 and transient receptor potential vanilloid 1, respectively. Genetic silencing of CB1 by siRNA, instead, elicited similar effects as SR141716. This is also in agreement with the recent observation that treatment of leptin-deficient obese mice with CB1 antagonists enhances glucose uptake by skeletal muscle (Liu et al., 2005). Therefore, Cavuoto et al. (2007) have shown that CB1 agonists and antagonists modify the expression of genes regulating skeletal muscle oxidative pathways. Altogether, these observations indicate that, in addition to its effect in the central nervous system (Matias et al., 2006), and similar as in liver cells and adipocytes (Teixeira-Clerc et al., 2006; Gasperi et al., 2007), ECS may directly modulate nutrient metabolism in the skeletal muscle.

Elevated levels of endocannabinoids, which have been found in obese animal models (Di Marzo et al., 2001) and humans (Cote et al., 2007), may enhance CB1 activity and interfere with glucose metabolism in muscle cells. Thus, it is conceivable that activation of CB1 may down-regulate glucose uptake. Consistently, either genetic silencing or pharmacological interference up-regulates this function. However, whether SR141716 works as an antagonist, by inhibiting constitutive CB1 activity in the L6 cells, or as an inverse agonist, as largely recognized in other cell types (Bouaboula et al., 1997, Xie et al., 2007), is currently under investigation in our laboratories. It should be pointed out that the SR141716 effect occurred in the absence of exogenous anandamide and 2-arachidonoyl-glycerol, suggesting an inverse agonist effect. However, autonomous cellular production of endocannabinoids cannot be excluded, also raising the possibility of an antagonist effect of the compound. It is intriguing that higher concentrations of the compound produced a paradoxical decrease of 2-DG uptake. The latter effect is possibly due to the partial agonist activity of SR141716 (De Vry and Jentzsch, 2004; Krylatov et al., 2005). One alternative explanation could be found in the up-regulation of CB1 occurring at micromolar concentrations of SR141716 in the L6 cells and in the primary myocytes (data not shown). However, this effect is most probably a feature of cultured cell systems, and it may not occur "in vivo" because of the drug turnover, mainly operated by liver metabolism (Padwal and Majumdar, 2007).

As shown by protein expression profiling, the regulatory effect of CB1 on glucose uptake is not due to changes in cellular abundance of the main glucose transporters GLUT1 and GLUT4. The expression of major proteins involved in the early events of insulin action on glucose uptake was also

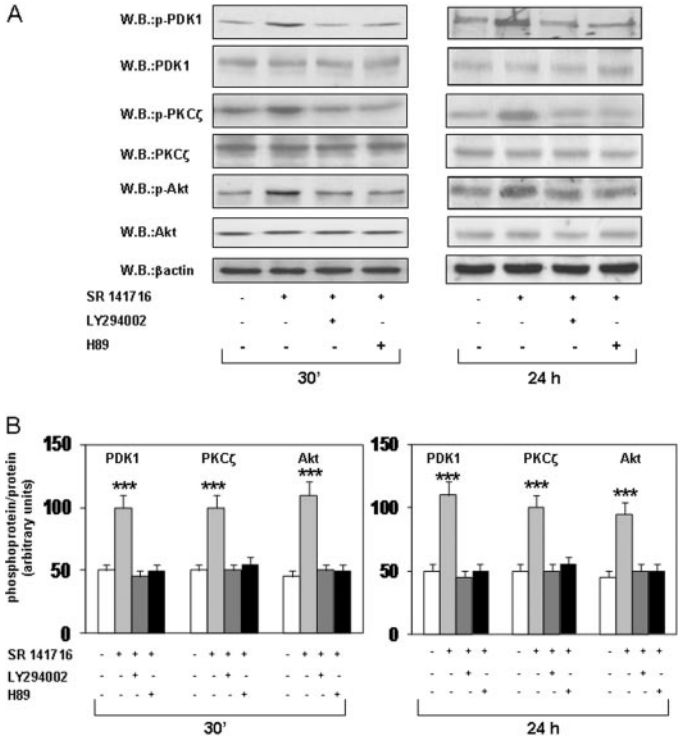

Fig. 8. SR141716 increases PI3K signaling via PKA. A, cells were serum-starved and incubated with LY294002 or with H-89, in the presence of 0.1 μM SR141716 for 30 min or for 24 h, as described in the legend to Fig. 2 and under *Materials and Methods*. Then cell extracts were subjected to SDS-PAGE followed by immunoblotting with specific anti phospho- or control antibodies, as indicated. The autoradiographs shown are representative of three independent experiments. B, filters obtained in A were analyzed by laser densitometry as described under *Materials and Methods*. Asterisks indicate statistically significant differences (**, $p < 0.01$).

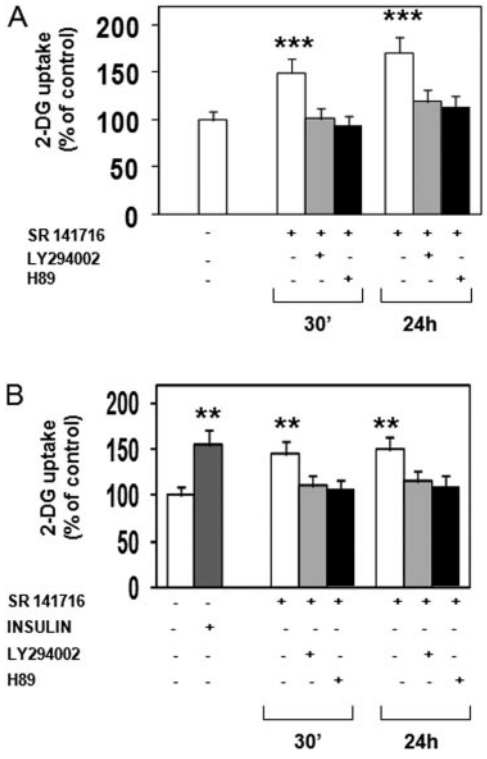

Fig. 9. SR141716 increases glucose uptake via PI3K and PKA. A, L6 myotubes were serum-starved and incubated with LY294002 or with H-89 in the presence of 0.1 μM SR141716 for 30 min or for 24 h. Then the cells were assayed for 2-DG uptake as described under *Materials and Methods*. Bars represent mean ± S.D. of three different experiments in triplicate (***, $p < 0.001$). B, primary myocytes were serum-starved for 24 h before exposure to 100 nM insulin for 30 min as indicated. On the other hand, myocytes were incubated with LY294002 or with H-89 in the presence of 0.1 μM SR141716 for 30 min or for 24 h. Then the cells were assayed for 2-DG uptake as described under *Materials and Methods*. Bars represent mean ± S.D. of three different experiments in triplicate (**, $p < 0.01$).

unmodified upon CB1 pharmacological targeting. Several lines of evidence indicate that CB1 regulation of glucose uptake occurs through PI3K signaling. First, dose- and time-dependent increases of both the regulatory (p85) and the catalytic (p110) subunits were observed after treatment with low concentrations of SR141716. Second, these effects were paralleled by increased activity of several PI3K downstream molecules (PDK1, PKCζ, and Akt/PKB). Third, the inhibition of PI3K activity counteracted the effect of SR141716 on glucose uptake.

It is noteworthy that the SR141716 effect occurred with both short- (30 min) and long-term incubation. This is only partially consistent with the timing of up-regulation of the PI3K subunits by the CB1 antagonist compound.

The molecular events involved in both short- and long-term CB1 regulation of PI3K require PKA activity. Indeed, in parallel with p85 and p110 expression, SR141716 induces increases in intracellular cAMP levels and CREB phosphorylation at a PKA consensus site. H-89, a pharmacological PKA blocker, inhibits both CREB phosphorylation and PI3K signaling as well as SR141716-induced glucose uptake. It is currently unknown whether CREB transcriptional activity is involved in CB1-mediated regulation of glucose uptake. It has been reported that CB1 is coupled to $G_{i/0}$ proteins (Howlett et al., 1986). Then, engagement of CB1 by endogenous ligands causes inhibition of adenylate cyclase and reduction of cellular cAMP levels (Bidaut-Russell et al., 1990). SR141716 may uncouple CB1 from the inhibitory proteins and increase cAMP levels, with a consequent activation of PKA. PKA, in turn, regulates the expression of both p85 and p110, at least in part, at the post-translational level as indicated by the experiments in the presence of protein synthesis inhibitors.

However, the rapid stimulatory effect of SR141716 on PI3K activity and glucose uptake cannot be accounted for by changes in the content of the PI3K subunits. CB1 modulation therefore may also either directly activate PI3K, independent of its expression, or regulate the activity of its downstream targets (i.e., Akt). This is consistent with the potential role of PKA to regulate PI3K activity in other cellular systems. It has been described recently that PKA phosphorylates p85 on Ser83 (Cosentino et al., 2007; De Gregorio et al., 2007). We have now shown that SR141716 increases serine phosphorylation of p85 in a PKA-dependent manner. Therefore, it could be inferred that CB1 modulates PI3K by a dual mechanism: 1) a short-term mechanism, which directly stimulates PI3K phosphorylation and activation, and 2) a long-term mechanism, mediated by the enhanced PI3K expression. Both effects are largely mediated by PKA activation.

Thus, at least in cultured cellular models, CB1 receptor exerts an inhibitory action on glucose uptake, which could be augmented by endocannabinoid stimulation. SR141716 removes the inhibitory constraint maintained by CB1 tonic activity and induces glucose uptake by cAMP/PKA- and PI3K-mediated pathways. Genetic silencing of CB1 in skeletal muscle cells further supports this hypothesis. In conclusion, beside antiobesity and antineoplastic effects (Van Gaal et al., 2005; Pi-Sunyer et al., 2006; Sarnataro et al., 2006; Bifulco et al., 2007), SR141716 may potentially possess a glucoregulatory function, which is exerted at least in part by direct regulation of glucose metabolism in skeletal muscle cells.

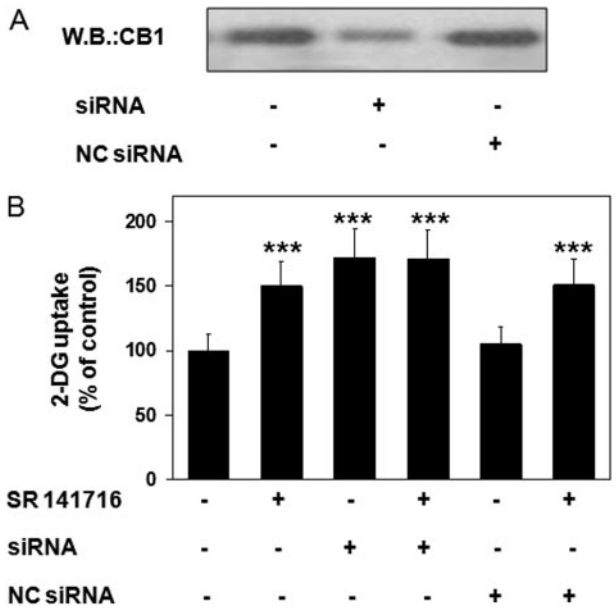

Fig. 10. Effect of CB1 silencing on glucose uptake. A, cells were transfected with siRNA-CB1 or with silencer negative control-1 siRNA. After 6 h, cells were serum-starved. Cell lysates were then analyzed by CB1 immunoblot as indicated. The autoradiographs shown are representative of three independent experiments. B, cells were treated as described above and incubated with 0.1 μM SR141716 for 16 h. Then they were assayed for 2-DG uptake as described under *Materials and Methods*.

References

Bensaid M, Gary-Bobo M, Esclangon A, Maffrand JP, Le Fur G, Oury-Donat F, and Soubrié P (2003) The cannabinoid CB1 receptor antagonist SR141716 increases Acrp30 mRNA expression in adipose tissue of obese fa/fa rats and in cultured adipocyte cells. *Mol Pharmacol* **63:**908–914.

Bidaut-Russell M, Devane WA, and Howlett AC (1990) Cannabinoid receptors and modulation of cyclic AMP accumulation in the rat brain. *J Neurochem* **55:**21–26.

Bifulco M, Grimaldi C, Gazzerro P, Pisanti S, and Santoro A (2007) Rimonabant: just an antiobesity drug? Current evidence on its pleiotropic effects. *Mol Pharmacol* **71:**1445–1456.

Bouaboula M, Perrachon S, Milligan L, Canat X, Rinaldi-Carmona M, Portier M, Barth F, Calandra B, Pecceu F, Lupker J, et al. (1997) A selective inverse agonist for central cannabinoid receptor inhibits mitogen-activated protein kinase activation stimulated by insulin or insulin-like growth factor 1. Evidence for a new model of receptor/ligand interactions. *J Biol Chem* **272:**22330–22339.

Boyd ST (2006) The endocannabinoid system. *Pharmacotherapy* **26:**218S–221S.

Caruso M, Miele C, Formisano P, Condorelli G, Bifulco G, Oliva A, Auricchio R, Riccardi G, Capaldo B, and Beguinot F (1997) In skeletal muscle, glucose storage and oxidation are differentially impaired by the IR1152 mutant receptor. *J Biol Chem* **272:**7290–7297.

Cavuoto P, McAinch AJ, Hatzinikolas G, Cameron-Smith D, and Wittert GA (2007) Effects of cannabinoid receptors on skeletal muscle oxidative pathways. *Mol Cell Endocrinol* **267:**63–69.

Cosentino C, Di Domenico M, Porcellini A, Cuozzo C, De Gregorio G, Santillo MR, Agnese S, Di Stasio R, Feliciello A, Migliaccio A, et al. (2007) p85 regulatory subunit of PI3K mediates cAMP-PKA and estrogens biological effects on growth and survival. *Oncogene* **26:**2095–2103.

Cota D, Marsicano G, Lutz B, Vicennati V, Stalla GK, Pasquali R, and Pagotto U (2003a) Endogenous cannabinoid system as a modulator of food intake. *Int J Obes Relat Metab Disord* **27:**289–301.

Cota D, Marsicano G, Tschöp M, Grübler Y, Flachskamm C, Schubert M, Auer D, Yassouridis A, Thöne-Reineke C, Ortmann S, et al. (2003b) The endogenous cannabinoid system affects energy balance via central orexigenic drive and peripheral lipogenesis. *J Clin Invest* **112:**423–431.

Cote M, Matias I, Lemieux I, Petrosino S, Almeras N, Despres JP, and Di Marzo V (2007) Circulating endocannabinoid levels, abdominal adiposity and related cardiometabolic risk factors in obese men. *Int J Obes (Lond)* **31:**692–699.

De Gregorio G, Coppa A, Cosentino C, Ucci S, Messina S, Nicolussi A, D'Inzeo S, Di Pardo A, Avvedimento EV, and Porcellini A (2007) The p85 regulatory subunit of PI3K mediates TSH-cAMP-PKA growth and survival signals. *Oncogene* **26:**2039–2047.

De Vry J and Jentzsch KR (2004) Partial agonist-like profile of the cannabinoid receptor antagonist SR141716A in a food-reinforced operant paradigm. *Behav Pharmacol* **15:**13–20.

Després JP, Golay A, and Sjöström L (2005) Rimonabant in Obesity-Lipids Study Group. Effects of rimonabant on metabolic risk factors in overweight patients with dyslipidemia. *N Engl J Med* **353:**2121–2134.

Di Marzo V, Goparaju SK, Wang L, Liu J, Bátkai S, Járai Z, Fezza F, Miura GI,

Palmiter RD, Sugiura T, et al. (2001) Leptin-regulated endocannabinoids are involved in maintaining food intake. *Nature* **410**:822–825.
Engeli S, Böhnke J, Feldpausch M, Gorzelniak K, Janke J, Bátkai S, Pacher P, Harvey-White J, Luft FC, Sharma AM, et al. (2005) Activation of the peripheral endocannabinoid system in human obesity. *Diabetes* **54:**2838–2843.
Formisano P, Oriente F, Miele C, Caruso M, Auricchio R, Vigliotta G, Condorelli G, and Beguinot F (1998) In NIH-3T3 fibroblasts, insulin receptor interaction with specific protein kinase C isoforms controls receptor intracellular routing. *J Biol Chem* **273:**13197–13202.
Gasperi V, Fezza F, Pasquariello N, Bari M, Oddi S, Agrò AF, and Maccarrone M (2007) Endocannabinoids in adipocytes during differentiation and their role in glucose uptake. *Cell Mol Life Sci* **64:**219–229.
Hirsch E, Costa C, and Ciraolo E (2007) Phosphoinositide 3-kinases as a common platform for multi-hormone signaling. *J Endocrinol* **194:**243–256.
Hollander P (2007) Endocannabinoid blockade for improving glycemic control and lipids in patients with type 2 diabetes mellitus. *Am J Med* **120 (2 Suppl 1):**S18–S32.
Howlett AC, Qualy JM, and Khachatrian LL (1986) Involvement of Gi in the inhibition of adenylate cyclase by cannabimimetic drugs. *Mol Pharmacol* **29:**307–313.
Jamshidi N and Taylor DA (2001) Anandamide administration into the ventromedial hypothalamus stimulates appetite in rats. *Br J Pharmacol* **134:**1151–1154.
Juan-Picó P, Fuentes E, Bermúdez-Silva FJ, Javier Díaz-Molina F, Ripoll C, Rodríguez de Fonseca F, and Nadal A (2006) Cannabinoid receptors regulate Ca^{2+} signals and insulin secretion in pancreatic beta-cell. *Cell Calcium* **39:**155–162.
Kahn SE (2003) The relative contributions of insulin resistance and beta-cell dysfunction to the pathophysiology of Type 2 diabetes. *Diabetologia* **46:**3–19.
Klip A, Logan WJ, and Li G (1982) Hexose transport in L6 muscle cells. Kinetic properties and the number of [^{3}H]cytochalasin B binding sites. *Biochim Biophys Acta* **687:**265–280.
Krämer DK, Al-Khalili L, Guigas B, Leng Y, Garcia-Roves PM, and Krook A (2007) Role of AMP kinase and PPARδ in the regulation of lipid and glucose metabolism in human skeletal muscle. *J Biol Chem* **282:**19313–19320.
Krylatov AV, Maslov LN, Lasukova OV, and Pertwee RG (2005) Cannabinoid receptor antagonists SR141716 and SR144528 exhibit properties of partial agonists in experiments on isolated perfused rat heart. *Bull Exp Biol Med* **139:**558–561.
Lazar MA (2005) How obesity causes diabetes: not a tall tale. *Science* **307:**373–375.
Liu YL, Connoley IP, Wilson CA, and Stock MJ (2005) Effects of the cannabinoid CB1 receptor antagonist SR141716 on oxygen consumption and soleus muscle glucose uptake in Lep(ob)/Lep(ob) mice. *Int J Obes (Lond)* **29:**183–187.
Matias I, Bisogno T, and Di Marzo V (2006) Endogenous cannabinoids in the brain and peripheral tissues: regulation of their levels and control of food intake. *Int J Obes (Lond)* **30 (Suppl 1):**S7–S12.
Nikodemova M, Kasckow J, Liu H, Manganiello V, and Aguilera G (2003) Cyclic adenosine 3′,5′-monophosphate regulation of corticotropin-releasing hormone promoter activity in AtT-20 cells and in a transformed hypothalamic cell line. *Endocrinology* **144:**1292–1300.
Osei-Hyiaman D, DePetrillo M, Pacher P, Liu J, Radaeva S, Bátkai S, Harvey-White J, Mackie K, Offertáler L, Wang L, et al. (2005) Endocannabinoid activation at hepatic CB1 receptors stimulates fatty acid synthesis and contributes to diet-induced obesity. *J Clin Invest* **115:**1298–1305.
Osei-Hyiaman D, Harvey-White J, Bátkai S, and Kunos G (2006) The role of the endocannabinoid system in the control of energy homeostasis. *Int J Obes (Lond)* **30 (Suppl 1):**S33–S38.
Padwal RS and Majumdar SR (2007) Drug treatments for obesity: orlistat, sibutramine, and rimonabant. *Lancet* **369:**71–77.
Pagotto U, Marsicano G, Cota D, Lutz B, and Pasquali R (2006) The emerging role of the endocannabinoid system in endocrine regulation and energy balance. *Endocr Rev* **27:**73–100.
Pi-Sunyer FX, Aronne LJ, Heshmati HM, Devin J, and Rosenstock J; RIO-North America Study Group (2006) Effect of rimonabant, a cannabinoid-1 receptor blocker, on weight and cardiometabolic risk factors in overweight or obese patients: RIO-North America: a randomized controlled trial [published erratum appears in *JAMA* **295:**1252]. *JAMA* **295:**761–775.
Poirier B, Bidouard JP, Cadrouvele C, Marniquet X, Staels B, O'Connor SE, Janiak P, and Herbert JM (2005) The anti-obesity effect of rimonabant is associated with an improved serum lipid profile. *Diabetes Obes Metab* **7:**65–72.
Ravinet Trillou C, Arnone M, Delgorge C, Gonalons N, Keane P, Maffrand JP, and Soubrie P (2003) Anti-obesity effect of SR141716, a CB1 receptor antagonist, in diet-induced obese mice. *Am J Physiol Regul Integr Comp Physiol* **284:**R345–R353.
Ravinet Trillou C, Delgorge C, Menet C, Arnone M, and Soubrié P (2004) CB1 cannabinoid receptor knockout in mice leads to leanness, resistance to diet-induced obesity and enhanced leptin sensitivity. *Int J Obes Relat Metab Disord* **28:**640–648.
Sarnataro D, Pisanti S, Santoro A, Gazzerro P, Malfitano AM, Laezza C, and Bifulco M (2006) The cannabinoid CB1 receptor antagonist rimonabant (SR141716) inhibits human breast cancer cell proliferation through a lipid raft-mediated mechanism. *Mol Pharmacol* **70:**1298–1306.
Teixeira-Clerc F, Julien B, Grenard P, Tran Van Nhieu J, Deveaux V, Li L, Serriere-Lanneau V, Ledent C, Mallat A, and Lotersztajn S (2006) CB1 cannabinoid receptor antagonism: a new strategy for the treatment of liver fibrosis. *Nat Med* **12:**671–676.
Van Gaal LF, Rissanen AM, Scheen AJ, Ziegler O, and Rössner S; RIO-Europe Study Group (2005) Effects of the cannabinoid-1 receptor blocker rimonabant on weight reduction and cardiovascular risk factors in overweight patients: 1-year experience from the RIO-Europe study [published erratum appears in *Lancet* **366:**370, 2005]. *Lancet* **365:**1389–1397.
Williams CM and Kirkham TC (2002) Observational analysis of feeding induced by Delta9-THC and anandamide. *Physiol Behav* **76:**241–250.
Xie S, Furjanic MA, Ferrara JJ, McAndrew NR, Ardino EL, Ngondara A, Bernstein Y, Thomas KJ, Kim E, Walker JM, et al. (2007) The endocannabinoid system and rimonabant: a new drug with a novel mechanism of action involving cannabinoid CB1 receptor antagonism—or inverse agonism—as potential obesity treatment and other therapeutic use. *J Clin Pharm Ther* **32:**209–231.
Yan ZC, Liu DY, Zhang LL, Shen CY, Ma QL, Cao TB, Wang LJ, Nie H, Zidek W, Tepel M, et al. (2007) Exercise reduces adipose tissue via cannabinoid receptor type 1 which is regulated by peroxisome proliferator-activated receptor-delta. *Biochem Biophys Res Commun* **354:**427–433.

Address correspondence to: Dr. Pietro Formisano, Dipartimento di Biologia e Patologia Cellulare e Molecolare, Università degli Studi di Napoli "Federico II", Via Pansini, 5-80131 Napoli, Italy. E-mail: fpietro@unina.it

SELECTIVE DISRUPTION OF INSULIN-LIKE GROWTH FACTOR-1 SIGNALLING VIA PHOSPHOINOSITIDE-DEPENDENT KINASE-1 PREVENTS PROTECTIVE EFFECTS OF IGF-1 ON HUMAN CANCER CELL DEATH.

A. Teresa Alberobello[1], Vittoria D'Esposito[1], Daniela Marasco[2], Menotti Ruvo[2], Roberto Bianco[3], Giampaolo Tortora[3], Iolanda Esposito[1], Francesca Fiory[1], Claudia Miele[1], Francesco Beguinot[1], and Pietro Formisano[1]

From Dipartimento di Biologia e Patologia Cellulare e Molecolare & Istituto di Endocrinologia ed Oncologia Sperimentale del CNR[1], Istituto di Biostutture e Bioimmagini del CNR[2], Dipartimento di Endocrinologia e Oncologia Molecolare e Clinica[3], Università di Napoli "Federico II", Naples, Italy

Running head: Targeting IGF-1R/PDK1 interaction in human cancer cells.

Address correspondence to: Pietro Formisano, Dipartimento di Biologia e Patologia Cellulare e Molecolare, Università di Napoli "Federico II", Via S. Pansini 5, 80131 Naples, Italy. Phone: +39-081-7464450; Fax: +39-081-7463235; e-mail: fpietro@unina.it

Insulin-like Growth Factor-1 (IGF-1) signaling system exerts a broad anti-apoptotic function and plays a crucial role in resistance to anti-cancer therapies. Exposure of MCF-7 breast cancer cells to IGF-1 rapidly and transiently induced tyrosine phosphorylation and activation of Phosphoinositide-Dependent Kinase-1 (PDK1). This was paralleled by Akt/Protein Kinase B and Protein Kinase C-ζ phosphorylation, at Thr308 and Thr410, respectively. IGF-1 treatment also enhanced PDK1 interaction with IGF-1 receptor (IGF-1R) in intact MCF-7 cells. Pull-down assays revealed that PDK1 bound IGF-1R in vitro, and the region encompassing amino acids 51-359 of PDK1 was necessary for the interaction. Synthetic peptides corresponding to IGF-1R C-terminus amino acids 1295-1337 (C43) reduced in vitro IGF-1R/PDK1 interaction and PDK1 tyrosine phosphorylation by activated IGF-1R, in a concentration-dependent manner. Similar peptides featuring replacement of Tyr1316 with phenylalanine were much less effective, however. Loading of fluoresceinated-C43 (FITC-C43) into MCF-7 cells significantly reduced IGF-1R/PDK1 interaction and phosphorylation of PDK1 substrates. Moreover, FITC-C43 intracellular loading reverted the protective effect of IGF-1 on growth factor deprivation-induced cell death. Finally, the inhibition of IGF-1R/PDK1 interaction and signalling by FITC-C43 was accompanied by 2-fold enhanced killing capacity of Cetuximab in human GEO colon adenocarcinoma cells and was sufficient to restore cell death in Cetuximab-resistant cell clones. Thus, disruption of PDK1 interaction with IGF-1R reduces IGF-1 survival effects in cancer cells and may enhance cell death by anti-cancer agents.

INTRODUCTION

The insulin-like growth factor (IGF) signalling system plays a key role in growth and development of many normal tissues and regulates overall growth of organisms (1). Type I insulin-like growth factor (IGF-1) has been identified as a regulator of cellular transformation and controls the acquisition of the tumorigenic phenotype by regulating multiple cellular functions that impact on the invasive/metastatic potential of cancer cells. These include cell survival, motility, invasion, growth potential in secondary organ sites, the induction of angiogenesis (2). There are also several lines of evidence that dysregulation of the IGF-1 system is involved in resistance to certain anticancer therapies, including cytotoxic chemotherapy, hormonal agents, biological therapies, and radiation (3). The link between cancer and IGF signalling is also consistent with recent epidemiological studies showing an increased relative risk for the development of colon, prostate, breast, lung, and bladder cancers in individuals with circulating IGF-1 levels in the upper tertile of the normal range (4). These findings were confirmed in animal models, where reduced circulating IGF-1 levels result in significant reductions in cancer development, growth, and metastases, whereas increased

circulating IGF-1 levels are associated with enhanced tumor growth (5).

Aberrant expression of the receptor for IGF-1 (IGF-1R) has been implicated in malignant transformation of cells (6, 7). IGF-1R is normally activated by binding of the secreted growth factor ligand to the extracellular domain. This, in turn, triggers a number of cellular signalling pathways, including the phosphatidylinositol 3-kinase (PI3K) pathway, the main mechanism by which IGF-1R protects cells from apoptosis (8, 9).

Phosphoinositide-dependent protein kinase 1 (PDK1) plays a crucial role in mediating signal transduction downstream of PI3K (10). PDK1 is a 64-kDa protein, of 556 amino acids, comprised of a serine/threonine kinase domain near the N-terminus, a C-terminal pleckstrin homology (PH) domain, and an ATP-binding site located between the two domains (11). PDK1 phosphorylates several protein kinases, including Akt/PKB and PKCs, at the activation loop phosphorylation sites (11-13). Phosphorylation of Ser_{241} at its own activation loop may be mediated by an intermolecular mechanism suggesting that dimerization and *trans*-phosphorylation may regulate PDK1 activity in cells (10, 11, 14). There is also evidence that PDK1 undergoes tyrosine phosphorylation in response to several growth factors. Studies with the tyrosine phosphatase inhibitor pervanadate and insulin indicate that full activation of PDK1 requires phosphorylation at $Tyr_{373/376}$ (15-17). Consistent with its role in transformation, PDK1 is highly expressed in a large number of invasive human breast cancer cell lines and in ovarian cancers (18, 19).

Collectively, a large body of evidence identifies the IGF-1R/PDK1 system as a target for molecular therapy with potential benefits for a wide spectrum of human malignancies (3, 4, 20). Various strategies have been used to target components of this system in established cancer cell lines and animal models, and some of these strategies may be advancing to clinical use. Among them, down-regulation of IGF-1R by antisense oligonucleotides, antisense RNA, small interfering RNA, single chain antibody, full humanized anti-IGF-1R monoclonal antibodies and specific kinase inhibitors have been attempted (8, 21). Some of these molecular strategies to target the IGF-1 system, however, have failed for the magnitude of toxicity, due, at least in part, to the cross reactivity with the insulin system.

Here, we show that IGF-1R directly interacts with and activates PDK1. Synthetic peptides corresponding to the IGF-1R C-terminus selectively displace the interaction *in vitro* and reduce IGF-1 signalling via PDK1 in human cancer cell lines, preventing IGF-1 pro-survival effects and facilitating cell killing by anti-cancer agents.

EXPERIMENTAL PROCEDURES

Materials. Media, sera, and antibiotics for cell culture were from Invitrogen (Invitrogen Corporation, Paisley, United Kingdom). Antibodies against PDK1, IGF-1 Receptor α subunit, IGF-1 Receptor β subunit, phospho-Thr_{308} Akt1/PKB and Akt/PKBα were purchased from Upstate Biotechnology (Lake Placid, NY). PKCζ, phospho-Thr_{410} PKCζ and extracellular signal-regulated kinases antibodies were from Santa Cruz Biotechnology (Santa Cruz, CA). Phospho-Ser_{473} Akt, phospho-Ser_{241} PDK1, Phospho-$Tyr_{373/376}$ PDK1 and phospho-Thr_{202}/Tyr_{204} ERK were obtained from Cell Signaling Technology (Danvers, MA). Recombinant human IGF-1 was from PeproTech (London, UK). The p-EBG-2T expression vector containing the cDNA of the human full length PDK1 and the cDNA of PDK1 deletion mutants were a generous gift of Dr. D.R. Alessi (University of Dundee) and have been previously described (22). Protein A-Sepharose beads and enhanced chemiluminescence (ECL) reagents were from Pierce (Rockford, USA). Agarose-bound Wheat Germ Agglutinin (WGA) was from Vector (Vector Laboratories Inc., Burlingame, CA), sodium dodecyl sulfate-polyacrylamide gel electrophoresis (SDS-PAGE) reagents from Bio-Rad (Richmond, VA). Nα-protected Fmoc-amino acid derivatives and coupling reagents for peptide synthesis were from Inbios (Pozzuoli, Italy). HPLC-grade solvents and trifluoroacetic acid (TFA) were from LabScan (Stillorgan, Dublin, Ireland). All the other chemicals were from Sigma-Aldrich (St. Louis, MO).

Cell cultures. MCF-7 cells, L6 cells and NIH-3T3 cells stably transfected with IGF-1 receptor (NIH-3T3^{IGF-1R}) (23) were plated (6×10^3 cells/cm^2) and grown in Dulbecco's modified Eagle's medium (DMEM) supplemented with 10% fetal bovine serum and 2 mM glutamine, 100 IU/ml penicillin, 100 IU/ml streptomycin. GEO and GEO-CR (24) colon cancer cells were cultured in McCoy's medium supplemented with 10% fetal bovine serum, 20 mM Hepes (pH 7.4), 2mM glutamine. Cultures were maintained in humidified atmosphere of 95% air and 5% CO_2 at 37 C. L6 differentiation has been achieved as previously described (Caruso et al., 1997).

Immunoblot and Immunoprecipitation Procedure. Cells were solubilized for 20 min at 4C with lysis buffer containing 50 mM HEPES, 150 mM NaCl, 10 mM EDTA, 10 mM $Na_4P_2O_7$, 2 mM sodium orthovanadate, 50 mM NaF, 1 mM phenylmethylsulfonyl fluoride, 10 µg/ml aprotinin, 10 µg/ml leupeptin, pH 7.4, and 1% (v/v) Triton X-100. The lysates were clarified by centrifugation at 12,000*g* for 20 min at 4C. Proteins were separated by SDS-polyacrylamide gel electrophoresis and blotted on Immobilon-P membranes (Millipore, Billerica, MA). Membranes were blocked for 1 h in TBS (10 mM Tris-HCl, pH 7.4, and 140 mM NaCl) containing 4% (w/v) bovine serum albumin and then incubated with the indicated antibodies. Detection of blotted proteins was performed by ECL according to the manufacturer's instruction. Immunoprecipitation experiments were performed as previously described (25). Densitometric analysis was performed using a Scion Image Analyzer. All the data were expressed as mean ± SD. Significance was assessed by Student's t test for comparison between two means. Data were analyzed with Statview software (Abacusconcepts) by one-factor analysis of variance. P values of less than 0.05 were considered statistically significant.

IGF-1 receptor purification. IGF-1R were partially purified by WGA affinity chromatography. Confluent monolayers of NIH-3T3^{IGF-1R} cells (corresponding to 6-8 x 10^7 cells) were solubilized in lysis buffer. The insoluble material was separated by ultracentrifugation at 100,000 x g for 1 h at 4 C. The supernatant was applied to a WGA-Sepharose column pre-equilibrated with HNT buffer (50 mM HEPES, 150 mM NaCl and 0.1% Triton) and the protease inhibitors described above. The column was extensively washed using the same buffer, and bound glycoproteins were eluted in the same buffer containing 0.3 M N-acetylglucosamine (26).

Pull down assay. PDK1-glutatione *S*-transferase (GST) fusion proteins were generated as described (22). Purified IGF-1R (50 µg protein extract) was incubated in the presence of Sepharose-bound GST-PDK1 (2 µg) for 2 h at 4 C. The beads were washed two times with HNT buffer, then resuspended in loading buffer, heated to 95 C for 5 min and centrifuged at 25,000 x g for 3 min. Supernatants were separated by SDS-PAGE followed by immunoblotting with appropriate antibodies.

In vitro PDK1 tyrosine phosphorylation. Purified IGF-1R (50 µg protein extract) was incubated in the presence of IGF-1 (100 ng/ml). Phosphorylation reactions were initiated by adding 2 mM CTP, 2 µM ATP, 10 mM HEPES, pH 7.4, 0.02% Triton X-100, 5 mM $MnCl_2$, 7 mM $MgCl_2$ (final concentrations) and prolonged for 30 min at 22 C. Recombinant PDK1 was added for 15 min. The reaction was stopped on ice and proteins were separated by SDS-PAGE and analyzed by Western blotting with phosphotyrosine antibodies.

Peptide synthesis and purification. Solid-phase peptide syntheses were carried out on a fully automated peptide synthesizer 433A (Applied Biosystems). Preparative RP-HPLC purifications were carried out on a Shimadzu LC-8A instrument, equipped with a SPD-M10 AV detector and using a Phenomenex Luna-COMBI C18 column (50x22 mm ID; 10 µm). LC-MS analyses were carried out on an LCQ DECA XP Ion Trap mass spectrometer (ThermoElectron, Milan, Italy) equipped with an OPTON ESI source, operating at 4.2 kV needle voltage and 320 C and with a complete Surveyor HPLC system. LC-MS columns were from ThermoElectron. Peptides were prepared by solid phase synthesis following standard Fmoc/tBu protocols (27). To monitor cell delivery, N-terminal fluoresceine labelling was

achieved by on-resin treatment with fluorescein isothiocyanate (FITC). Cleavage from the solid support was performed by treatment with a trifluoroacetic acid (TFA)/tri-isopropyl-silane (TIS)/water (90:5:5, v/v/v) mixture for 90 min at RT, then crude peptides were precipitated in cold ether, dissolved in a water/acetonitrile (1:1, v/v) mixture and lyophilized. Products were purified by RP-HPLC applying a linear gradient of CH_3CN, 0.1% TFA (Solvent B) from 5% to 65% over 40 min. Solvent A was 0.1% TFA in water. Flow rate was 20 ml/min. Peptides purity and identity were confirmed by LC-MS.

Peptide loading into cultured cells. Peptides were delivered onto MCF-7 cells by using the ProVectin Protein delivery reagents method according to the manufacture's instructions. Briefly, the dry film of ProVectin reagent found in glass vial was dissolved with 250 µl of methanol and vortexed for 10-20 seconds. 20 µl of ProVectin reagent for a 60-mm-diameter dishes were recommend. The total amount of ProVectin needed was pipetted into an eppendorf tube and left under a laminar flow hood to evaporate the solvent for at least 2 hours at room temperature and then hydrated with PBS. Peptides, diluted in PBS, were added to ProVectin reagent at different concentrations and let stand at room temperature for 5 min. The ProVectin/peptide complexes were added directly onto the cells cultured in serum-free DMEM for 24 h.

Cell death analysis. For detecting apoptosis, the cells were kept in the presence or in the absence of serum or incubated with 10 mM synthetic peptides, as indicated in the description of the individual experiments. Apoptosis was then assayed using the Apoptosis ELISA Plus kit (Roche Diagnostics GmbH, Mannheim, Germany), according to the manifacturer's instructions or by cytometric analysis. Briefly, cells were harvested and suspended in 0.3 ml of PBS. After adding 0.7 ml of cold absolute ethanol, cells were fixed and stored for at least 2 h at –20 C. For analysis, cells were centrifuged, resuspended in PBS containing 0.1mg/ml RNaseA and 40 µg/ml propidium iodide and incubated in dark for 30 min at room temperature. Samples were kept on ice and the analysis was performed using FACS Cyan cytometer (Dako Cytomation, USA). A minimum of 30000 events were collected for each sample. Sub-G1 phase cells were identified using Summit V 4.3 software (Dako).

Fluorescence microscopy. Cells, loaded with FITC-peptides, were fixed with 3% formaldehyde for 15 min at 37 C, washed three times with PBS and incubated for 10 min at RT with DAPI diluted 1: 1000 in TBS. All slides were then washed three times with TBS 0.1% Tween and kept in dark until examined under a fluorescence microscope.

2-Deoxy-D-glucose Uptake. The measurement of 2-deoxy-D-[14C] glucose uptake was taken as a readout of glucose uptake by muscle cells, as previously described (Klip et al., 1982). Cells were incubated in serum free DMEM supplemented with 0.2% (w/v) bovine serum albumin for 18 h in the presence or absence of C43 or SP 10 µM. Cells were incubated in glucose-free 20 mM HEPES, pH 7.4, 140 mM NaCl, 2.5 mM MgSO4, 5 mM KCl, 1 mM CaCl2 (HEPES buffer) and exposed or not to 100 nM insulin for 30 min. Glucose uptake was measured by incubating cells with 0.15 mM 2-deoxy-D-[^{14}C]glucose (0.5µCi/assay) for 15 min in HEPES buffer. The reaction was terminated by the addition of 10 µM cytochalasin B, and the cells were washed three times with ice-cold isotonic saline solution prior to lysis in 1 M NaOH. Incorporated radioactivity was measured in a liquid scintillation counter.

RESULTS

IGF-1 induces PDK1 tyrosine phosphorylation and co-precipitation with IGF-1R in MCF-7 cells. We analyzed tyrosine phosphorylation of PDK1 in response to IGF-1 in human breast cancer cells. MCF-7 cells were incubated with serum-free medium and treated with IGF-1 (100 ng/ml) for 5 and 30 min. Western blot analysis with antibodies specifically recognizing $pTyr_{373/376}$-PDK1, revealed that IGF-1 rapidly induces tyrosine phosphorylation of endogenous PDK1, compared to the control cells. Tyrosine phosphorylation returned close to the basal levels after 30 min, with no change in the total

PDK1 levels (Fig. 1A). To gain further insights into the molecular mechanism of PDK1 phosphorylation, we tested the ability of IGF-1R to interact with PDK1. To this aim, MCF-7 cells were stimulated with IGF-1 (100ng/ml) and cell lysates were precipitated with IGF-1R antibodies followed by blotting with PDK1 antibodies. As shown in Fig. 1B, an interaction between IGF-1R and PDK1 occurred after 5 min of IGF-1 exposure while, as in the case of tyrosine phosphorylation, the interaction was poorly detectable after 30 min. Immunoblotting with specific antibodies also revealed that IGF-1R-associated PDK1 was phosphorylated at Ser_{241} (Fig. 1B). Moreover, stimulation of MCF-7 cells with IGF-1 increased phosphorylation of Akt/PKB and PKCζ, at the PDK1 consensus sites, indicating the induction of PDK1 activity. Control detection with Akt/PKB and PKCζ antibodies revealed no difference in the total levels (Fig.1C).

IGF-1R directly interacts with and phosphorylates PDK1 *in vitro*. In order to determine the PDK1 portion involved in the interaction with IGF-1R, recombinant GST fused with full-length PDK1 protein (residues 1-556), two PDK1 mutants lacking the PH domain (corresponding to residues 1-359 and 51-359, respectively), and the PH domain alone (residues 408-556) were used in pull-down experiments with purified IGF-1R. IGF-1R was detectable in GST-pull down experiments with the full length PDK1. The interaction was also well detectable for $PDK1_{51-359}$ and $PDK1_{1-359}$, while it was almost completely absent with $PDK1_{408-556}$ (Fig. 2A).

It has been previously reported (17) that the region corresponding to the insulin receptor (IR) C-terminus is critical for the interaction with PDK1. With this background, peptides corresponding to the C-terminal residues 1295-1337 of IGF-1R (C43), 1316-1337 (C22) and similar peptides featuring tyrosine replacement with phenylalanine (C43F and C22F) were synthesized (Fig. 2B). In pull-down assays (Fig. 2C), C43 peptide displayed the highest ability to reduce IGF-1R/PDK1 interaction (ED_{50} = 80 nM). At variance C43F (ED_{50} = 1 μM), C22 (ED_{50} >1 μM) and C22F (ED_{50} >1 μM) were significantly less effective (Fig. 2C). Furthermore, a synthetic peptide corresponding to the IR C-terminus (C-IR) and a scrambled peptide (SP) did not significantly impair IGF-1R/PDK1 interaction (Fig. 2C). Similarly, co-incubation with C43 reduced tyrosine phosphorylation of PDK1 by activated IGF-1R in a concentration-dependent manner (Fig. 2D).

IGF-1R C-terminus peptides reduce PDK1 signalling and prevent IGF-1 protection from apoptosis in MCF-7 cells. In order to evaluate the ability to reduce IGF-1R/PDK1 interaction in intact cells, C43 was conjugated to fluorescein isothiocyanate (FITC-C43) and loaded into MCF-7 cells at different concentrations (range: 100 nM – 10 μM). Peptide loading was confirmed by FACS analysis (Fig. 3A) and fluorescence microscopy (Fig. 3B). Next, MCF-7 cells were loaded with 10 μM FITC-C43 and stimulated for 5 min with 100 ng/ml IGF-1. As shown in Fig. 4A, peptide loading decreased IGF-1R/PDK1 co-precipitation in response to IGF-1, as compared to a scrambled peptide (FITC-SP). Consistently, FITC-C43 loading was paralleled by reduced Akt/PKB and PKCζ phosphorylation in response to IGF-1 (Fig. 4B and 4C). ERK1/2 phosphorylation was preserved, instead.

In the MCF-7 cells, exposure to IGF-1 for 16 h rescued cell death induced by growth factor deprivation (Fig. 5A and 5B). Therefore, we wanted to prove the principle that IGF-1 protective effect on cell death could be reverted by disrupting the interaction between IGF-1R and PDK1. To this aim, 10μM FITC-peptides (C43, C43F, C22, C22F and C-IR) were loaded into MCF-7 cells before the treatment with IGF-1. Interestingly, loading of C43 completely reverted IGF1 protective action, while no significant effect was elicited by the other peptides (Fig. 5A and 5B).

Effect of C43 on glucose uptake in L6 cells. In order to investigate whether reduced IGF-1R/PDK1 interaction may affect glucose uptake in a skeletal muscle cell model we have performed a 2-deoxy-glucose (2-DG) uptake assay in L6 cells in the absence or in the presence of 10 μM of C43 or SP (Fig. 5C). No significant effect was achieved following treatment of L6 cells with C43 or SP (Fig. 5C).

Synergic effect of C43 and Cetuximab on GEO and GEO-CR cells. It has been shown that switching to the IGF-1R pathway is a common mechanism to promote resistance to anti-EGFR treatment (28). The correlation between IGF-1R activation and acquired resistance to EGFR inhibitors has been demonstrated for several cancer cell lines (29). Therefore, we investigated whether C43 could affect the response to Cetuximab (C225) in human colon adenocarcinoma cells (GEO cells) and in a clone of GEO cells resistant to Cetuximab action (GEO-CR). FITC-C43 or FITC-SP (10 μM) were loaded into GEO and GEO-CR and the entry was assessed by FACS and fluorescence microscopy (data not shown). In GEO cells, C225 increased cell death by 1,5-fold. FITC-C43 loading did not significantly change basal cell death, compared to the control, but enhanced the effect of C225 up to 2-fold (Fig. 6). As expected, C225 was ineffective in GEO-CR cells. However, when FITC-C43 was loaded into the cells, C225 effect was detectable at levels similar to those observed in GEO cells. No effect was elicited when FITC-SP was loaded in the cells (Fig. 6).

Next, we analyzed the effect of C43 on IGF-1 signalling in GEO and GEO-CR cells. IGF-1R total content and tyrosine phosphorylation were unchanged by the peptide (data not shown). In both cell lines FITC-C43 loading decreased IGF-1-induced PDK1 tyrosine phosphorylation (Fig. 7A) and IGF-1R co-precipitation (Fig. 7B), while no effect was elicited by FITC-SP. We also analyzed Akt/PKB phosphorylation, as a marker for PDK1 activity. As shown in Fig. 6C, FITC-C43, but not FITC-SP, reduced Akt/PKB phosphorylation in response to IGF-1, both in GEO and GEO-CR cells. Nevertheless, upon FITC-C43 loading, IGF-1-induced ERK1/2 phosphorylation was preserved in GEO cells, but reduced in GEO-CR cells (Fig. 7C).

DISCUSSION

Targeting IGF-1R signalling pathways represents an attractive strategy for innovative therapeutic approaches (3, 30-32). Therefore, understanding the details of IGF-1R signalling may be beneficial to envision tailored strategies.

We have described that upon ligand binding, IGF-1R directly interacts with and phosphorylates PDK1 at $Tyr_{373/376}$. The molecular interaction may account, at least in part for the specificity of IGF-1 signals via PDK1. Indeed, recruitment of kinases in close proximity of specific ligand-receptor complexes may selectively direct their further action (12). The interaction between PDK1 and IGF-1R requires residues 51-359 of PDK-1, and not the PH domain (aa 408-556), which is located at the C-terminus of the molecule. However, the substrate tyrosines are distal to the former portion. Thus, one may hypothesize that the PH domain of PDK1 binds to plasma membrane lipids (33, 34), and the N-terminal portion interacts with the IGF-1R β-subunit, thereby locating the tyrosines in proximity of IGF-1R catalytic domain. IGF-1R C-terminal residues are likely involved in PDK1 binding. Indeed, *in vitro*, a synthetic peptide corresponding to the IGF-1R C-terminus (residues 1295-1337; C43) inhibits the interaction between the two molecules.

This hypothesis is further supported by the finding that intracellular loading of C43 peptide prevents co-precipitation of PDK1 with IGF-1R antibodies, both in MCF-7, breast cancer, and in GEO, colon cancer cells. Moreover, C43 loading in intact cells reduced IGF-1-stimulated phosphorylation of the PDK1 substrates Akt/PKB and PKCζ, suggesting that either interaction with IGF-1R or tyrosine phosphorylation are needed for eliciting downstream effects. Similarly, C43 loading is sufficient to impair IGF-1 anti-apoptotic effect. This is consistent with previous findings indicating that PI3K activation is a relevant mechanism for IGF-1-mediated cell survival (35). This is also consistent with previous work by Baserga and LeRoith groups, demonstrating that the C-terminus portion is required for the transforming potential of the IGF-1R (36). In addition, a peptide bearing substitution of Tyr_{1316} with a phenylalanine (C43F) failed to be as effective as the wild-type C43. These observations suggest that Tyr_{1316} is necessary for the interaction with PDK1. However, neither a similar peptide, corresponding to the insulin receptor C-terminus (containing a tyrosine in a similar position), nor shorter peptides containing or not Tyr_{1316} (residues 1316-1337; C22, C22F), were able to elicit comparable effects. Noteworthy, the upper segment of C43

(residues 1295-1316) displayed weaker homology with the corresponding IR fragment, compared to the lower segment (see Fig. 2B) Thus, one might speculate that the specificity of interaction resides in the amino acid stretch immediately upstream Tyr_{1316}.

Reiss et al. reported that a peptide encompassing residues 1282-1298 (peptide 2) induces apoptosis in mouse embryo fibroblasts, with minor changes in IGF-1 signalling, suggesting that peptide 2 *per se* could elicit the activation of caspase cascade (37). While we cannot exclude the possibility that C43 may directly impinge on the caspase pathway as well, our *in vitro* data indicate that the main mechanism could be related to its ability to interfere with IGF-1R/PDK1 interaction. Nevertheless, the other peptides at the concentration used (10 μM) slightly increased apoptosis in the absence of alterations in IGF-1 signalling, further exploiting the concept that the C-terminus fragment of the IGF-1R may possess an intrinsic pro-apoptotic function (38, 39).

Previous findings indicated that IGF-1 alters sensitivity to several anticancer drugs by inhibiting apoptosis (40). More recent evidence also points to IGF-1 as a major candidate for the acquired resistance to tyrosine kinase inhibitors and monoclonal antibodies as cancer therapeutics (41, 42). Up-regulation of IGF-1 or IGF-1R (43), down-regulation of IGF-binding proteins (44), heterodimerization of the IGF-1R with other tyrosine kinase receptors (28, 45) are putative mechanisms accounting for drug resistance. On the other hand, the use of mAbs or inhibitors of IGF-1R tyrosine kinase, although effective in a number of human tumors (46), have encountered difficulties, at least in part, because of the cross-interference with insulin receptor signalling (47). One of the potential mechanisms involves the signalling through PDK1 by both pathways.

Indeed, PDK1 beside being a potential molecular target for cancer therapy (20) is largely involved in the control of glucose metabolism. Pharmacologic or genetic blockade of PDK1 enhances apoptosis but severely affects glucose metabolism in animal models (48, 49). Moreover, 7-Hydroxystaurosporine (UCN-01), a non-selective inhibitor of PDK1, has shown anti-apoptotic activity in cancer cells (50) and has been tested in Phase I trials (51, 52). Although displaying an acceptable toxicity profile, hyperglycaemia is a relevant adverse event, possibly due to the major role exerted by PDK1 in regulation of insulin-stimulated glucose metabolism (51). We now show that pathway-selective strategies may help to discriminate between IGF-1R and IR signalling via PI3K/PDK1. In this regard, C43 loading into L6 skeletal muscle cells does not significantly inhibit insulin-stimulated glucose uptake (Fig. 5C).

Disrupting communication between IGF-1R and PDK1, by means of C43, is sufficient to prevent IGF-1 protection from apoptosis induced by growth factor deprivation. In addition, C43 exposure of GEO cells enhanced cell death following treatment with cetuximab and, importantly, restored cell killing in cetuximab-resistant clones. It has been recently suggested that combined inhibition of IGF-1 signals, which mainly occurs via PI3K, and EGF signals, mainly via ERK, results in a synergistic effect in colon cancer cells (53). We now observe that targeting IGF-1R C-terminus in a cetuximab-resistant clone of colon cancer cells, although *per se* not sufficient to induce cell death, blocked both PDK1 and ERK1/2 activation and restored sensitivity to cetuximab, supporting the hypothesis that both pathways are needed to escape cell death. The mechanism by which C43 may also interfere with ERK activation remains to be elucidated. Since no hyper-expression/hyper-activation of IGF-1 signalling components has been detected in GEO-CR cells, IGF-1R/EGFR hybrid formation could explain the differential impairment of the ERK pathway by C43. This is a less likely possibility, however, since C43 failed to inhibit EGF signalling in both GEO and GEO-CR cells (data not shown). Alternatively, as also described in other cell types (54), PDK1 may directly regulate MEK/ERK pathway. Whether and how this occurs in GEO-CR and not in GEO cells, however remains unclear. In addition, in drug resistant cells, IGF-1R may have acquired the ability through its C-terminus to recruit different signalling complexes, finally leading to ERK1/2 activation (55).

Thus, we have provided the proof of principle that targeted disruption of IGF-1R/PDK1 interaction prevents anti-apoptotic action of IGF-1 and may facilitate cell killing by anticancer

agents. Moreover, selectively interfering with IGF-1R signalling restores cell death in cetuximab resistant colon cancer cells.

ACKNOWLEDGMENTS

A.T. Alberobello and V. D'Esposito equally contributed. The authors wish to thank Dr. Dario R. Alessi (University of Dundee) for generously providing PDK1 constructs and Prof. Massimo Santoro for critical reading of the manuscript. This study was supported by the European Community's FP6 EUGENE2 (LSHM-CT-2004–512013) and the FP7 PREPROBEDIA (#201681) grants, European Federation for the Study of Diabetes, grants from the Associazione Italiana per la Ricerca sul Cancro (AIRC), and from the Ministero dell'Università e della Ricerca Scientifica (PRIN and FIRB). The financial support of Telethon – Italy is also gratefully acknowledged.

REFERENCES

1. Samani, A. A., Yakar, S., LeRoith, D., and Brodt, P. (2007) *Endocr. Rev.* **28**, 20-47
2. Samani, A. A., and Brodt, P. (2001) *Surg. Oncol. Clin. N. Am.* **10**, 289-312
3. Ryan, P. D., and Goss, P. E. (2008) *Oncologist* **13**, 16-24
4. LeRoith, D., and Helman, L. (2004) *Cancer Cell.* **5**, 201-202
5. Wu, Y., Cui, K., Miyoshi, K., Hennighausen, L., Green, J.E., Setser, J., LeRoith, D., and Yakar, S. (2003) *Cancer Res.* **63**, 4384
6. Zhang, L., Zhou, W., Velculescu, V. E., Kern, S. E., Hruban, R. H., Hamilton, S. R., Vogelstein, B., and Kinzler, K. W. (1997) *Science* **276**, 1268–1272
7. Ouban, A., Muraca, P., Yeatman, T., and Coppola, D. (2003) *Hum. Pathol.* **34**, 803-8
8. Pollak, M. (2008) *Nat. Rev. Cancer* **8**, 915-28. Erratum in: *Nat. Rev. Cancer.* (2009) **9**, 224
9. Chitnis, M. M., Yuen, J. S., Protheroe, A. S., Pollak, M., and Macaulay, V. M. (2008) *Clin. Cancer Res.* **14**, 6364-70
10. Mora, A., Komander, D., van Aalten, D. M., and Alessi, D. R. (2004) *Semin. Cell. Dev. Biol.* **15**, 161-70
11. Biondi, R. M., Komander, D., Thomas, C. C., Lizcano, J. M., Deak, M., Alessi, D. R., and van Aalten, D.M. (2002) *EMBO J.* **21**, 4219-28
12. Casamayor, A., Morrice, N. A., and Alessi, D. R. (1999); *Biochem. J.* **342**, 287-92
13. Toker, A., and Newton, A. C. (2000) *J. Biol. Chem.* **275**, 8271-4
14. Wick, M. J., Ramos, F. J., Chen, H., Quon, M. J., Dong, L. Q., and Liu, F. (2003) *J. Biol. Chem.* **278**, 42913-9
15. Grillo, S., Grémeaux, T., Casamayor, A., Alessi, D. R., Le Marchand-Brustel, Y., and Tanti, J. F. (2000) *Eur. J. Biochem.* **267**, 6642-9
16. Park, J., Hill, M. M., Hess, D., Brazil, D. P., Hofsteenge, J., and Hemmings, B. A. (2001) *J. Biol. Chem.* **276**, 37459-71
17. Fiory, F., Alberobello, A. T., Miele, C., Oriente, F., Esposito, I., Corbo, V., Ruvo, M., Tizzano, B., Rasmussen, T. E., Gammeltoft, S., Formisano, P., and Beguinot, F. (2005) *Mol. Cell. Biol.* **25**, 10803-14
18. Xie, Z., Zeng, X., Waldman, T., and Glazer, R. I. (2003); *Cancer Res.* **63**, 5370-5
19. Ahmed, N., Riley, C., and Quinn, M. A. (2008);*Br. J. Cancer* **98**, 1415-24
20. Peifer, C., and Alessi, D. R. (2009) *Biochem J* **417**, 5-7
21. Riedemann, J., and Macaulay, V. M. (2006) *Endocr. Relat. Cancer* **13**, S33-43
22. Alessi, D. R., James, S. R., Downes, C. P., Holmes, A. B., Gagaffney, P. R. J., Reese, C. B., and Cohen, P. (1997) *Curr. Biol.* **7**, 261-269
23. Kato, H., Faria, T. N., Stannard, B., Roberts, C. T. Jr, and LeRoith, D. J. (1993) *Biol. Chem.* **268**, 2655-61
24. Ciardiello, F., Bianco, R., Caputo, R., Caputo, R., Damiano, V., Troiani, T., Melisi, D., De Vita, F., De Placido, S., Bianco, A. R., and Tortora, G. (2004) *Clin. Cancer Res.* **10**, 784-93

25. Formisano, P., Oriente, F., Miele, C., Caruso, M., Auricchio, R., Vigliotta, G., Condorelli, G., and Beguinot, F. (1998) *J. Biol. Chem.* **273**, 13197-202
26. Formisano, P., Sohn, K. J., Miele, C., Caruso, M., Auricchio, R., Vigliotta, G., Condorelli, G., and Beguinot, F. (1993) *Mutation J. Biol. Chem.* **268**, 5241-8
27. Fields, G. B., and Noble, R. L. (1990) *Int. J. Pept. Protein Res.* **35**, 161-214
28. Jones, H. E., Gee, J. M., Hutcheson, I. R., Knowlden, J. M., Barrow, D., and Nicholson, R. I. (2006) *Endocr. Relat. Cancer* **13**, S45- 51
29. Tortora, G., Bianco, R., Daniele, G., Ciardiello, F., McCubrey, J. A., Ricciardi, M. R., Ciuffreda, L., Cognetti, F., Tafuri, A., and Milella, M. (2007) *Drug Resist. Updat.* **10**, 81-100
30. Miller, B. S., and Yee, D. (2005) *Cancer Res.* **65**, 10123-7
31. Huang, F., Greer, A., Hurlburt, W., Han, X., Hafezi, R, Wittenberg, G. M., Reeves, K., Chen, J, Robinson, D., Li, A., Lee, F. Y, Gottardis, M. M., Clark, E., Helman, L., Attar, R. M., Dongre, A., and Carboni, J. M. (2009) *Cancer Res.* **69**, 161-70
32. Buck, E., Eyzaguirre, A., Rosenfeld-Franklin, M., (2008) *Cancer Res.* **68**, 8322-32
33. Harris, T. K. (2003) *IUBMB Life* **55**, 117-26
34. Komander, D., Fairservice, A., Deak, M., Kular G. S., Prescott, A. R., Peter Downes, C., Safrany, S. T., Alessi, D. R., and van Aalten, D. M. (2004) *EMBO J.* **23**, 3918-28
35. Valentinis, B., and Baserga, R. (2001) *Mol. Pathol.* **54**, 133-7
36. Surmacz, E., Sell, C., Swantek, J., Kato, H., Roberts, C. T. Jr, LeRoith, D., and Baserga, R. (1995) *Exp. Cell. Res.* **218**, 370-80
37. Reiss, K., Yumet, G., Shan, S., Huang, Z., Alnemri, E., Srinivasula, S. M., Wang, J. Y., Morrione, A., and Baserga, R. (1999) *J. Cell. Physiol.* **181**, 124-35
38. Hongo, A., Yumet, G., Resnicoff, M., Romano, G., O'Connor, R., and Baserga, R. (1998) *Cancer Res.* **58**, 2477-84
39. Liu, Y., Lehar, S., Corvi, C., Payne, G., and O'Connor, R. (1998) *Cancer Res.* **58**, 570-6
40. Dunn, S. E., Hardman, R. A., Kari, F. W., and Barrett, J. C. (1997) *Cancer Res.* **57**, 2687-93
41. Wang, Q., and Greene, M. I. (2008) *J. Clin. Invest.* **118**, 2389-92
42. Guix, M., Faber, A. C., Wang, S. E., Olivares, M. G., Song, Y., Qu, S., Rinehart, C., Seidel, B., Yee, D., Arteaga, C. L., and Engelman, J. A. (2008) *J. Clin. Invest.* **118**, 2609-19
43. Takahari, D., Yamada, Y., Okita, N. T., Honda, T., Hirashima, Y., Matsubara, J., Takashima, A., Kato, K., Hamaguchi, T., Shirao, K., Shimada, Y., and Shimoda, T. (2009) *Oncology* **76**, 42-8
44. Gallego, R., Codony-Servat, J., García-Albéniz, X., Carcereny, E., Longarón, R., Oliveras, A., Tosca, M., Augé, J. M., Gascón, P., and Maurel, J. (2009) *Endocr. Relat. Cancer* **16**, 311-317
45. Nahta, R., Yuan, L. X., Zhang, B., Kobayashi, R., and Esteva, F. J. (2005) *Cancer Res.* **65**, 11118-28. Erratum in: *Cancer Res.* (2008) **68**, 9566
46. Barnes, C.J., Ohshiro, K., Rayala, S. K., El-Naggar, A. K., and Kumar, R. (2007) *Clin. Cancer Res.* **13**, 4291-9
47. Sachdev, D., Singh, R., Fujita-Yamaguchi, Y., and Yee, D. (2006) *Cancer Res.* **66**, 2391-402
48. Hashimoto, N., Kido, Y., Uchida, T., Asahara, S., Shigeyama, Y., Matsuda, T., Takeda, A., Tsuchihashi, D., Nishizawa, A., Ogawa, W., Fujimoto, Y., Okamura, H., Arden, K. C., Herrera, P. L., Noda, T., and Kasuga, M. (2006) *Nat. Genet.* **38**, 589-93
49. Duronio, V. (2008); *Biochem. J.* **415**, 333-44
50. Seynaeve, C. M., Stetler-Stevenson, M., Sebers, S., Kaur, G., Sausville, E. A., and Worland, P. J. (1993) *Cancer Res.* **53**, 2081-6
51. Kortmansky, J., Shah, M. A., Kaubisch, A., Weyerbacher, A., Yi, S., Tong, W., Sowers, R., Gonen, M., O'reilly, E., Kemeny, N., Ilson, D. I., Saltz, L. B., Maki, R. G., Kelsen, D. P., and Schwartz, G. K. (2005) *J. Clin. Oncol.* **23**, 1875-84
52. Jimeno, A., Rudek, M. A., Purcell, T., Laheru, D. A., Messersmith, W. A., Dancey, J., Carducci, M. A., Baker, S. D., Hidalgo, M., and Donehower, R. C. (2008) *Cancer Chemother. Pharmacol.* **61**, 423-33

53. Hu, Y. P., Patil, S. B., Panasiewicz, M., Li, W., Hauser, J., Humphrey, L. E., and Brattain, M. G. (2008) *Cancer Res.* **68**, 8004-13
54. Sato, S., Fujita, N., and Tsuruo, T. (2004) *J. Biol. Chem.* **279**, 33759-67
55. Michel, J. J., Townley, I. K., Dodge-Kafka, K. L., Zhang, F., Kapiloff, M. S., and Scott, J. D. (2005) *Mol. Cell.* **20**, 661-72

FIGURE LEGENDS

Figure 1. **PDK1 tyrosine phosphorylation, IGF-1R co-precipitation and substrate phosphorylation.** A) MCF-7 cells were exposed to 100 ng/ml IGF-1 for 5 and 30 min, as indicated, and then solubilized as described in Experimental Procedures. Cell lysates (50 μg protein/sample) were blotted with phospho-tyrosine-373/376-PDK1 antibodies ($pTyr_{373/376}$-PDK1). To ensure the equal PDK1 transfer, membranes were blotted with PDK1 antibodies (PDK1). The filters were revealed by ECL and autoradiography. B) MCF-7 cell lysates (200μg/sample) were immunoprecipitated with IGF-1R α-subunit antibodies, followed by blotting with PDK1 antibodies and then re-blotted with phospho-serine-241-PDK1 antibodies ($pSer_{241}$-PDK1). To ensure equal immunoprecipitation, membranes were blotted with α-subunit-IGF-1R antibodies (α–sub-IGF-1R). Membranes were revealed by ECL and autoradiography. C) MCF-7 total cell lysates (50 μg protein/sample) were blotted with phospho-threonine-308-Akt/PKB ($pThr_{308}$-Akt/PKB) and phospho-threonine-410-PKCζ ($pThr_{410}$-PKCζ) antibodies and then re-blotted with Akt/PKB and PKCζ antibodies. Membranes were revealed by ECL and autoradiography.
The autoradiographs shown are representative of four independent experiments.

Figure 2. ***In vitro*** **interaction of IGF-1R with PDK1.** A) IGF-1R was partially purified from $NIH3T3^{IGF\text{-}1R}$ by WGA affinity chromatography and subjected to pull-down using full length GST-PDK1 and deletion mutants (aa 1-359, aa 51-359 and aa 408-556). Equal amounts of IGF-1R were incubated with each fusion protein, then eluted and analyzed by 7,5% SDS-PAGE; IGF-1R bound to fusion proteins was detected by Western blotting using anti-β subunit IGF-1R antibodies. B) Amino acid sequence alignment of synthetic peptides corresponding to IGF-1R C-terminus fragment (C43; C22), to a mutated version, in which Tyr_{1316} has been substituted with Phe (C43F; C22F), and to insulin receptor C-terminus (C-IR). C) Partially purified IGF-1R was incubated for 2 h at 4 C with Sepharose-GST-PDK1, in the presence or in the absence of synthetic peptides (C43, C43F, C22, C22F, C-IR and SP) at increasing concentration as indicated. Pulled-down proteins were blotted with anti IGF-1R (β subunit) antibody and the results quantitated by laser densitometry. D) Equal amounts of purified IGF-1R were stimulated with 100 ng/ml IGF1, as described in Materials and Methods, and incubated with GST-PDK1 in the presence of increasing concentrations of C43, as indicated. Proteins were blotted with $pTyr_{373/376}$-PDK1 antibodies. Membranes were re-blotted with PDK1 and IGF-1R (α subunit) antibodies, as shown on the bottom. Blots were revealed by ECL and autoradiography.
The autoradiographs shown are representative of at least four independent experiments.

Figure 3. **Transduction of FITC-C43 into MCF-7 cells.** A). MCF-7 cells were incubated with increasing concentrations of the fluoresceine-conjugated peptide (FITC-C43), as indicated. Peptide uptake in MCF7 cells was detected by FACS analysis of fluorescein-labelled cells. B) MCF-7 cells were incubated with FITC-C43 peptide (10 μM) and fixed in formaldehyde at 37 C. Uptake and intracellular distribution were monitored by fluorescence with appropriate filters. *Panel I* shows the FITC-C43 peptide internalized in the cells with prevalent sub-membrane localization; *panel II* shows cell nuclei stained with DAPI reagent, *panel III* shows the overlay…
These experiments were repeated three times with similar findings.

Figure 4. **Effect of C43 on IGF-1 signalling in intact MCF-7cells.** A) MCF-7 cells, treated with FITC-Scrambled Peptide (FITC-SP) or with FITC-C43, were starved for 16 h and stimulated for

indicated time with 100 ng/ml IGF-1. Cell lysates (200μg/sample) were immunoprecipitated with anti IGF-1R (α sub) antibody, then immunoprecipitated proteins were separated on SDS-PAGE and Western blot analysis was performed with anti PDK1 and anti IGF-1R α subunit antibodies. Blots were revealed by ECL and autoradiography. B) MCF-7 cells, loaded with FITC-SP or FITC-C43, were incubated for 5 min with 100 ng/ml IGF-1. Total cell lysates (50μg protein/sample) were blotted with $pThr_{308}$-Akt/PKB or $pThr_{410}$-PKCζ or phospho-Threonine-202/Tyrosine-204-ERK1/2 (pERK) antibodies and then re-blotted with Akt/PKB, PKCζ or ERK1/2 antibodies. Membranes were revealed by ECL and autoradiography. The autoradiographs shown are representative of four independent experiments. C) Filters obtained in B have been analyzed by laser densitometry as described in Experimental Procedures. Asterisks indicate statistically significant differences (***, $p<0.001$).

Figure 5. **Biological effect of reduced IGF-1R/PDK1 interaction in intact cells.** A) MCF-7 cells, loaded with FITC-C43, -C43F, -C22, -C22F , -C-IR or SP, were incubated in serum-free DMEM for 16 h in the presence or in the absence of IGF-1and apoptosis was quantified by the ELISA plus apoptosis detection kit as described under Experimental Procedures.B) MCF-7 cells, loaded with FITC-C43, -C43F, -C22, -C22F ,-C-IR or SP, were incubated in serum-free DMEM for 16 h in the presence or in the absence of IGF-1. Cells were stained with propidium iodide and ratio of cells in sub-G1 phase was determined by cytometric analysis, as described in Experimental Procedures. C) L6 cells were incubated in serum-free media for 16 h before exposure to 100 nM insulin for 30 min, as indicated. Alternatively, 10 μM of C43 or SP were simultaneously added to serum-free media in the presence or absence of insulin. Then the cells were assayed for 2-DG uptake as described in Experimental Procedures. Bars represent mean ± S.D. of three different experiments in triplicate. Asterisks indicate statistically significant differences vs untreated cells (***, $p<0.001$).

Figure 6. **Synergistic effect of C43 and Cetuximab on GEO and GEO-CR cells.** 10 μM FITC-C43 or FITC-SP was loaded into GEO and GEO-CR cells. After 24 h treatment with Cetuximab (C225), the cells were harvested, fixed and stained with propidium iodide. The ratio of cells in sub-G1 phase was determined by cytometric analysis, as described in Experimental Procedures.

Figure 7. **Effect of C43 on IGF-1 signalling in GEO and GEO-CR cells.** A) GEO and GEO-CR cells, treated with FITC-SP or FITC-C43, were exposed to 100 ng/ml IGF-1, as indicated, and then solubilized. Cell lysates (50 μg protein/sample) were blotted with $pTyr_{373/376}$-PDK1 antibody. To ensure equal PDK1 transfer, membranes were further blotted with PDK1 antibodies. Blots were revealed by ECL and autoradiography. B) GEO and GEO-CR cells were loaded with FITC-SP or with FITC-C43 and then stimulated for indicated time with 100 ng/ml IGF-1. Cell lysates (200 μg/sample) were immunoprecipitated with anti IGF-1R (α sub) antibody, then immunoprecipitated proteins were separated on SDS-PAGE. Western Blot analysis was performed with anti PDK1 and anti IGF-1R β subunit antibodies. Blots were revealed by ECL and autoradiography. C) GEO and GEO-CR cells, loaded with FITC-SP or with FITC-C43 were stimulated with 100 ng/ml IGF-1 and then solubilized as described in Material and Methods. Total cell lysates (50 μg protein/sample) were blotted with $pThr_{308}$-Akt/PKB or pERK antibodies and then re-blotted with Akt/PKB or ERK1/2 antibodies. Membranes were revealed by ECL and autoradiography.
The autoradiographs shown are representative of four independent experiments.

Fig. 1

A

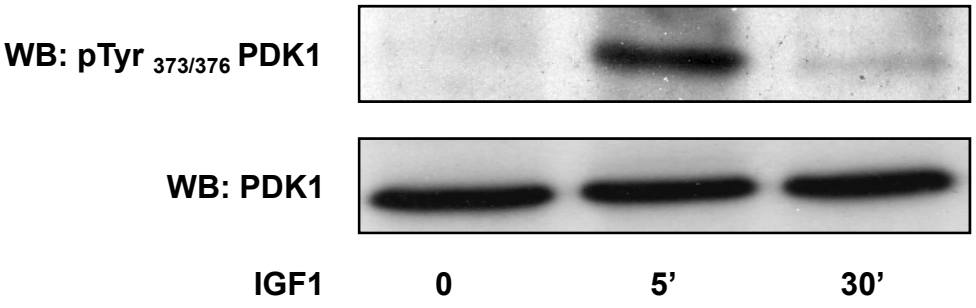
WB: pTyr 373/376 PDK1
WB: PDK1
IGF1
0
5'
30'

B

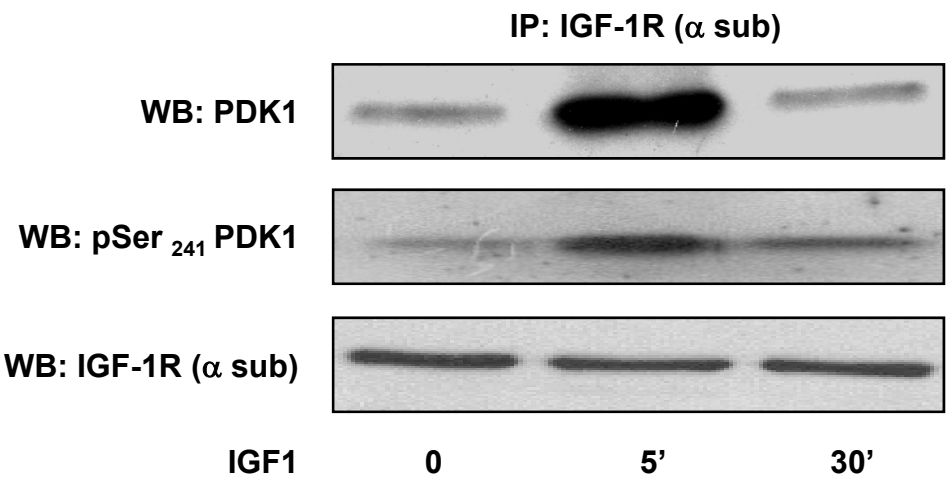
IP: IGF-1R (α sub)
WB: PDK1
WB: pSer 241 PDK1
WB: IGF-1R (α sub)
IGF1
0
5'
30'

C

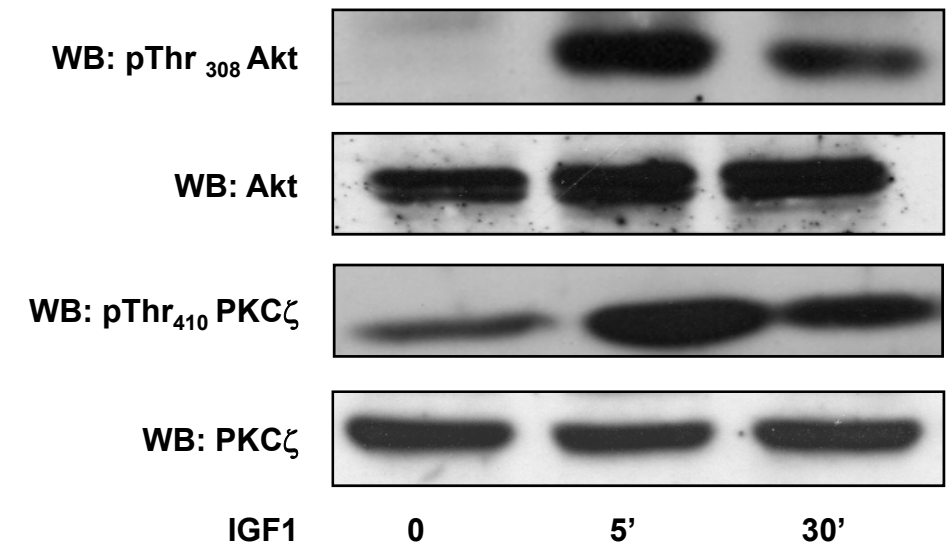
WB: pThr 308 Akt
WB: Akt
WB: pThr410 PKCζ
WB: PKCζ
IGF1
0
5'
30'

A

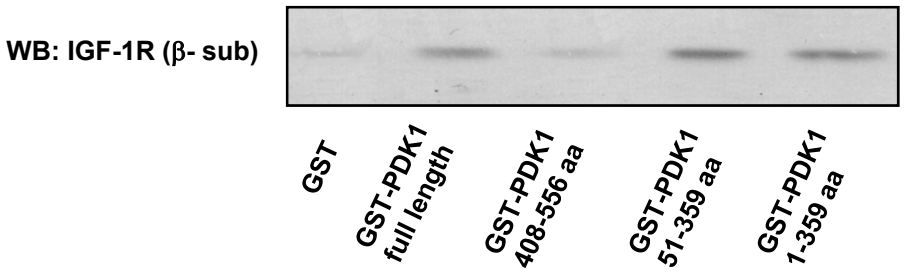
WB: IGF-1R (β- sub)
GST
GST-PDK1 full length
GST-PDK1 408-556 aa
GST-PDK1 51-359 aa
GST-PDK1 1-359 aa

B

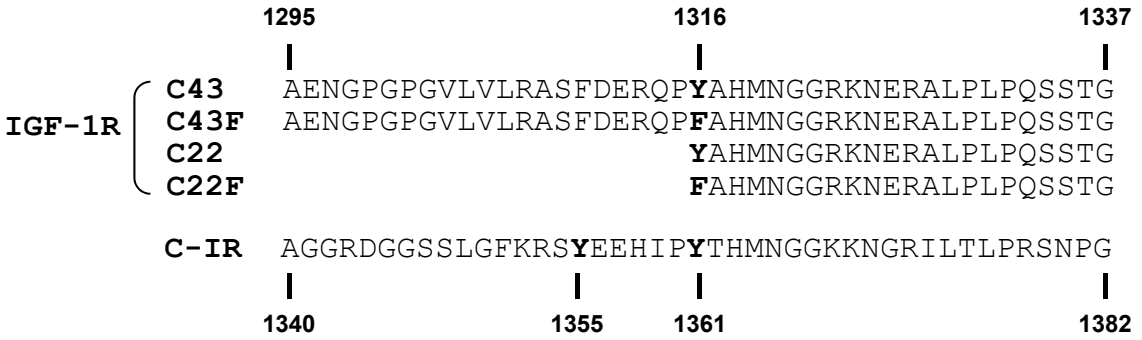
1295
1316
1337
IGF-1R
C43 AENGPGPGVLVLRASFDERQPYAHMNGGRKNERALPLPQSSTG
C43F AENGPGPGVLVLRASFDERQPFAHMNGGRKNERALPLPQSSTG
C22 YAHMNGGRKNERALPLPQSSTG
C22F FAHMNGGRKNERALPLPQSSTG
C-IR AGGRDGGSSLGFKRSYEEHIPYTHMNGGKKNGRILTLPRSNPG
1340
1355
1361
1382

C

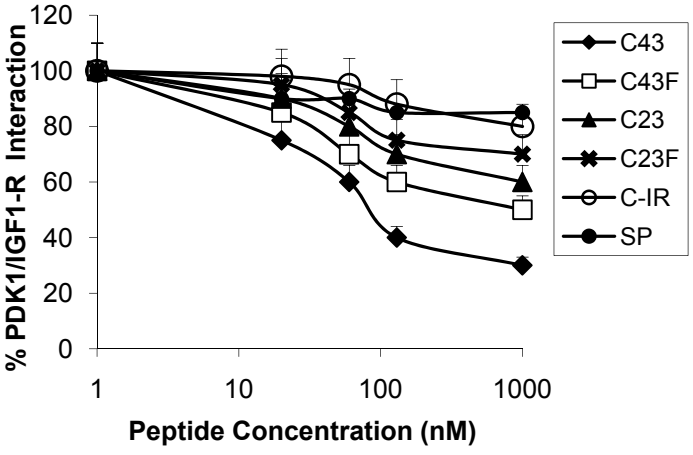
% PDK1/IGF1-R Interaction
120
100
80
60
40
20
0
1
10
100
1000
Peptide Concentration (nM)
C43
C43F
C23
C23F
C-IR
SP

D

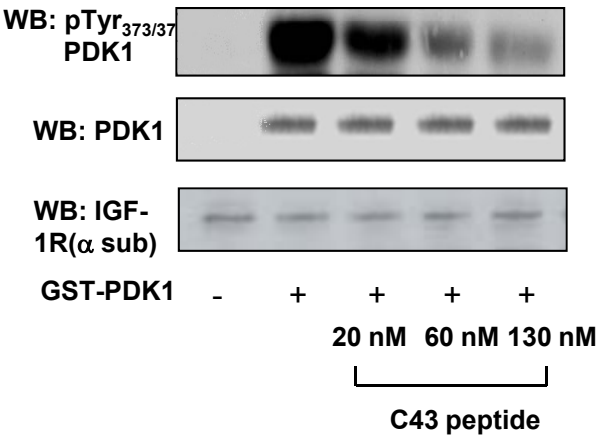
WB: pTyr373/37 PDK1
WB: PDK1
WB: IGF-1R(α sub)
GST-PDK1 - + + + +
20 nM 60 nM 130 nM
C43 peptide

A

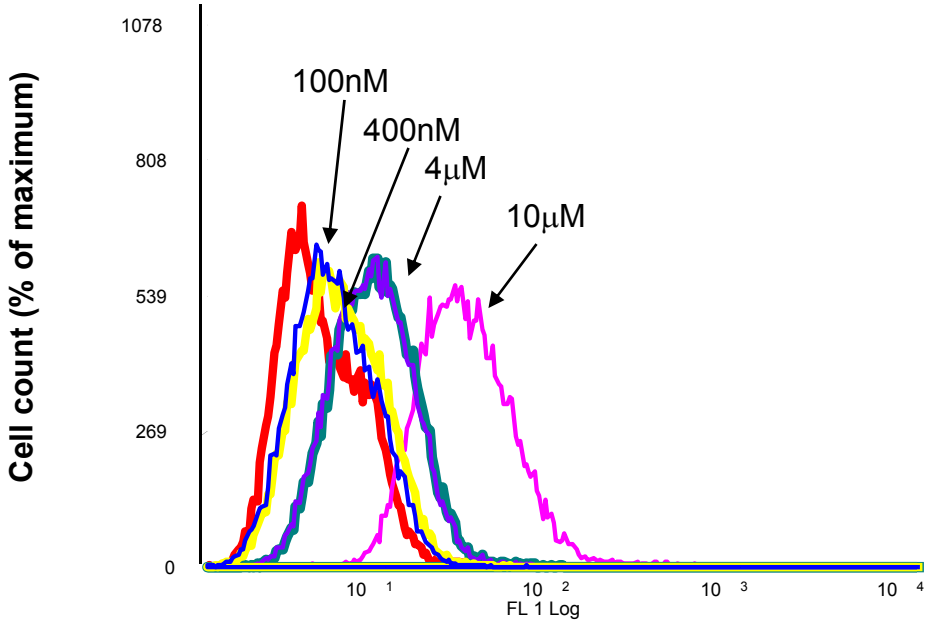
Cell count (% of maximum)
1078
808
539
269
0
100nM
400nM
4μM
10μM
10 1
10 2
10 3
10 4
FL 1 Log

B

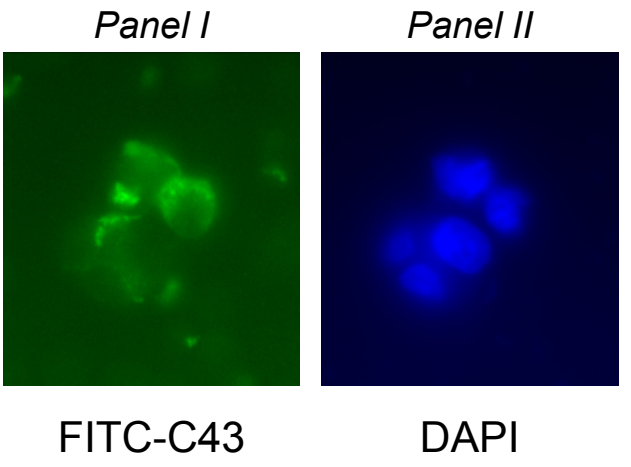
Panel I
Panel II
FITC-C43
DAPI

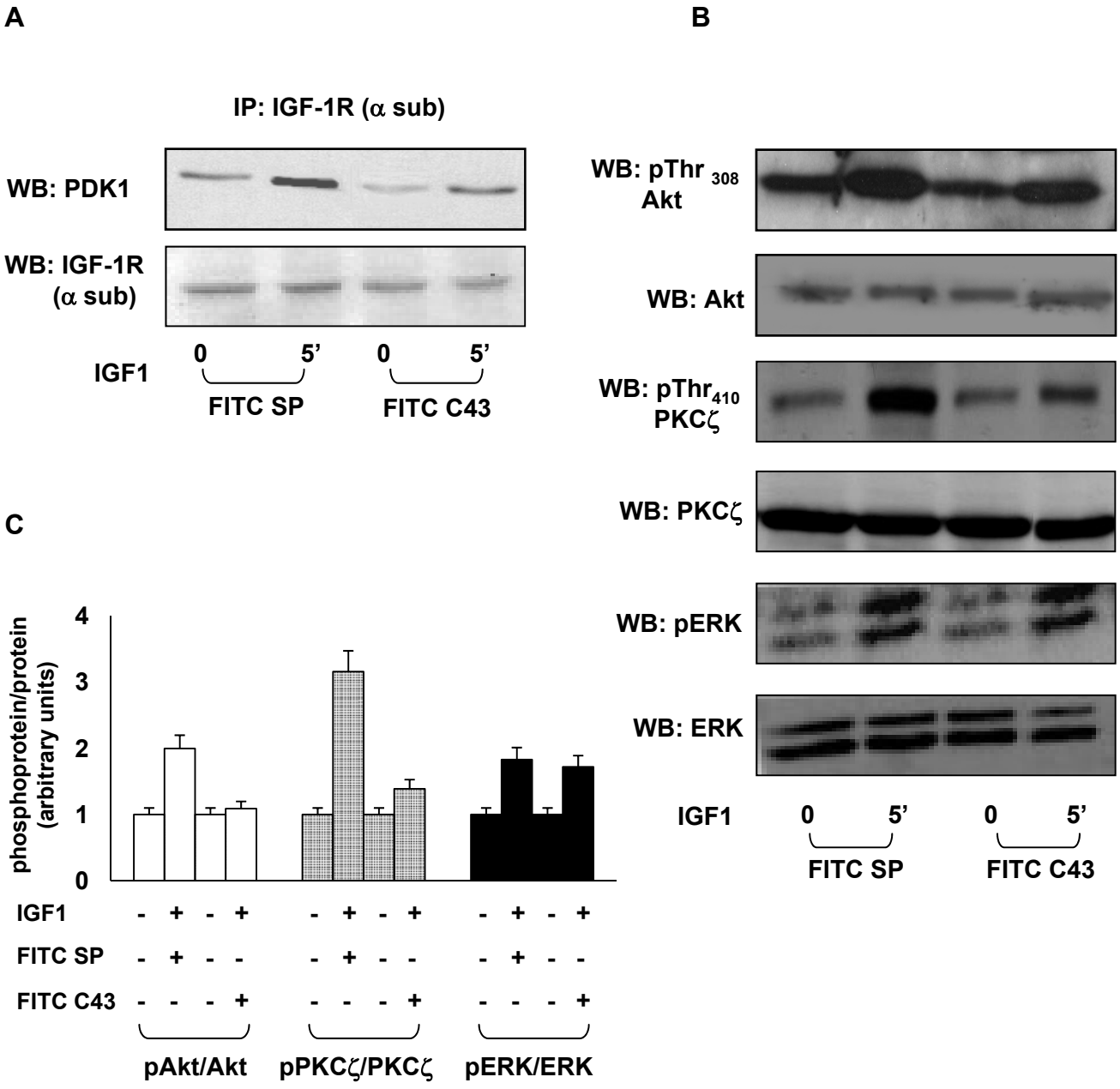
A
IP: IGF-1R (α sub)
WB: PDK1
WB: IGF-1R (α sub)
IGF1
0
5'
0
5'
FITC SP
FITC C43
B
WB: pThr 308 Akt
WB: Akt
WB: pThr410 PKCζ
WB: PKCζ
WB: pERK
WB: ERK
IGF1
0
5'
0
5'
FITC SP
FITC C43
C
phosphoprotein/protein (arbitrary units)
4
3
2
1
0
IGF1
FITC SP
FITC C43
pAkt/Akt
pPKCζ/PKCζ
pERK/ERK

A

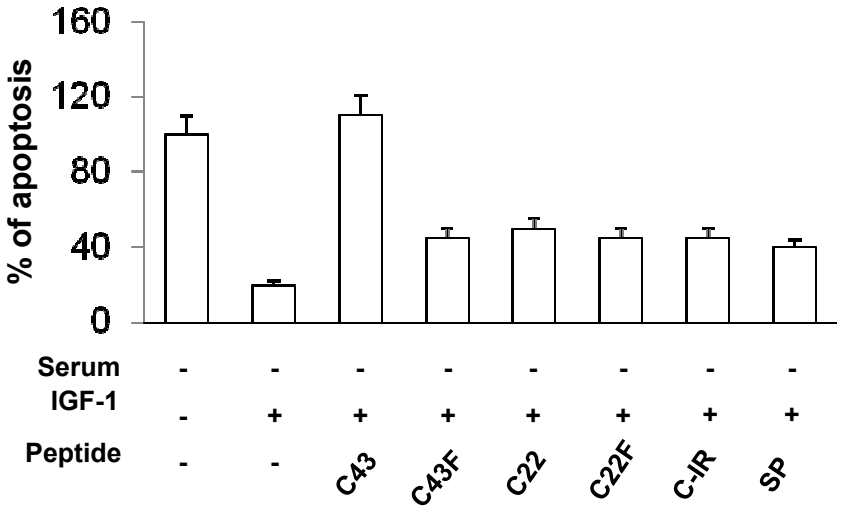
160
120
80
40
0
% of apoptosis
Serum - - - - - - - -
IGF-1 - + + + + + + +
Peptide - - C43 C43F C22 C22F C-IR SP

B

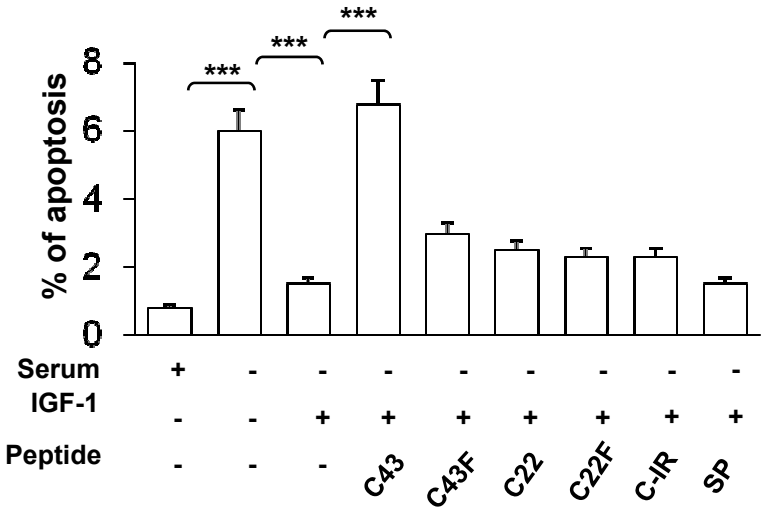
***
***
***
8
6
4
2
0
% of apoptosis
Serum + - - - - - - - -
IGF-1 - - + + + + + + +
Peptide - - - C43 C43F C22 C22F C-IR SP

C

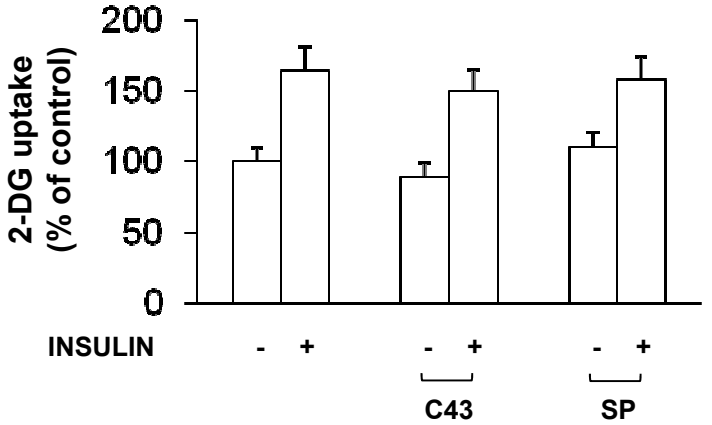
200
150
100
50
0
2-DG uptake (% of control)
INSULIN - + - + - +
C43
SP

Fig. 6

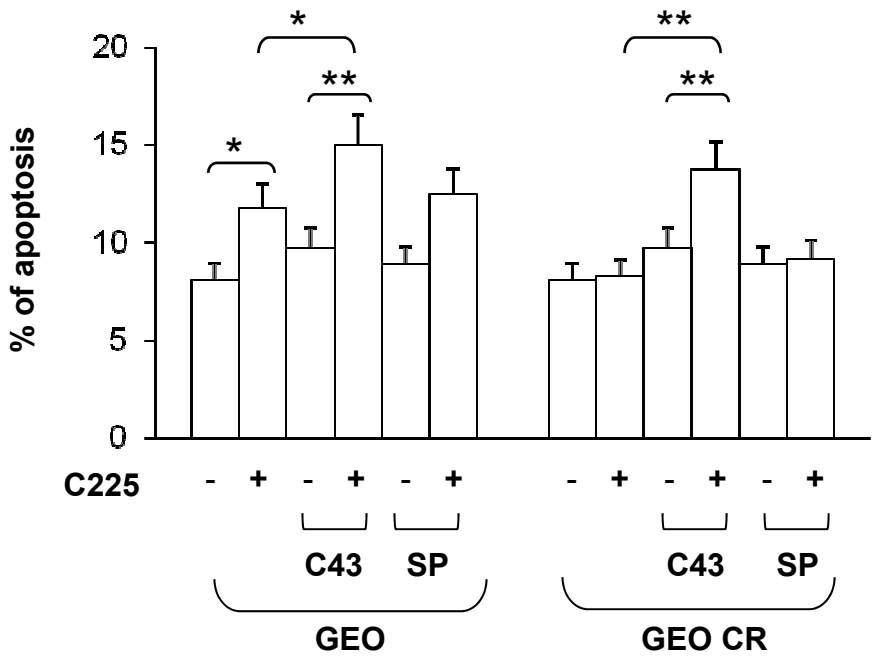

Fig. 7

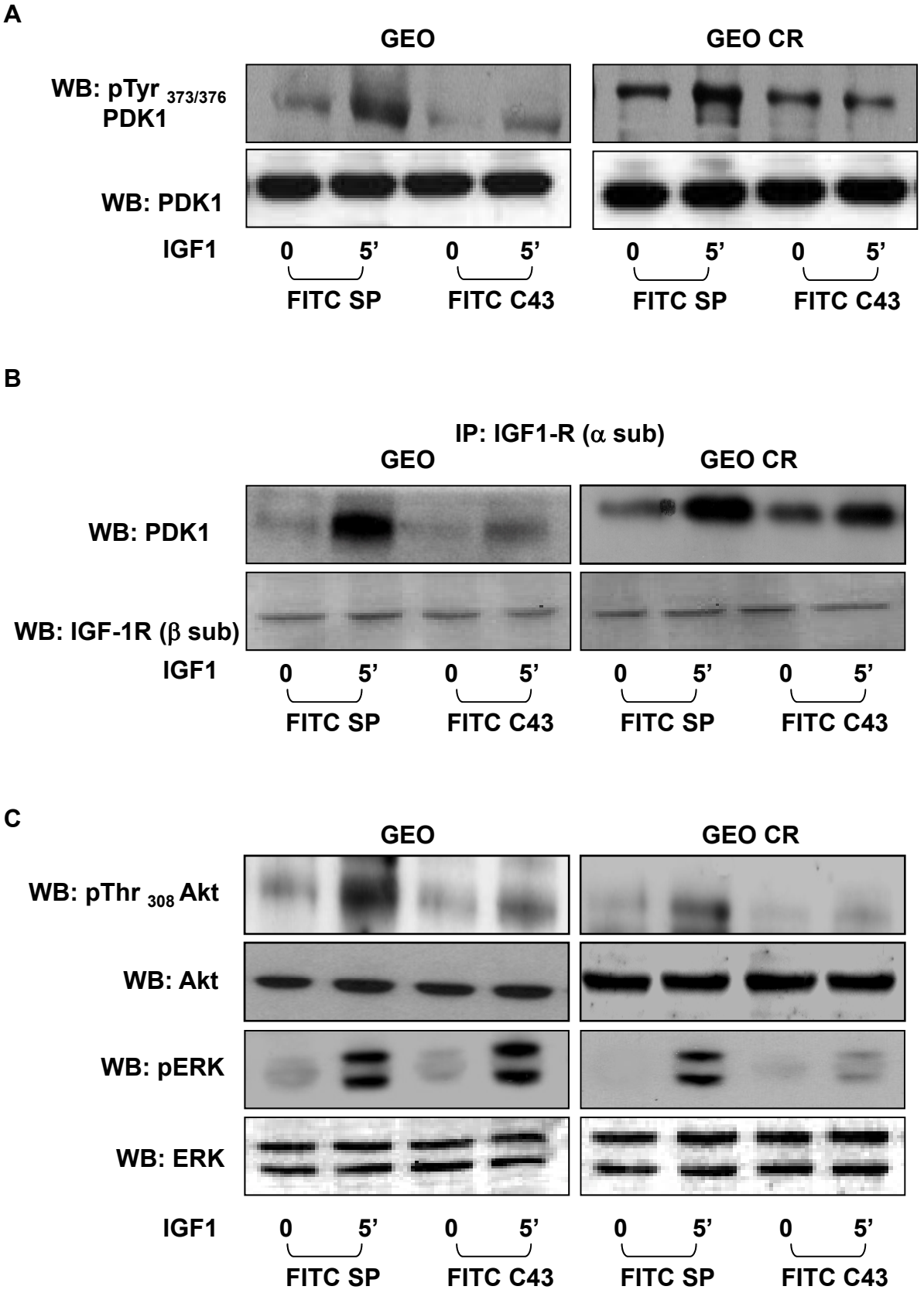
A
GEO
GEO CR
WB: pTyr 373/376 PDK1
WB: PDK1
IGF1
0
5'
0
5'
0
5'
0
5'
FITC SP
FITC C43
FITC SP
FITC C43
B
IP: IGF1-R (α sub)
GEO
GEO CR
WB: PDK1
WB: IGF-1R (β sub)
IGF1
0
5'
0
5'
0
5'
0
5'
FITC SP
FITC C43
FITC SP
FITC C43
C
GEO
GEO CR
WB: pThr 308 Akt
WB: Akt
WB: pERK
WB: ERK
IGF1
0
5'
0
5'
0
5'
0
5'
FITC SP
FITC C43
FITC SP
FITC C43